Spherical Collapse in Dark Energy Models

Master of Science Thesis by

Robert Mardoff Nielsen

Institute of Theoretical Astrophysics
University of Oslo

June 1, 2011

Abstract

This thesis is a study of the dynamics and virialization of cosmic structures in the framework of flat cosmological models where the properties of the dark energy component plays an important role in the global and local dynamics of the Universe. In particular, the analysis focuses on the study of the spherical collapse model which represents a spherical homogeneous density perturbation in the cosmic fluid. It is a two-component system, made of cold dark matter and dark energy, which initially evolves with the Universe and with time begins to decouple from the background expansion and starts to "turn around" and finally collapse. It is taken into account many models with an equation of state which are constant in time. Three main conditions for virialization will be considered and compared, and some differences in characteristic parameters will be pointed out, such as the radius and density contrast when the structures have virialized to a final size.

Acknowledgments

I wish to thank:

David F. Mota: My thesis supervisor. Thank you for helping me through this work.

My fellow students at Stjernekjelleren: Thank you for a pleasant working environment. Especially I would like to thank Svein Rune Saxrud and Håkon Skogsrud for helping me with computer and academic problems.

My grandmother: Thank you for helping me financially.

My mother and father: Thank you for being who you are and for always supporting me.

Contents

Chapter 1

Outline

In 1972 the spherical collapse model was presented by Gunn and Gott (GG) [1]. Since then it has proven to be a powerful tool for understanding and analysing the growth of inhomogeneities in the Universe [2, 3, 4, 19, 20, 21, 22, 23, 24, 25, 27]. It describes the evolution of how a spherical overdensity decouples from the expansion of the background, eventually ceases to expand, and then collapse towards its center. It is assumed that the collapse of this sphere never reaches a singularity but at some stage virializes and stabilizes at a finite size. How to define the epoch of virialization depends on what type of properties one impose the components of the sphere to have, what type of universe model it is in, and also on considerations of energy conservation.

There exists an analytical solution to this model when it is applied for the EdS universe. In this case the ratio of the radius at virialization R_{vir} to the maximal radius at turnaround R_{ta} is equal to a half, i.e. $\frac{R_{vir}}{R_{ta}} = \frac{1}{2}$. Among others it also gives analytical values for the *nonlinear density contrast* at turnaround, i.e. $\Delta_{ta} \approx 4.55$, and an analytical value for the nonlinear density contrast at virialization, i.e. $\Delta_{vir} \approx 145.84$ (or ≈ 176.65).

Because the EdS model only contains nonrelativistic dust (CDM) these parameter values do not apply when one wish to consider an additional component of dark energy (X). Then the situation becomes more complicated and it has been the subject of many studies. Lahav and Lilje (LL) et al. [2] generalized the formalism to a Universe composed of CDM and a specific X component, i.e. the cosmological constant Λ. They considered Λ to be *passive*, i.e. it only contributed with an extra potential U_Λ 'felt' by CDM, and only CDM virialized. This resulted in $\frac{R_{vir}}{R_{ta}} < \frac{1}{2}$. In the article by Maor and Lahav (ML) [3] they commented briefly this result saying that this scenario also corresponds to the dynamics implemented in N-body simulations for the concordance ΛCDM model which means that Λ only affects the time evolution of the scale factor a of the *background* Universe. Horellou and Berge (HB) [4] used the same condition for virialization as LL when using the spherical collapse model to investigate the effects of X on the formation of virialized structures. They considered dark energy models with

a constant equation of state, i.e. $w = constant$, and mainly $w = (-1.0, -0.8, -0.6)$. Among other things, HB concluded that for $-1 < w < -\frac{1}{3}$ clusters form *earlier* and are *more* concentrated in dark energy models than in the ΛCDM model (where $w = -1$).

In the article by ML they point out that most existing works look at virialization of the CDM component which only feels an additional potential due to the presence of X. They argued that by using this procedure, one implicitly assumes that X either does not virialize, or does so separately from the CDM component. Therefore their work aimed at critically contrast two different approaches - the assumption that the CDM virializes separately (as in LL and HB) and the assumption that both the CDM and X of the sphere virializes as a whole. In this context they also considered another interesting issue relating to the way of finding the right condition of virialization. They first concluded that if X do not participate in the spherical collapse, i.e. it remains homogeneous in the same way as the background, then the sphere must lose energy as it collapses. That is, X will 'leak out' during the collapse. Yet, the virialization condition assumes energy conservation between turnaround and virialization. This is an inconsistency for dark energy models with an equation of state with $w \neq -1$. ML introduce a correction to the equation that defines the final virialized radius to take into account this energy loss for X. They show that the inclusion of X in the virialization process (as not done in LL and HB) changes the results in a fundamental manner; the ratio of final to maximal size of the sphere is *larger* if X *is part* of the virialization.

A short summary is now appropriate. The article by GG implies that by using the correct virialization condition for a sphere in the EdS model then $\frac{R_{vir}}{R_{ta}} = \frac{1}{2}$. The virialization condition introduced in the article by LL results in $\frac{R_{vir}}{R_{ta}} < \frac{1}{2}$, and the virialization condition introduced in the article by ML results in $\frac{R_{vir}}{R_{ta}} > \frac{1}{2}$. Thus, these fundamental different results indicates that by observing virialized structures in the Universe and to measure their radius, they have the potential to reveal the type and dynamical nature of the energy components of the Universe, and in addition its correct equation of state.

This thesis will use the specific virialization condition used in LL and HB, and the specific virialization condition used in ML and also the corrected version accounting for energy loss from the same article. That is, three different considerations of virialization will be investigated:

- The dark energy is *passive*, it does *not* participate in the virialization process but only sets up an additional potential U_X 'felt' by the CDM. Energy conservation is neglected.

- The dark energy is *dynamical*, it *does* participate in the virialization process, but does not cluster and thus energy is *not* conserved.

- The dark energy is *dynamical*, it *does* participate in the virialization process, it does cluster and thus energy *is* conserved.

These three different conditions will be applied to homogeneous overdense spheres evolving mainly inside many different dark energy universe models with a *constant* equation of state where $w \in [-1, 0]$. Their radius at virialization $\frac{R_{vir}}{R_{ta}}$ will be simulated, and also the two other parameters already mentioned, i.e. the density contrast Δ_{ta} at turnaround, and the density contrast Δ_{vir} at virialization. It will be shown that these virial conditions gives significant different results.

In addition will the dynamics of overdense spheres be studied and simulated for different initial density perturbations, inside dark energy models with a constant equation of state. That is, when no virialization condition is included to halt the collapse.

The simulations are done by a code developed for this thesis. In all of the dark energy universe models where the evolution of the sphere takes place are flat and based on the FLRW metric and with two energy components with density parameters $\Omega_{m0} = 0.3$ for CDM and $\Omega_{X0} = 0.7$ for X.

Note that for this thesis there is no characteristic length scales associated to the collapsing system so the spherical collapse remains independent of the size of the object.

Chapter 2

Preliminaries

"..in order to make an apple pie from scratch, you must first invent the Universe."
-Carl Sagan

For describing the Universe in a scientific manner, one need certain basic physical theories. A complete theory is yet to be fully discovered, but luckily one do not really need it, because in most situations one is interested in describing only specific physical processes and not the whole universal machinery at ones.

Cosmology depends on a theory describing the Universe on very large scales and *The theory of General Relativity* is capable of doing this. It tells us what we observe but not, on a fundamental level, what causing the things we observe. Derived from this theory is basic mathematical models which describes specific types of simplified, but very useful, universes where their topological, geometrical and dynamical properties depends on their contents. These universes serves as a kind of basis, or framework, for building more complicated and more realistically universe models to describe the real Universe we inhabits and is a part of.

In the first section of this chapter, Albert Einstein's theory of general relativity will be introduced. In the second section will an introduction of basic cosmology be given.

2.1 The Theory of General Relativity

"..mass tells spacetime how to curve, and spacetime tells mass how to move."
-John Wheeler

With Albert Einstein's *Theory of General Relativity* (GR) - no longer is gravity a force, as we know it from Newtonian mechanics, but instead an intrinsic property of the so called 'fabric' of the four dimensional spacetime. GR describes the interaction between spacetime and energy (mass is a form of energy). It tells us that mass or any kind of matter distribution actually bends the spacetime surrounding it and warps its properties. By using its mathematical framework we are capable of calculating this warping and its effects on the trajectories of *test particles* (ch. 2.1.2) in its vicinity.

The following three subsections will be based on the books [5], [6], [7], [8], and [9].

2.1.1 The metric tensor and the line element

The most central quantity in GR is the concept of a *metric*. This metric has significant implications crucial for the physics treated by GR because it defines the geometry of spacetime. It is a *symmetric second rank tensor* represented by a 4×4 - matrix and conventionally labelled g. In its most general form it is given as

$$g_{\alpha\beta} = \begin{pmatrix} g_{00} & g_{01} & g_{02} & g_{03} \\ g_{10} & g_{11} & g_{12} & g_{13} \\ g_{20} & g_{21} & g_{22} & g_{23} \\ g_{30} & g_{31} & g_{32} & g_{33} \end{pmatrix} \tag{2.1}$$

where the elements can be zero, constants, and functions of spacetime coordinates.

A second very important quantity in GR is the *line element*. At its most fundamental level one could say that it is just the Pythagorean theorem giving the distance between two points on a flat two-dimensional surface. In a more general sense it can be defined as 'a measurement of the distance between two points in some defined metric space', i.e. the two points is not necessarily limited to a two-dimensional space and the space itself does not need to be flat and it can even expand or contract. This calls for modifications of the Pythagorean theorem and it is carried out by the machinery of the mathematical field of *differential geometry*.

We can find a standard example of a line element, conventionally labelled ds, in the theory of *Special Relativity* (SR). Here the *flat* spacetime geometry can be summarized

in Cartesian coordinates by

$$ds^2 = -c^2dt^2 + dx^2 + dy^2 + dz^2 \tag{2.2}$$

where c is the speed of light, dt is an infinitesimal interval in the time dimension and dx, dy and dz are infinitesimal intervals in the three space dimensions. With two sets of coordinates (t, x, y, z) and (t', x', y', z') representing *events* (the terminology for points in the spacetime) this line element gives the distance ds between them. Note that the time-dimension is included in this distance. Now, this particular line element is not unique as goes for many others. The same flat geometry of spacetime can be represented by equivalent line elements because different coordinate systems can be used. One specific transformation of (2.2) results into

$$ds^2 = -c^2dt^2 + dr^2 + r^2d\theta^2 + sin^2\theta d\phi^2 \tag{2.3}$$

where the spatial part of the line element have been transformed to spherical polar coordinates. It looks different than (2.2) but it represents the exact same geometry only with the events labeled in a different way.

With these two examples in mind, it is easy to see that when we know the elements of the metric $g_{\alpha\beta}$ (2.1), the line element easily follows as

$$ds^2 = \sum_{\alpha,\beta} g_{\alpha\beta}(x)dx^\alpha dx^\beta \equiv g_{\alpha\beta}(x)dx^\alpha dx^\beta \tag{2.4}$$

This is the general formula for the line element and it also defines *Einstein's convention for summation*. Here the metric $g_{\alpha\beta} = g_{\alpha\beta}(x)$ is position-dependent and dx is an infinitesimal interval between two spacetime events defined by x and x'. Note that x in the literature is used to represent all four spacetime coordinates. Also note that the two metrics $g_{\alpha\beta}$ defining (2.2) and (2.3) has to be diagonal, i.e. all off-diagonal elements are zero in these cases.

For example, if

$$g_{\alpha\beta} = \begin{pmatrix} -c^2 & 0 & 0 & 0 \\ 0 & 1 & 0 & 0 \\ 0 & 0 & r^2 & 0 \\ 0 & 0 & 0 & r^2sin^2\theta \end{pmatrix} \tag{2.5}$$

then

$$\begin{aligned} ds^2 &= g_{\alpha\beta}(x)dx^\alpha dx^\beta \\ &= g_{00}dx^0dx^0 + g_{11}dx^1dx^1 + g_{22}dx^2dx^2 + g_{33}dx^3dx^3 \\ &= -c^2dt^2 + dr^2 + r^2d\theta^2 + sin^2\theta d\phi^2 \end{aligned} \tag{2.6}$$

which is the explicit derivation of (2.3) using the summation convention.

Thus, by knowing the actual form of the metric (2.1) we can calculate and define the line element which describes the corresponding geometry of the spacetime. The metric and the line element is two sides of the same coin and because of that one needs to be aware of that they get treated interchangeably in the wide literature of GR.

2.1.2 The geodesic equation and the Christoffel symbols

A *geodesic* is defined as 'the shortest line between two points on a specific surface'. This line is given by the *geodesic equation*.

Firstly, when talking about geodesics one needs to know the meaning of a *test particle* and a *free particle*. A test particle is a body with so little mass that it produces no significant spacetime curvature by itself. This makes it capable of moving in response to the spacetime curvature produced by other bodies with significant masses. A man made satellite is one of many examples of this. A free particle in the following context means a test particle free from any influences (e.g. electric forces) other than the curvature of spacetime. Thus, the curved spacetime of general relativity are explored by studying how these test particles (and also light rays) move through them.

The geodesic equation[1] can be derived using the method of variations and it says

$$\frac{d^2x^\alpha}{d\lambda^2} = -\Gamma^\alpha_{\beta\gamma}\frac{dx^\beta}{d\lambda}\frac{dx^\gamma}{d\lambda} \tag{2.7}$$

where λ is a parameter that monotonously increases along the *worldline* (i.e. a path in spacetime) of the test particle. For test particles with mass is $\lambda = \tau$, and represents its *proper time* which is the time measured by the test particle itself. The coefficients $\Gamma^\alpha_{\beta\gamma}$, called the *Christoffel symbols*, are constructed from the metric (2.1) and its first derivatives. At each event in spacetime, for any *local* coordinate system, it is an array

[1] [6] p. 173.

with three dimensions, n × n × n, where each of the n^3 components is a real number and represent a gravitational force field. The general formula[2] is

$$\Gamma^{\delta}_{\beta\gamma} = \frac{1}{2} g^{\alpha\delta} \left(\frac{\partial g_{\alpha\beta}}{\partial x^{\gamma}} + \frac{\partial g_{\alpha\gamma}}{\partial x^{\beta}} - \frac{\partial g_{\beta\gamma}}{\partial x^{\alpha}} \right) \tag{2.8}$$

and with a known metric g this formula gives the corresponding Christoffel symbols when substituting the metric elements done by the correct "notation gymnastics".

The geodesic equation (2.7) is the GR equivalent of Newton's second law in the absence of external forces. The left side being the acceleration of the test particle, and the right side involving the curvature of spacetime.

2.1.3 Einstein's field equations

Einstein's vision was that there exists no gravitational force at all but rather the non-euclidean geometry of spacetime causing an illusion of a force. This is incorporated in the 'backbone' of his theory of general relativity; *Einstein's Field Equations*[3] (EFE):

$$\boxed{E_{\alpha\beta} + \Lambda g_{\alpha\beta} = \frac{8\pi G}{c^4} T_{\alpha\beta}} \tag{2.9}$$

where its schematic form is

$$\begin{pmatrix} \text{a measure of local} \\ \text{spacetime curvature} \end{pmatrix} \quad = \quad \begin{pmatrix} \text{a measure of} \\ \text{mass-energy density} \end{pmatrix} \tag{2.10}$$

This tensor equation is equivalent to a set of ten scalar equations which describes the fundamental interaction of gravitation as a result of spacetime being warped by mass (i.e. all forms of energy).

The first term of (2.9), $E_{\alpha\beta}$, is the *Einstein tensor* which describes the gravitational fields, i.e. the spacetime curvature. It is *covariant* (i.e. the components changes with a change of basis from one coordinate system to another) and it is defined as

[2] [6] p. 174.
[3] [7] p. 180.

$$E_{\alpha\beta} \equiv R_{\alpha\beta} - \frac{1}{2}\mathrm{R}g_{\alpha\beta} \tag{2.11}$$

where $R_{\alpha\beta}$ is the *Ricci tensor*, $g_{\alpha\beta}$ is the metric tensor (2.1) and R is the *Ricci curvature scalar*.

The Ricci tensor is calculated from the *Riemann curvature tensor*[4]. Without going into details of differential geometry one can say that the Riemann curvature tensor is involved in the change in separation of neighbouring geodesics or, equivalently, the *tidal force* experienced by a rigid body moving along a geodesic. In other words, it has to do with the curving of spacetime. Its general expression is

$$R^{\alpha}_{\beta\gamma\delta} = \frac{\partial\Gamma^{\alpha}_{\beta\delta}}{\partial x^{\gamma}} - \frac{\partial\Gamma^{\alpha}_{\beta\gamma}}{\partial x^{\delta}} + \Gamma^{\alpha}_{\gamma\epsilon}\Gamma^{\epsilon}_{\beta\delta} - \Gamma^{\alpha}_{\delta\epsilon}\Gamma^{\epsilon}_{\beta\gamma} \tag{2.12}$$

which is a rank-four tensor given by the Christoffel symbols (2.8) and its derivatives. By a contraction, $R_{\alpha\beta} \equiv R^{\gamma}_{\alpha\gamma\beta}$, of this tensor the *Ricci tensor* follows;

$$R_{\alpha\beta} = \frac{\partial\Gamma^{\gamma}_{\alpha\beta}}{\partial x^{\gamma}} - \frac{\partial\Gamma^{\gamma}_{\alpha\gamma}}{\partial x^{\beta}} + \Gamma^{\gamma}_{\alpha\beta}\Gamma^{\delta}_{\gamma\delta} - \Gamma^{\gamma}_{\alpha\delta}\Gamma^{\delta}_{\beta\gamma} \tag{2.13}$$

which is a second rank symmetric tensor. Finally, using contraction on this Ricci tensor, we obtain the *Ricci scalar*

$$\mathrm{R} = g^{\alpha\beta}R_{\alpha\beta} \tag{2.14}$$

It assigns a single real number to each point in spacetime determined by the geometry near that point. This number represents the amount by which the volume of a geodesic ball deviates from that of a corresponding standard ball in flat space.

Now, the second term on the left of (2.9) represents the *cosmological constant* Λ. It is a type of *vacuum energy*, responsible for the observed accelerated expansion of the Universe. This vacuum energy is often given by its density ($\frac{kg}{m^3}$) and is defined as[5]

$$\rho_{\Lambda} = \frac{c^2\Lambda}{8\pi G} \tag{2.15}$$

[4] [5] p. 85.
[5] [5] p. 138.

where G is the gravitational constant. Note that in this thesis the dimension of Λ is defined as $[\Lambda] = 1/m^2$.

The right hand side of (2.9) is the *source* of spacetime curvature and represents the densities of energy and momentum. It is important to note that the famous equation $E = mc^2$ states the equivalence between mass and energy, and thus all forms of energy gravitate. The quantity $T^{\alpha\beta}$ is a second-rank symmetric tensor called the *energy-momentum-stress tensor* or, for short, the *energy-momentum tensor*. It describes the energy contents in the *cosmological fluid*, that is the gravitational sources responsible for the curvatures in the Universe. Its elements in general is

$$T^{\alpha\beta} = \begin{pmatrix} T^{00} & T^{01} & T^{02} & T^{03} \\ T^{10} & T^{11} & T^{12} & T^{13} \\ T^{20} & T^{21} & T^{22} & T^{23} \\ T^{30} & T^{31} & T^{32} & T^{33} \end{pmatrix} \tag{2.16}$$

where

$T^{00} = \rho =$ *mass-energy density* crossing a surface of constant time.
$T^{i0} = \pi =$ *momentum density* = momentum crossing a surface of constant time.
$T^{ii} = p =$ flux of force per unit area $> 0 \Rightarrow$ *pressure*.
$T^{ii} = p =$ flux of force per unit area $< 0 \Rightarrow$ *tension*.
$T^{ij} =$ *shear forces* for $i \neq j$.

This applies for an inertial frame of reference. That means the frame is stationary relative to a body moving at constant velocity and on which no force is being exerted.

2.1.4 Final words about GR

The theory of general relativity has now been introduced and with the goal of presenting its essence. It is a highly successful theory that so far has past all tests trying to disprove it. In physics we seek laws that can be written in an *invariant form* which means it is true for all observers. In this context tensors plays a key role because if a tensor equation is true in one coordinate system then it is true in all coordinate systems. This property can greatly simplify analysis by transforming the 'problem' to a coordinate system where the mathematics are easier. It has now been shown that Einstein's field equations (2.9), the 'backbone' of GR, is a tensor equation and thus possesses these advantages.

2.2 Basic Cosmology - The Homogeneous Isotropic Universe

"..the history of astronomy is a history of receding horizons."
-Edwin Hubble

Looking back on the scientific history of astronomy, as time has gone by, humanity have experienced the Universe to appear greater and greater. Our and the rest of Earth's place in the Universe has only been more and more negligible in line with the scientists harvesting more and more knowledge about it. This enormous work reveals the Universe to appear greater and more complex for each day.

The aim of cosmology, which is a subfield of astronomy, is to place all known physical phenomena within a single coherent framework. It is by far an ambitious goal with still significant gaps of knowledge to be filled. Albert Einstein himself failed this goal after working on it tirelessly in his last twenty years of life, and one can understand his motivation from what he said back then; "I want to know God's thoughts. The rest are details".

It is important to have in mind that despite much of the presented theory and equations of GR in chapter 2.1 not will be directly used in what follows (and in the rest of this thesis for that matter) one must be aware of that GR is the foundation of this cosmological theoretical framework. Any dynamical process taking place in the Universe, and not least those treated in this thesis, happens embedded in the fabric of spacetime described by GR.

In this section on basic cosmology, mainly what concerns this thesis will be presented. There will be some emphasis on the Friedmann equations because they are very central in the simulation of the spherical collapse model. Based on the derivation of them in this section is the appendix A (B.1) which further on change their variable dependency and perform modifications to them. These modified Friedmann equations have then been implemented in the program code.

This section with its subsections are based on the books [9], [6], [8], [7], [10], [11], [12], and [13].

2.2.1 The Cosmological Principle and the Copernican Principle

Principles are introduced in order to allow some progress to be made when one has no data to go on. Cosmology is no exception to this rule.

Einstein published his general theory of relativity in 1915 and almost immediately sought to exploit it to explain the large-scale behaviour of the Universe. No doubt is GR an elegant physical theory, but he was aware of the harsh truth that it involves some of the most difficult mathematics ever applied to a description of nature. He realized that to be able to make any progress he needed to assume that the Universe had some simplifying symmetry or uniformity. A smooth Universe on a grand scale appealed to him; if the Universe where the same everywhere he could set his wanted cosmological theory on a solid footing by allowing the distribution of matter to define a special reference frame that would help him deal with the effects of gravity.

Thus, Einstein decided to make the following simplifications on a *grand* scale:

- *The Universe is homogeneous - the same in every place.*
- *The Universe is isotropic - looks the same in every direction.*

(2.17)

These two assumptions together form the *Cosmological Principle*. But they are not equivalent even though they are related. Isotropy does not necessarily imply homogeneity without an additional assumption; that the observer is *not* in a special place. That is, if an observer is at the center of a spherical symmetric distribution of matter where the density decreases further away from the center it will appear isotropic but the whole distribution is *not* homogeneous. Nor homogeneity does necessarily imply isotropy. For example; a homogeneous universe which contracts in one space-dimension and expands in the other two space-dimensions is not isotropic.

A second important principle says:

- *We do not live in a special place in the Universe.*

(2.18)

This is called the *Copernican Principle* and is, at present time, a generalisation of its original meaning which displaced the Earth from the center of the Universe and replaced it with the Sun. Thus, observed isotropy together with the Copernican Principle implies the Cosmological Principle. The first and basic models of the Universe are fully based on these two principles.

2.2.2 Hubble's law

The general theory of relativity led to major developments in cosmological theory in the 1920s. But as in all fields of physics, new theories only gain acceptance when confirmed by experiments - and for the science of cosmology this means confirmation by observations.

The beginning of this chapter implied that Edwin Hubble was the man who discovered that the Universe is expanding. This was, and still is, a fact even though he misinterpreted the underlying physics of his observational data leading to this great discovery (ch. 2.2.3). He encapsulated this property of the Universe in one simple equation known as the *Hubble Law*:

$$v = H_0 d \tag{2.19}$$

Here v is the expansion velocity of the Universe (ch. 2.2.3), d is the distance to where this velocity is being measured and H_0 is the so called *Hubble constant*. Hubble derived this equation from his observational data. By plotting a graph of measured velocities and distances of galaxies he found it as a straight line. The slope of this line is the Hubble constant H_0. This implies that if two galaxies are being observed where one of them is twice as far away, this most distant galaxy will have twice the receding velocity than the other one. In other words, what Hubble discovered was that by looking in any direction in the Universe one will see that (almost) all galaxies are receding from us and with increasing speed as further away they are. However, he were not capable of explaining the true reason for this.

The Hubble constant at present time H_0 is defined as

$$H_0 \equiv H(t = t_0) \equiv \frac{\dot{a}(t_0)}{a(t_0)} \tag{2.20}$$

where a is the *scale factor* (ch. 2.2.4), t is the *cosmic time* (ch. 2.2.3), t_0 refers to the present cosmic time, and $\dot{a} \equiv \frac{da}{dt}$ is the time derivative of the scale factor. The Hubble constant $H = H(t)$ at any other time than present time is when $t \neq t_0$.

The definition (2.20) gives the connection of the Hubble constant to the geometry of spacetime. This is because it is the scale factor a which controls how the equations of motion of a certain universe model evolves (ch. 2.2.6). Note that the Hubble constant H_0 refers to the value measured at present time t_0. It is *not* a constant in time but a constant in the sense that it is the same at all points in the Universe for any given cosmic time t. In other words, it is being a number describing the expansion of the Universe from our perspective.

Hubble's constant (2.20) is quoted in units of $\frac{(km/s)}{Mpc}$ where Mpc is approximately three million light years. Because there is still uncertainties with this constant, a way to express it is

$$H_0 = 100h\frac{(km/s)}{Mpc} \tag{2.21}$$

where the common value for h used today is

$$h = 0.72 \pm 0.08 \tag{2.22}$$

which is also used in this thesis.

2.2.3 The expanding Universe and cosmic time

Expanding universe

How can Hubble's law (2.19) and its consequences be compatible with the Copernican Principle (2.18)? Which it is. The answer is that any other observer in any other place in the Universe will see the same as us; every galaxy is still moving away according to Hubble's law (2.19). The only way this can be the case is that the space of the Universe itself is expanding - and *not* the galaxies moving *through* the Universe.

The standard analogy to visualize this statement is to scale down the three expanding space-dimensions to a two-dimensional surface of a perfectly spherical balloon. By painting dots (representing galaxies) onto its surface and then inflate it more, one will observe that, from the perspective of *any* dot, all the other dots are moving away. Thus the separations between all of them increases uniformly in all directions. Note that it is important to be aware of that, in this analogy, the universe only constitute the *surface* of the balloon and thus has no center (as it would have if submerged in a three-dimensional space). That is, it exists and evolves in only two space-dimensions and one time-dimension.

This implies that every point in the Universe is equivalent as far as the expansion is concerned. Without further explanations the Hubble Law is then consistent with the Cosmological Principle (2.17).

Note that not everything takes part in the expansion. This include elementary particles, atoms, molecules, and greater things as elephants and buildings here on Earth. These are held together by the three other - much stronger - forces of nature (without necessarily asserting that gravity is a force, even though that is what the standard model of particle physics says). Likewise, objects in which gravity is dominant also resist the expansion, such as planets, stars, galaxies and massive clusters of galaxies. Some objects larger than this can too be bound, but not like individual galaxies are. However, their gravity may be strong enough to actually cause distortions of Hubble's Law (2.19) by perturbing the trajectories of objects in their vicinity which are following the so called *cosmic flow* caused by the expansion.

But on the largest scales of all, no forces are strong enough to counteract the global

tendency of the Universe to expand with the cosmic time. By ignoring all these 'local' perturbations, all matter is rushing apart from all other matter with a velocity described by Hubble's Law (2.19).

Cosmic time

Now, based on the explanation of the expanding Universe, it is appropriate to also explain the concept of *cosmic time*. It is a central quantity in the equations of motion of universe models which will be presented in chapter 2.2.6. A well known fact (at least for a physicist) is that SR and GR dramatically changed our perception of time and made it more difficult to grasp compared to its role in Newtonian mechanics. However, cosmic time for universe models is easy to understand:

> *The evolution of energy density is the same in the whole universe so this evolution can be thought of as a measure of time. This 'time' must therefore be the same everywhere and it is called the cosmic time t.* (2.23)

Thus, every spatial point in space has a "clock" and all these clocks are synchronized.

A more abstract explanation of cosmic time is; due to the nature of the four-dimensional spacetime one can imagine to slice it up in a line of three-dimensional spatial sections in which all of them are separated because they are all embedded in a higher dimensional room, i.e. spacetime. Each of the sections are labelled with a parameter t and each of these along the line are representing an increasing cosmic time. One can say that the time-dimension is orthogonal to the three space-dimensions.

2.2.4 The redshift and the scalefactor

Redshift

By utilizing spectroscopy Hubble obtained his law (2.19). Light from a galaxy is splitted up into its colour components and analysed separately. These components constitute a spectra which contains sharp features called emission lines and they occur at definite wavelenghts depending on the chemistry of the source. By comparing these lines with the positions they are supposed to have, Hubble observed that they were almost always shifted to the red end of the spectrum, i.e. towards longer wavelengths. He interpreted this as the well known *Doppler shift* and concluded that the light sources (galaxies) was moving away from him. This is the explanation behind the expression *redshift* and which is usually given the symbol z. A definition of redshift is:

Redshift z measures the fractional change in wavelength of an observed emission line relative to its expected position.	(2.24)

Redshift is an inevitably tool when dealing with distances in cosmology and will be frequently used in this thesis, especially with the numerical data presented in plots.

However, what was causing this redshift was not as obvious as Hubble first thought. It is not caused by the source moving away from the observer *through* space. Instead it moves away because *the space itself* between the source and observer is expanding (ch. 2.2.3). This is why his law is now taken to represent the expansion of the Universe. Himself never made this interpretation of his results.

Scalefactor

There is another way of picturing the effect of redshift (2.24). As explained in chapter 2.2.3, separation between any points in the Universe increases uniformly in all directions. If one imagine an elastic sheet of graph paper perfectly covering 'the balloon' (from this last chapter), then the regular grid on the paper at some particular time will look like a blown up version of the way it looked at an earlier time. It is intuitive that the symmetry of the situation is preserved and that is why one only needs to know the *factor* by which the grid has been expanded in order to recover the past grid from the later one.

Analogue to this modification of the balloon example is the universe that satisfies the Cosmological Principle (2.17). It preserves its symmetry as it expands in the same way everywhere and one only needs to know an overall scale factor to obtain a picture of its past physical conditions from present data. This factor, simply called the *scale factor*, is given the symbol a and its behaviour is governed by the *Friedmann equations* which will be presented in chapter 2.2.5.

The concept of the scalefactor a is easy to grasp and can be illustrated by a simple example: If the Universe has expanded by some factor between the emission of light from a galaxy and its detection at a telescope, the light waves would be stretched by the same factor as the scalefactor a during its travelling time through the intermediate space. If the Universe expanded by a scalefactor $a = 3$ then the wavelength would triple.

Comoving coordinates and physical Coordinates

The scalefactor a relates two different types of coordinates used in cosmology; the *comoving* coordinates and the *physical* coordinates. A given set of spatial comoving

coordinates $(r_x, r_y, r_z) \implies \boldsymbol{r} = r_x\hat{x} + r_y\hat{y} + r_z\hat{z}$ will remain the same during the evolution of the Universe. But a given set of spatial physical coordinates $(x, y, z) \implies \boldsymbol{x} = x\hat{x} + y\hat{y} + z\hat{z}$ will change corresponding to the evolution of the Universe. Their relation is

$$\boldsymbol{x} = a(t)\boldsymbol{r} \tag{2.25}$$

Cosmological redshift formula

Following from what have been said about wavelength, redshift and the scalefactor, their relations can be described in the *cosmological redshift formula*

$$1 + z \equiv \frac{\lambda_0}{\lambda} = \frac{a_0}{a} \tag{2.26}$$

where z is the redshift, and λ_0 and a_0 are the wavelength and the scalefactor at present time t_0, respectively. λ and a are the wavelength and the scalefactor at the time of emission, respectively.

2.2.5 The FLRW metric and the line element - the geometry of the Universe

It is the metric (2.1) that defines the geometry of a given spacetime. This whole chapter 2.2 deals with homogeneous and isotropic universes which satisfies the cosmological principle (2.17) and the Copernican principle (2.18). The metric which meets these principles is the *FLRW metric*.

The simplest edition of this metric is the *flat* FLRW metric

$$g_{\alpha\beta} = g_{\alpha\beta}(t) = \begin{pmatrix} -c^2 & 0 & 0 & 0 \\ 0 & a^2(t) & 0 & 0 \\ 0 & 0 & a^2(t) & 0 \\ 0 & 0 & 0 & a^2(t) \end{pmatrix} \tag{2.27}$$

where c is the speed of light, and $a(t)$ is the scalefactor as a function of cosmic time t. By using the formula for a general line element (2.4) one get the corresponding line element[6]

[6] [6] p. 368.

$$ds^2 = -c^2dt^2 + a^2(t)(dx^2 + dy^2 + dz^2) = -c^2dt^2 + dS^2 \tag{2.28}$$

which describes the geometry of the spacetime corresponding to a flat homogeneous isotropic cosmological model. The term dS is the part of the line element describing the geometry of the three-dimensional spatial section of the spacetime which also 'homogeneous and isotropic' refers to. Until further notice, by 'flat' means that the angles of a triangle, when submerged in this spatial section dS, will add up to exactly 180 degrees. So here this is the same as the well known euclidean space. Thus, each $t = constant$ implies $dt = 0$ which corresponds to a specific spatial section - also called a *spacelike surface* - described by dS as

$$ds^2 = 0 + a^2(t)(dx^2 + dy^2 + dz^2) = dS^2 \tag{2.29}$$

Here $a(t)$ provides the symmetrical *spatial* expansion as explained in chapter 2.2.4. Now, for a new infinitesimally increased cosmic time $t' > t$ new spatial coordinates (X, Y, Z) can be introduced as

$$\begin{aligned} & X = a(t')x, \quad Y = a(t')y \quad \text{and} \quad Z = a(t')z \\ \Rightarrow \quad & dX = x - X \quad dY = y - Y \quad \text{and} \quad dZ = z - Z \end{aligned} \tag{2.30}$$

Note that (x, y, z) and (X, Y, Z) are identical in a *comoving* coordinate frame following the symmetrical expansion of space, but they are different when representing *physical* coordinates because then the physical distance in space between them has really increased. Then from (2.30) the spatial line element (2.29) takes the form

$$dS^2 = dX^2 + dY^2 + dZ^2 \tag{2.31}$$

and thus describes the geometry in the new spatial section 'labeled' with the time t'.

As mentioned with the line elements (2.2) and (2.3) in the GR chapter, the particular line element (2.28) nor is unique. The same flat geometry can be represented by equivalent line elements using other coordinate systems through transformations. For example in spherical coordinates which gives

$$ds^2 = -c^2dt^2 + a^2(t)(dr^2 + r^2d\theta^2 + sin^2\theta d\phi^2) = -c^2dt^2 + a^2(t)dS^2 \tag{2.32}$$

corresponding to (2.3), but with the additional scale factor $a(t)$ multiplied with the spatial part dS.

Now, the flat FLRW metric does not represent the only homogeneous isotropic spacetime geometry. Any line element of the form

$$ds^2 = -c^2dt^2 + a^2(t)d\xi^2 \tag{2.33}$$

can be a homogeneous isotropic spacetime. That is if $d\xi$ is the line element of a time-independent homogeneous isotropic three-dimensional spatial space. Then (2.33) is known collectively as *FLRW metrics*. The flat FLRW metric (2.28) and (2.32) is one type, but there exists also two *curved* types. In this thesis one assumes that the Universe is perfectly flat so these two metrics will not be presented in details. It is sufficient to say that they represents two different spacetimes with *positive*- and *negative* curvature in their three-dimensional spatial surfaces, respectively. That is,

• *Positive curvature* - implies a *closed* universe model which means it has a final volume and the angles in a triangle adds up to *more* than 180 degrees inside its three-dimensional spatial surface. The analogy of this surface, with one less spatial dimension, is the surface of the familiar sphere submerged in a three-dimensional euclidean space.

• *Negative curvature* - implies an *open* universe model which means it has an infinite volume and the angles in a triangle adds up to *less* than 180 degrees inside its three-dimensional spatial surface. The analogy of this surface, with one less spatial dimension, is the surface of a saddle (with infinite extent) submerged in a three-dimensional euclidean space.

And for the universe model used in this thesis applies

• *Zero curvature* - implies an *open* universe model which means it has an infinite volume and the angles in a triangle adds up to exactly 180 degrees inside the spatial surface. The analogy of this surface, with one less spatial dimension, is just a normal sheet of paper (though with infinite extent) submerged in a three-dimensional euclidean space.

It is important to note that because these three models are homogeneous they require that the spatial curvature is the same at each point of these geometries. The corresponding line elements (the 'flat' one already shown in (2.28) and (2.32)) of these three metrics can be written in a unified form in spherical coordinates as[7]

[7] [6] p. 387.

$$\boxed{ds^2 = -c^2dt^2 + a^2(t)\Big[\frac{dr^2}{1-kr^2} + r^2(d\theta^2 + sin^2\theta d\phi^2)\Big]} \tag{2.34}$$

where $k = +1, -1$ and 0 implies open, closed, and flat universes, respectively. One sees that by substituting $k = 0$ the flat metric (2.32) follows. These spatial polar coordinates are comoving (see (2.25)) with *free reference particles* such as galaxies without any motion except that due to the expansion of the Universe itself. The time coordinate t is the cosmic time (2.23) which is the same as the *proper time* of the reference particles. This is the *FLRW line element*. All of the homogeneous and isotropic universe models can be represented by this.

About the flat universe model, which this thesis is based on, it is not necessary a simplification. The large amount of observational data so far indicates that it is the flat homogeneous isotropic model that most closely represent our Universe. Thus, the simplest model is also the most realistic and it is represented by the flat FLRW metric (2.32).

2.2.6 Foundation of the FLRW models - dynamics of the Universe

In order to describe how the Universe evolves, one need to know what is in it. For a homogeneous isotropic universe, the FLRW models assume a simple model for its contents. These contents constitute a certain *cosmological fluid* which can consists of three noninteracting components, or less, depending on the model. They have no heat conduction or viscosity and are therefore called *perfect fluids*.

Components of the Universe

• *Dust* - short hand for pressureless matter, which means *non-relativistic matter* and refers to any type of material which exerts negligible pressure ($p = 0$) and are sources to gravitational fields, i.e. both *baryonic*- and *dark* matter. In a universe consisting only of this dust and the fact that typical random motions of galaxies is $\sim 10^2$ km/s, gives a thermal energy (i.e. *kinetic* energy) much less than the *rest* energy ($E = mc^2$). Thus, the thermal energy, which causes pressure, can be neglected. The type of dust handled in this thesis is only cold dark matter (CDM).

• *Radiation* - includes the cosmic background photons and e.g. neutrino species with zero or sufficiently small rest masses so that they move relativistically today (i.e. the kinetic energy is much greater than the rest energy). Radiation is not handled in this thesis.

• *Dark energy* - its physical nature is so far unidentified. It can be the result of a new type of energy component or it can be interpreted as a modification of GR. Regardless, it is responsible for the observed accelerated expansion of the Universe. Note that dark energy is a general expression and for example the cosmological constant is a special form of dark energy. Dark energy is handled in this thesis.

What is crucial to know about the cosmological fluid, when it comes to describing the evolution of the Universe, is how its density ρ and pressure (or tension) p evolves with cosmic time t. This process is described by the *fluid equation*.

The fluid equation

The fluid equation can be derived by considering the first law of thermodynamics

$$dE + pdV = TdS \tag{2.35}$$

where E is the energy, p is the pressure, V is the volume, T is the temperature, and S is the entropy. For convenience the expanding volume V is given a *unit comoving* radius. By doing this the scalefactor a (ch. 2.2.4) represents the physical radius (ch. 2.2.5) with an arbitrary distance unit. Thus has the volume V a physical radius a and the energy E can be expressed as

$$E = V \cdot \rho c^2 = \frac{4\pi}{3} a^3 \rho c^2 \tag{2.36}$$

where ρc^2 is the energy density $[\frac{kgm^2}{s^2}]$ of the cosmic fluid and c is the light speed. The change of energy in a time dt is

$$\frac{dE}{dt} = 4\pi a^2 \rho c^2 \frac{da}{dt} + \frac{4\pi}{3} a^3 \frac{d\rho}{dt} c^2 \tag{2.37}$$

and the rate of change in volume V is

$$\frac{dV}{dt} = 4\pi a^2 \frac{da}{dt} \tag{2.38}$$

By assuming a *reversible adiabatic expansion* $dS = 0$, substitute (2.37) and (2.38) into (2.36), and rearranging gives

$$\boxed{\dot{\rho} = -3\frac{\dot{a}}{a}\left(\rho + \frac{p}{c^2}\right) \equiv -3H\left(\rho + \frac{p}{c^2}\right)} \tag{2.39}$$

where H is the Hubble constant (2.20). This is the *fluid equation* and it describes the change in the energy density of the cosmic fluid. The ρ term corresponds to the dilution in the density because the volume V grows bigger. The p-term corresponds to the loss of energy because the pressure of the fluid has done work as the Universe's volume increase. Thus the energy lost from this work has gone into *gravitational potential energy* because energy is always conserved.

So, the fluid equation (2.39) tells how the energy density ρ of the cosmic fluid evolves given that one knows how the scale factor $a = a(t)$ acts with cosmic time and what the pressure p is. These answers are given by the *Friedmann equations* and the *equation of state*, respectively, which now will be presented.

The Friedmann equations - Newtonian approach

It was not Einstein but the Russian physicist Alexander Friedmann who first developed mathematical models of an expanding universe from GR. These formed the basis of modern cosmology. His work was published in 1922 and the models are represented by the two *Friedmann equations* which describes the evolution of the Universe. To begin with, these equations can be derived in the frame of *Newtonian physics* to give a first impression and a more intuitive understanding of what they represents[8]. But there are problems with these derivations and they will be discussed during and after the derivation.

Consider the whole Universe as a *uniform spherical symmetric* cosmological fluid consisting *only* of classical mass with density ρ. Because of the cosmological principle (2.17) and the Copernican principle (2.18) any point can be its center. A test particle (ch. 2.1.2) with mass m and a physical distance r from the center, only feels a gravitational force from the fluid at smaller radii $r' = |\vec{r'}| < |\vec{r}|$. This part of the fluid has total mass

$$M = \frac{4\pi}{3} r^3 \rho \tag{2.40}$$

which contributing a gravitational force

$$F = -G\frac{Mm}{r^2} = -\frac{4\pi G}{3}\rho r m \tag{2.41}$$

[8] [10] p. 18-20.

directed inward toward the center. This gives the test particle a gravitational potential energy

$$U = -G\frac{Mm}{r} = \frac{4\pi G}{3}\rho r^2 m \tag{2.42}$$

and a kinetic energy

$$K = \frac{1}{2}m\dot{r}^2 \tag{2.43}$$

where $\dot{r} \equiv \frac{dr}{dt}$ means the (cosmic) time derivative. This is a dynamical system and thus by require energy conservation

$$E = K + U \tag{2.44}$$

for the test particle, where E is its total energy, and then substitute (2.42) and (2.43) for U and K in (2.44) gives

$$E = \frac{1}{2}m\dot{r}^2 - \frac{4\pi G}{3}\rho r^2 m \tag{2.45}$$

This equation represent the evolution of the physical separation r between the center and the particle. By considering a second test particle placed in the center the crucial step is now to realize that, because of the principles (2.17) and (2.18), this derivation applies to *any* two separated particles in the Universe. This allows one to use comoving coordinates

$$\boldsymbol{r} = a(t)\boldsymbol{x} \tag{2.46}$$

as presented in ch. 2.2.4, because the expansion is uniform. By substituting this for r in (2.45), remembering $\dot{x} = 0$ for comoving coordinates, gives

$$E = \frac{1}{2}m\dot{a}^2x^2 - \frac{4\pi G}{3}\rho a^2 x^2 m \tag{2.47}$$

Now, by multiplying each side by $\frac{2}{ma^2x^2}$ and rearranging the terms then gives

$$\frac{\dot{a}^2}{a^2} + \frac{kc^2}{a^2} = \frac{8\pi G}{3}\rho \tag{2.48}$$

where

$$k \equiv -\frac{2E}{c^2 m x^2} \tag{2.49}$$

The equation (2.48) is the *first Friedmann equation* given in Newtonian physics and it describes how the scalefactor a changes with cosmic time t. In GR the constant k corresponds to the three types of spacetime curvatures as presented in ch. 2.2.5 and (2.34), though this derivation is based on Newtonian physics and thus the spacetime is euclidean with no curvature. From its definition (2.49) one can only say that it is a constant and unchanging in both space and time because all its factors are constants in the evolution of a given universe model. That means any kind of universes must have a unique k because the constant factor E in (2.45) depends on the contents and density which defines the evolution and dynamics of the given universe.

Now, in this same physical system, one can instead of using energy conservation (2.44), start from *Newton's second law* (force = acceleration $\cdot$ mass) applied to the test particle which implies

$$m\ddot{r} = -G\frac{Mm}{r^2} \tag{2.50}$$

where $\ddot{r} \equiv \frac{d^2 r}{dt^2}$ is the acceleration of the physical separation of any two particles and the right hand side is the gravitational force F from (2.41). Then substitute (2.46) for r and (2.40) for M which results in

$$\frac{\ddot{a}}{a} = -\frac{4\pi G}{3}\rho \tag{2.51}$$

This is the *second Friedmann equation* given in Newtonian physics. Here $\ddot{a} \equiv \frac{d^2 a}{dt^2}$ is the acceleration of the scalefactor, i.e. this equation describes the *acceleration* of the evolution of a given universe model.

However, there are many problems with these derivations. It is assumed that spatial space is euclidean, and then it is not consistent to interpret k as spatial curvature (as already mentioned). It also turns out that the density ρ of the cosmological fluid needs to include more than the classical mass density. In addition it must have a term representing either *pressure* or *stress*, i.e. $\rho \longrightarrow \rho + \frac{3p}{c^2}$. The reason for this is that *all* forms of energy are sources to gravity according to the equivalence between mass and energy ($E = mc^2$) as mentioned in the GR chapter. A third problem is that it does not consider the fact that the Universe has an (positive) accelerated expansion, i.e. they do not include a dark energy component.

There are also other important points missing in this Newtonian approach, but the main message here is to illustrate that it is incomplete when it comes to describing nature. So, to get the correct Friedmann equations, i.e. in accordance with GR, one needs to derive them from Einstein's field equations (2.9).

The Friedmann equations - GR approach

The EFE with a cosmological constant Λ was given in (2.9) and (2.11) as

$$E_{\alpha\beta} + \Lambda g_{\alpha\beta} \equiv R_{\alpha\beta} - \frac{1}{2}\mathrm{R}g_{\alpha\beta} + \Lambda g_{\alpha\beta} = \frac{8\pi G}{c^4}T_{\alpha\beta} \tag{2.52}$$

To go from here one needs to specify the cosmic fluids described by the energy-momentum tensor (2.16) presented generally in ch. 2.1.3. Cosmic fluids which meets the physical conditions of the evolution of a FLRW universe model, i.e. which are encapsulated in the unified line element (2.34), is *perfect* fluids. They are characterized by their energy-mass density ρ and pressure (or tension) p. Measured in these fluids *rest frames*, their energy-momentum tensor[9] is

$$T_{\alpha\beta} = \Big(\rho + \frac{p}{c^2}\Big)u_\alpha u_\beta + p g_{\alpha\beta} \tag{2.53}$$

where u_α are the components of the 4-velocity and the metric $g_{\alpha\beta}$ in (2.1) are the FLRW metric implied by the FLRW line element (2.34). In a comoving *orthonormal* basis the metric $g_{\alpha\beta}$ is given as

$$g_{\hat{\alpha}\hat{\beta}} = \begin{pmatrix} -1 & 0 & 0 & 0 \\ 0 & 1 & 0 & 0 \\ 0 & 0 & 1 & 0 \\ 0 & 0 & 0 & 1 \end{pmatrix} \tag{2.54}$$

and the 4-velocity is $u^{\hat{\mu}} = (c, 0, 0, 0)$, thus the energy-momentum tensor (2.53) is given by

$$T_{\hat{\alpha}\hat{\beta}} = \begin{pmatrix} \rho c^2 & 0 & 0 & 0 \\ 0 & p & 0 & 0 \\ 0 & 0 & p & 0 \\ 0 & 0 & 0 & p \end{pmatrix} \tag{2.55}$$

[9] [8] p. 151.

It will now only be referred to a tedious calculation in book [7] by Øyvind Grøn on the pages 267-271, where the components of the Einstein tensor (2.11) is derived in an orthonormal basis $g_{\hat{\alpha}\hat{\beta}}$ for a FLRW universe model. That is, based on the FLRW line element (2.34) where its physical meaning was explained in ch. 2.2.5. The results is

$$E_{\hat{t}\hat{t}} = 3\frac{\dot{a}^2 + kc^2}{c^2a^2} \tag{2.56}$$

$$E_{\hat{i}\hat{i}} = -2\frac{\ddot{a}}{c^2a} - \frac{\dot{a}^2 + kc^2}{c^2a^2} \tag{2.57}$$

where the natural unit $c = 1$ is *not* in use here. Now there are explicit expressions for all three tensors in EFE (2.52). By substituting (2.56) and (2.57) for the Einstein tensor $E_{\alpha\beta}$, (2.54) for the metric $g_{\alpha\beta}$ and (2.55) for the energy-momentum tensor $T_{\alpha\beta}$ this gives

$$3\frac{\dot{a}^2 + kc^2}{c^2a^2} - \Lambda = \frac{8\pi G}{c^4}\rho c^2 \tag{2.58}$$

and

$$-2\frac{\ddot{a}}{c^2a} - \frac{\dot{a}^2 + kc^2}{c^2a^2} + \Lambda = \frac{8\pi G}{c^4}p \tag{2.59}$$

By moving Λ to the right hand side of (2.58) and then substituting one third of this side for the second term on the left hand side in (2.59) and then do some simple rearranging on both equations one ends up with

$$\boxed{\frac{\dot{a}^2}{a^2} + \frac{kc^2}{a^2} = \frac{8\pi G}{3}\rho + \frac{\Lambda c^2}{3}} \tag{2.60}$$

and

$$\boxed{\frac{\ddot{a}}{a} = -\frac{4\pi G}{3}\left(\rho + \frac{3p}{c^2}\right) + \frac{\Lambda c^2}{3}} \tag{2.61}$$

These are the Friedmann equations within the realm of GR. Note the dimensions in use here: $[\rho] = kg/m^3$, $[\Lambda] = 1/m^2$ and $[k] = 1/m^2$. A comparison of these two

with the other two Friedmann equations (2.48) and (2.51), derived with the Newtonian approach, shows

• *First Friedmann equation*: The constant k has now a defined physical meaning. It represents the curvature of spatial space. A factor $\frac{1}{c^2}$ in the second term on the RHS which takes into account the equivalence between mass and energy in GR, i.e. now the unit of ρ is *energy density* and not (Newtonian-) mass density. A new term $\frac{\Lambda}{3}$ on the RHS involving the cosmological constant which represents the accelerated expansion of the Universe.

• *Second Friedmann equation*: A new second term on the RHS involving p which represents pressure (or tension) in the cosmic fluid. A factor $\frac{1}{c^2}$ in the second and third term on the RHS which takes into account the equivalence between mass and energy in GR. A new term $\frac{\Lambda}{3}$ on the RHS involving the cosmological constant which represents the accelerated expansion of the Universe.

Note that in these new equations, (2.60) and (2.61), p or Λ can be zero, or *both* can be zero, depending on what kind of universe model one wish to describe. They are a generalisation of (2.48) and (2.51) derived from the realm of Newtonian physics.

Another important thing to note is that, despite the fact that the Friedmann equations are fundamental, they are of no use without the fluid equation (2.39). That is, (2.60) and (2.61) governs the time evolution of the scalefactor $a(t)$, and the fluid equation (2.39) governs the evolution of the mass-energy density $\rho(t)$ and the pressure (or tension) $p = p(\rho(t))$ of the cosmic fluid. These three equations are the foundation which to built universe models.

2.2.7 Crucial information from the cosmological fluid

As already mentioned, in order to discover how the Universe evolves, one needs to know what is in it. When this is clear one can extract crucial information about its evolution from its cosmological fluid.

Equation of state

To know the relationship between the energy-mass density ρ and the pressure-tension p is very important. From thermodynamics one knows that many of the properties of a low-density gas can be summarized in the *ideal gas law*

$$pV = Nk_BT \tag{2.62}$$

where p is the pressure, V is the volume, N is the particle number, k_B is the Boltzmann's constant, and T is the temperature. A rewriting of this is

$$p = \frac{Nk_BT}{V} = \frac{Nmc^2}{Vmc^2}k_BT = \frac{k_BT}{mc^2}\rho c^2 \tag{2.63}$$

where $\rho = \frac{Nm}{V}$ is the mass density of the gas and c is the light speed. Again, from thermodynamics, the kinetic energy of the gas particles are related to the gas temperature as

$$\frac{1}{2}m\langle v^2\rangle = \frac{3}{2}k_BT \quad \Leftrightarrow \quad m\langle v^2\rangle = 3k_BT \tag{2.64}$$

where $\langle v^2\rangle$ is the mean-square speed of the particles. By substituting (2.64) for k_BT in (2.62) gives

$$p = \frac{\langle v^2\rangle}{3c^2}\rho c^2 \equiv w\rho c^2 \tag{2.65}$$

This is the simplest *equation of state* and it is used much in cosmology. Note that ρ is the Newtonian mass density and thus ρc^2 is the mass-energy density. Also note that w can be negative but which seems impossible in this context. For example the ΛCDM universe model has $w = -1$. More on this in subsection 2.2.9 where this model is introduced.

The critical density and the density parameter

If the Universe is flat ($k = 0$), which means it has an euclidean spatial geometry, its cosmological fluid needs to meet a certain density. Starting out with the first Friedmann equation (2.60) the condition for this can be found by

$$\frac{\dot{a}^2}{a^2} + \frac{kc^2}{a^2} = \frac{8\pi G}{3c^2}\rho + \frac{\Lambda}{3} \quad \Longrightarrow \quad \frac{\dot{a}^2}{a^2} \equiv H^2 = \frac{8\pi G}{3c^2}\rho \tag{2.66}$$

where H is the Hubble constant, $k = 0$ as it has to be for a flat universe, and also $\Lambda = 0$ in this context. By rearranging (2.66) one get an expression for the mass-energy density

$$\rho = \frac{3H^2c^2}{8\pi G} \quad \Longrightarrow \quad \rho_c = \rho_c(t) = \frac{3H(t)^2c^2}{8\pi G} \tag{2.67}$$

where $[\rho_c] = \frac{J}{m^3} = \frac{kgm/s^2}{m^3} = \frac{kg}{s^2m}$. This density is the mass-energy density which the cosmological fluid needs to have for the Universe to be flat. It is called the *critical density*. Note that it is time dependent because the Hubble constant $H(t)$ is time dependent, as explained in chapter 2.2.2. Also note that the critical density is not necessary the true density, since the Universe need not to be flat.

A useful way of specifying the density of the Universe, i.e. each of the components (with the notation '*comp*') which constitute the cosmic fluid, is by introducing a certain parameter involving the critical density (2.67) which sets a natural scale for the density of the Universe. One can quote the density relative to the critical density and thus get a dimensionless quantity

$$\Omega_{comp}(t) \equiv \frac{\rho_{comp}(t)}{\rho_c(t)} \tag{2.68}$$

This is the *density parameter*. It can be used to rewrite the Friedmann equations in a very useful form, expressed in this *dimensionless* density parameter $\Omega(t)$ instead of the density $\rho(t)$. One particular benefit is that if $\Omega(t) = 1$, where $\Omega(t)$ is the sum of all the fractional parts relative to the critical density $\rho_c(t)$, one can immediately conclude that the corresponding universe model is flat. For example

$$\frac{\rho_{dust}(t)}{\rho_c(t)} + \frac{\rho_{radiation}(t)}{\rho_c(t)} \equiv \Omega_{dust}(t) + \Omega_{radiation}(t) = \Omega(t) = 1 \tag{2.69}$$

means that in a universe consisting only of dust and radiation their sum of densities equals accurately the critical density $\rho_c(t)$ at all cosmic times t. Thus this universe is flat at all t.

2.2.8 The EdS universe model

Finally, the basics for a general FLRW universe model are in place and thus the next step is to make specific models. This means finding *solutions* to the fluid equation (2.39), and the Friedmann equations (2.60) and (2.61). The simplest model is the matter dominated universe which is flat, consists only of dust, and is pressureless. This is the *Einstein - de Sitter* universe model (EdS). Note that in this thesis 'dust' will be referred to as *cold dark matter* (CDM).

From equation (2.69) this implies

$$\Omega_{dust} \equiv \Omega_{CDM} = \Omega_{CDM}(t) \equiv \Omega(t) = 1 \quad \Longrightarrow \quad \textit{flat} \text{ universe} \tag{2.70}$$

at any cosmic time t. That it has no pressure ($p = 0$) makes sense when considering the equation of state (2.65). The velocity v of the typical random motions of the dust particles (i.e. galaxies) are much less than the speed of light c. Thus $v^2/c^2 \approx 0 \Rightarrow w = 0 \Rightarrow p = w\rho c^2 = 0$. By substituting this $p = 0$ in the fluid equation (2.39) one gets

$$\dot{\rho} + 3\frac{\dot{a}}{a}\rho = 0 \quad \Rightarrow \quad \frac{1}{a^3}\frac{d}{dt}(\rho a^3) = 0 \quad \Rightarrow \quad \frac{d}{dt}(\rho a^3) = 0 \quad \Rightarrow \quad \rho a^3 = constant \tag{2.71}$$

This shows that the density gets diluted $\propto \frac{1}{a^3}$ which means it falls off in proportion to the expanding volume of this universe. Now, because the scalefactor usually is defined as $a(t_0) \equiv a_0 = 1$ at present cosmic time $t = t_0$ (ch. 2.2.4), this convention allows one to define the present density by $\rho(t_0) \equiv \rho_0$. This can be substituted for the constant in (2.71) which gives

$$\rho = \frac{\rho_0}{a^3} \quad \Longrightarrow \quad \rho(t) = \frac{\rho_0}{a^3(t)} \tag{2.72}$$

This equation describes how the CDM component evolves, and thus for the EdS universe, how the total cosmological fluid density $\rho(t)$ evolves with the universe model. That is, the fluid dilutes in proportion to the volume expansion represented by the scalefactor $a(t)$. But then one needs to know how the scalefactor $a(t)$ evolves with cosmic time t. In the EdS universe (flat and only filled with CDM) the first Friedmann equation is the same as (2.66). By substituting (2.72) in it this gives

$$\dot{a}^2 = \frac{8\pi G}{3c^2}\frac{\rho_0}{a} \tag{2.73}$$

Now, a power-law solution $a \propto t^{-q}$ as an 'educated guess' leads, through a short and simple calculation, to $q = \frac{2}{3}$, and so the solution is $a \propto t^{2/3}$. Because $a(t = t_0) \equiv a_0 = 1$ the full solution has to be

$$a(t) = \left(\frac{t}{t_0}\right)^{\frac{2}{3}} \tag{2.74}$$

This is how the scalefactor $a(t)$ for the EdS universe model evolves with cosmic time t. An important thing to note is that it will expand forever, but the expansion rate will always decrease and go to zero when time approach infinity. This is easy to see from the definition of the Hubble constant $H(t)$ in (2.20) when substituting (2.74) for a:

$$H(t) \equiv \frac{\dot{a(t)}}{a(t)} = \frac{2}{3t} \tag{2.75}$$

Thus, despite the pull of gravity from the dominating CDM, it is not able to recollapse this universe.

2.2.9 The ΛCDM universe model

The cosmological constant Λ is one of the most important and enigmatic objects in cosmology today. It can be positive or negative, but the positive case is much more commonly considered. This is because the observational data from the last decade is telling that the Universe has an accelerated expansion, i.e. $\ddot{a} > 0$, and that Λ, which is driving this acceleration, actually dominates the dynamics of the Universe. The data also indicates a flat geometry ($k = 0$), and in addition to Λ, a non-negligible dust component mostly in the form of CDM. This realistic model of the Universe is called the ΛCDM *universe model*.

To start with the component constituents, the observational data indicates that at *present time* t_0 approximately 70% of the Universe consist of Λ and 30% consist of CDM. Thus, the equation (2.69) says

$$\begin{aligned} \Omega_m(t_0) + \Omega_\Lambda(t_0) = 0.7 + 0.3 = \Omega(t_0) = \Omega_0 = 1 \\ \implies \quad \textit{flat} \text{ universe} \end{aligned} \tag{2.76}$$

and also at *any* time t

$$\Omega_m(t) + \Omega_\Lambda(t) = \Omega(t) = 1 \quad \implies \quad \textit{flat} \text{ universe} \tag{2.77}$$

Note that m is short for CDM in the subnotation. This means that in the past ($t < t_0$) the CDM density $\rho_m(t)$ was *greater* than the Λ density $\rho_\Lambda(t) = \textit{constant}$ because $\rho_m(t) \propto \frac{1}{a(t)^3}$. But their respective density parameters always added up to 'one' and thus the Universe has been flat at all times.

The constant Λ, can be described as if it where a *fluid* with energy density $\rho_\Lambda c^2$ and pressure p_Λ. This energy density was presented in equation (2.15) reproduced here:

$$\rho_\Lambda = \frac{c^2\Lambda}{8\pi G} \tag{2.78}$$

To describe how the cosmological fluid of the ΛCDM universe evolves, only a small modification to the density evolution (2.72) for the EdS universe is needed. As presented, the ΛCDM universe consists of only one additional energy content to the EdS universe which is the constant dark energy density $\rho_\Lambda c^2$ (2.78). Note that it is a true constant, e.g. not like the Hubble constant $H_0 = H_0(t)$. That is, it is a constant *independent* of cosmic time t. Thus, the evolution of the cosmic fluid density $\rho(t)$ in a ΛCDM universe is a modification of (2.72) and it says

$$\rho(t) = \frac{\rho_0}{a^3(t)} \quad \longrightarrow \quad \rho(t) = \frac{\rho_m(t_0)}{a^3(t)} + \rho_\Lambda \tag{2.79}$$

where $\rho_m(t_0)$ is the present time ($t = t_0$) density of the CDM and $\rho_\Lambda \equiv \rho_\Lambda(t_0) =$ *constant*. As for the EdS model, the fluid dilutes in proportion to the volume expansion represented by the scalefactor $a(t)$. Again one needs to know how the scalefactor $a(t)$ evolves with cosmic time. This expression for $a(t)$ demands some tedious calculations and its derivation will only be referred to the compendium 'Cosmology I' by Øystein Elgarøy [11] page 37-39. The result is

$$a(t) = \Big(\frac{\Omega_{m0}}{\Omega_{\Lambda 0}}\Big)^{1/3}\Big[\sinh\Big(\frac{3}{2}\sqrt{\Omega_{\Lambda 0}}H_0 t\Big)\Big]^{2/3} \tag{2.80}$$

where $a(t = t_0) \equiv a_0$ is given as 1. From the same pages also an expression for the cosmic time t in this model is given. It says

$$t = \frac{2}{3H_0\sqrt{\Omega_{\Lambda 0}}}\sinh^{-1}\Big[\Big(\frac{a}{a_\Lambda}\Big)^{\frac{3}{2}}\Big] \tag{2.81}$$

where a_Λ is a constant value of the scale factor which represent the scale of the Universe when $\Omega_m(t) = \Omega_\Lambda(t)$, i.e. at the cosmic time when the density of the cosmological constant Λ begins to be greater than the density of the CDM. Without going into the details on these pages, this equation gives, when using todays best data for H_0 and $\Omega_\Lambda(t_0)$, the age of the Universe to be $t = t_0 \approx 13.5$ billion years which turns out to be consistent with the age of the oldest observed objects in the Universe.

By substituting a_Λ with a in (2.81) another interesting age reveals itself; the time $t = t_\Lambda \approx 9.8$ billion years. It indicates *when* the accelerated expansion begun. Hence in this realistic (i.e. consistent with observations) ΛCDM universe model the Universe has had an accelerating expansion for the last ~ 3.7 billion years. Now, this accelerating expansion ($\ddot{a} > 0$), which is the effect of Λ, can be outlined from the second Friedmann equation (2.61) as

$$\frac{\ddot{a}}{a} = -\frac{4\pi G}{3c^2}\Big(\rho_m + \frac{3p_\Lambda}{c^2}\Big) + \frac{\Lambda}{3} \tag{2.82}$$

In this equation, a positive cosmological constant Λ must contribute to a positive accelerated scale factor $\ddot{a}$. This implies that Λ acts effectively as a *repulsive* force and if it is sufficiently large, it can overcome the gravitational *attraction* (represented by the first term $-\frac{4\pi G}{3c^2}\rho_m$) and then lead to an accelerated expansion.

In order to determine the effective pressure p_Λ corresponding to Λ one consider the fluid equation (2.39) and substitute the ρ with $\rho_\Lambda = \textit{constant}$ and p with p_Λ. This gives

$$\dot{\rho}_\Lambda + 3\frac{\dot{a}}{a}\Big(\rho_\Lambda + \frac{p_\Lambda}{c^2}\Big) = 0 \quad \Longrightarrow \quad \Big(\rho_\Lambda + \frac{p_\Lambda}{c^2}\Big) = 0 \tag{2.83}$$

and then

$$p_\Lambda = -\rho_\Lambda c^2 \tag{2.84}$$

This is the equation of state for the ΛCDM model and it is a specification of the general *equation of state* (2.65). One sees that the cosmological constant Λ has a *negative* effective pressure p_Λ because w is here derived to be $w = -1$. Note that this negative value of w is impossible to explain in the realm of Newtonian physics when it was derived in chapter 2.2.7 to be $w \equiv \frac{\langle v^2 \rangle}{3c^2} > 0$. By 'negative effective pressure' it is meant that as the Universe expands, work is done on the cosmic fluid. This permits its energy density ρ_Λ to remain constant even though the volume of the Universe is increasing.

2.2.10 A short summary

The theory of basic cosmology needed for this thesis has now been introduced with the aim of laying down a foundation for building upon more complex theories when, from the next chapter, we start to consider a universe that is not so smooth after all. It is important to remember that beneath this basic cosmological foundation lies the theory of general relativity.

Chapter 3

The Inhomogeneous Universe

"..who are we? We find that we live on an insignificant planet of a humdrum star lost in a galaxy tucked away in some forgotten corner of a universe in which there are far more galaxies than people."
-Carl Sagan

In the preliminary section 2.2, a 'homogeneous and isotropic' universe was presented and it contained a perfectly smooth cosmological fluid. By the fact that we exists it fails to describe the real Universe accurately and can thus only serve as an approximation. This is because the real Universe is lumpy, i.e. it is *inhomogeneous*. Its cosmological fluid is full of lumps as for example stars and galaxies.

This chapter discusses how structures in the Universe develops from tiny lumps, i.e. small density imperfections in the early cosmic fluid, to become gravitational bound objects on different size scales that we observes today.

3.1 Large-Scale Structures in the Universe - A short introduction

This section is based on [9]. Galaxies are the basic building blocks in cosmology. They tend not to be isolated, but like to band together and the way they are distributed over cosmological distances is termed *large-scale structure*.

Other terms included in this are such as *galaxy cluster* which is used to describe a physical aggregation of galaxies and can be systems of greatly varying size and richness. A *small galaxy cluster* can consists of as few as 30 galaxies and at the other extreme there are the *rich galaxy clusters* which can contain many thousands of galaxies in a region just a few million light years across (the Milky Way is about 100 000 light years across). In between these two extremes, galaxies appear to be distributed in systems of varying density in a roughly hierarchical manner.

Individual galaxy clusters are not the largest structures to be seen. The distribution of galaxies on scales larger than 30 million light years reveals a wealth of complexity where they are not simply distributed in quasi-spherical *blobs* (a group that lacks definite shape) but can also lie in extended quasi-linear structures called *filaments* (like a heated glowing wire), or flattened sheet-like structures (a roughly two-dimensional concentration of galaxies). These structures can contain $\sim 10^{16}$ solar masses.

Even greater structures exist. The rich clusters themselves are clustered into enormous loosely bound *agglomerations* (a state of being collected in a mass) called *superclusters*. They can contain from ten rich clusters to more than fifty and can have sizes as large as 300 million light years (the observable universe is $\sim$ 14000 million light years), containing as much as $\sim 10^{17}$ solar masses.

The structures now presented are complemented by vast nearly empty regions, many of which appear to be roughly spherical. These so called *voids* contain fewer galaxies than average, or even no galaxies at all, and appears on scales up to 200 million light years. Their existence is not surprising, given the existence of clusters and superclusters, because it is necessary to create regions of less than average density for there to be regions of greater than average density.

These voids and lumps which constitutes these large-scale structures can be illustrated with 2- and 3-dimensional maps from redshift observation and created in computer simulations. They look like something which is called a *cosmic web*; a vast complex 3-dimensional network of intersecting chains and sheets. A simplified way to describe how 'parts' of this complexity arise will be presented, to some extent, in this chapter.

3.2 Linear Perturbations in the Cosmic Fluid

The homogeneous isotropic universe and its corresponding Friedmann equations from section 2.2 provides important insights into how the bulk properties of the Universe change with time. But, as already mentioned, they describe an idealized world that is perfectly smooth without any lumps and thus must be unrealistic. A universe that starts out like that will remain perfectly smooth forever. Thus, in a realistic situation, there will always be *imperfections* all the way from 'the beginning'.

These imperfections in the cosmic fluid starts out like 'seeds' called *primordial density perturbations* from where the densities starts to grow. Such a denser piece of the Universe exerts a stronger gravitational pull on its surroundings than what an average corresponding piece will do. It will therefore attract material in, and depleting its neighbourhood. This effect is a runaway growth of the cosmic lumpiness and is called *gravitational instability*. Eventually strongly bound lumps form and begin to collect into galaxy clusters, filaments and sheets (ch. 3.1). A major challenge in cosmology is to understand how the imperfections grows and become all these structures one sees in the Universe today[1].

3.2.1 The density contrast

Density perturbations in the the cosmic fluid are commonly characterized by the *density contrast*. Its definition is given as[2]

$$\Delta(\boldsymbol{x},t) \equiv \frac{\rho(\boldsymbol{x},t)-\rho_b(t)}{\rho_b(t)} \equiv \frac{\delta\rho(\boldsymbol{x},t)}{\rho_b(t)} \tag{3.1}$$

where $\boldsymbol{x}=(x,y,z)$ represent spatial coordinates, $\rho_b(t)$ is the average *background density* at cosmic time t and $\rho(\boldsymbol{x},t)$ is the *local density* at point $\boldsymbol{x}$ at the same cosmic time t as the background density.

This density contrast $\Delta(\boldsymbol{x},t)$ will divide the Universe into two regions

$$\begin{aligned} &\bullet\ \Delta(\boldsymbol{x},t)>0 \quad\Longrightarrow\quad \text{the cosmic fluid is } \textit{overdense}. \\ &\bullet\ \Delta(\boldsymbol{x},t)<0 \quad\Longrightarrow\quad \text{the cosmic fluid is } \textit{underdense}. \end{aligned} \tag{3.2}$$

[1] This introduction was based on [9].
[2] [11] p. 119.

Thus the density will *grow* where the density contrast is positive and the density will continue to be *diluted* where the density contrast is negative. Another important thing to note about the value of the density contrast is

- If $0 < \Delta(\boldsymbol{x}, t) < 1$: The inhomogeneities are in the *linear regime*, and the gravitational instability is very weak. Thus *linear* perturbation theory can be used.

- If $\Delta(\boldsymbol{x}, t) > 1$: The inhomogeneities are in the *nonlinear* regime, the gravitational instability is strong and the inhomogeneity are starting to collapse and form gravitationally bound structures. *Nonlinear* perturbation theory must be used. (3.3)

3.2.2 Dynamics of linear perturbations

This subsection is based on [14] p. 460-464 and [11] p. 120-127. Much of the essential physics of linear perturbations (3.3) in the cosmological fluid can be extracted from a Newtonian approach and not involve GR. One reason for this is that small perturbations imply weak gravitational fields. Though a prerequisite is that the evolution of perturbations studied is on scales smaller than the *particle horizon*, i.e. the observable Universe, and that only speeds much less than the light speed are involved. Thus the types of cosmological fluids discussed in the following are so called *non-relativistic fluids*. Note that this thesis mainly considers the nonlinear regime, so a full derivation of the equation that describes the density evolution *before* the density contrast Δ gets bigger than one, will not be given. However, a brief review is appropriate.

The simplest situation to consider is a universe with only one component. The equations describing its corresponding cosmic fluid are called the *fluid equations* (or the *Euler equations*) and are given as

$$\begin{aligned} \tfrac{\partial \rho}{\partial t} + \nabla \cdot (\rho \boldsymbol{v}) &= 0 \\ \tfrac{\partial \boldsymbol{v}}{\partial t} + (\boldsymbol{v} \cdot \nabla)\boldsymbol{v} &= -\tfrac{1}{\rho}\nabla p - \nabla \phi \\ \nabla^2 \phi &= 4\pi G \rho \end{aligned} \tag{3.4}$$

where ρ is the density, $\boldsymbol{v} = v_x\hat{x} + v_y\hat{y} + v_z\hat{z}$ is the velocity field, p is the pressure and ϕ is the gravitational potential. And for the following derivations, the del operator ∇, the time partial derivative $\frac{\partial}{\partial t}$, and the operator $(\boldsymbol{v} \cdot \nabla)$ is given in *Cartesian coordinates* as

$$\begin{gathered}\nabla \equiv \frac{\partial}{\partial x}\hat{x} + \frac{\partial}{\partial y}\hat{y} + \frac{\partial}{\partial z}\hat{z} \\ \frac{\partial}{\partial t} = \frac{d}{dt} - (\boldsymbol{v} \cdot \nabla) \\ (\boldsymbol{v} \cdot \nabla) = v_x \frac{\partial}{\partial x}\hat{x} + v_y \frac{\partial}{\partial y}\hat{y} + v_z \frac{\partial}{\partial z}\hat{z}\end{gathered} \tag{3.5}$$

The form of the fluid equations (3.4) has *Eulerian coordinates*. In these coordinates the partial derivatives ($\frac{\partial}{\partial t}$) describes time variations in the respective quantities at a fixed spatial point in the Universe.

By using (3.5) these equations can be written in another form where one follows the motion of a particular fluid *element*. This is called the *Lagrangian description*[3] of a fluid and the corresponding fluid equations takes the form

$$\begin{gathered}\frac{d\rho}{dt} = -\rho(\nabla \cdot \boldsymbol{v}) \\ \frac{d\boldsymbol{v}}{dt} = -\frac{1}{\rho}\nabla p - \nabla\phi \\ \nabla^2\phi = 4\pi G\rho\end{gathered} \tag{3.6}$$

and will be the form used in the following. These equations has *solutions* and will be called $\boldsymbol{v} = \boldsymbol{v}_0$, $\rho = \rho_0$, $p = p_0$ and $\phi = \phi_0$, which together with (3.6) represents a perfectly smooth fluid, i.e. no lumps involved. To introduce inhomogeneities one add small perturbations to the solutions

$$\begin{gathered}\boldsymbol{v} = \boldsymbol{v}_0 + \delta\boldsymbol{v} \\ \rho = \rho_0 + \delta\rho \\ p = p_0 + \delta p \\ \phi = \phi_0 + \delta\phi\end{gathered} \tag{3.7}$$

Because this is about the linear regime (3.3), these perturbations is assumed to be sufficiently small so that when substituting them into their respective equations in (3.6), an expansion of these to *first* order is enough. Furthermore, it is assumed that the unperturbed pressure solution p_0 is homogeneous, i.e. $\nabla p_0 = 0$. With these assumptions now presented, the *linearized* fluid equations can be derived from (3.6) with the perturbed quantities (3.7). Then by referring to some tedious calculations in the compendium [11] p. 122-123, the results are

[3] [14] p. 462.

$$\frac{d}{dt}\left(\frac{\delta\rho}{\rho_0}\right) = -\nabla\cdot\delta\boldsymbol{v}$$

$$\frac{d}{dt}\delta\boldsymbol{v} + (\delta\boldsymbol{v}\cdot\nabla)\boldsymbol{v}_0 = -\frac{1}{\rho_0}\nabla\delta p - \nabla\delta\phi \tag{3.8}$$

$$\nabla^2\delta\phi = 4\pi G\delta\rho$$

These are thus the *linearized* equations describing how the perturbations evolve with cosmic time t.

The perturbations are supposed to evolve, i.e. getting denser, inside the uniformly expanding background universe, so it is convenient to change from physical coordinates $\boldsymbol{x}$ to comoving coordinates $\boldsymbol{r}$. Their relation was given in equation (2.25) and are reproduced here:

$$\boldsymbol{x} = a(t)\boldsymbol{r} \tag{3.9}$$

where $a(t)$ is the background scalefactor. This change gives a perturbed expression $\delta\boldsymbol{x}$ for the physical coordinates

$$\delta\boldsymbol{x} = \delta[a(t)\boldsymbol{r}] = \boldsymbol{r}\delta a(t) + a(t)\delta\boldsymbol{r} \tag{3.10}$$

and the effect on the velocity field

$$\boldsymbol{v} \equiv \frac{\delta\boldsymbol{x}}{\delta t} = \boldsymbol{v}_0 + \delta\boldsymbol{v} = H\boldsymbol{x} + a(t)\boldsymbol{u} \tag{3.11}$$

where $H = H(t)$ is the Hubble constant and $\boldsymbol{u}$ has the definition

$$\delta\boldsymbol{v} = a(t)\frac{\delta\boldsymbol{r}}{\delta t} \equiv a(t)\boldsymbol{u} \tag{3.12}$$

Here $\boldsymbol{u} \equiv \frac{\delta\boldsymbol{r}}{\delta t}$ is, by considering (3.11), a velocity and describes the *deviations* from the *smooth* Hubble expansion (ch. 2.2.2) represented by $H\boldsymbol{x}$. This deviation velocity $\boldsymbol{u}$ is called *peculiar velocity*.

More tedious calculations now follows in [11] p. 123-125. Here the del operator ∇ with physical coordinates is replaced with a corresponding del operator ∇_c which use comoving coordinates. Their relation is

$$\nabla = \frac{1}{a}\nabla_c \tag{3.13}$$

where the notation c denotes 'comoving'. The calculation starts out with the second equation in (3.8) and uses the rest of the equations (3.9) - (3.13) together with the rest of the two equations in (3.8). The final result is

$$\boxed{\frac{d^2\Delta}{dt^2} + 2\frac{\dot{a}}{a}\frac{d\Delta}{dt} = \frac{c_s^2}{\rho_0 a^2}\nabla_c^2\delta\rho + 4\pi G\rho_0\Delta} \tag{3.14}$$

where $\Delta \equiv \frac{\delta\rho}{\rho_0}$ is the density contrast (3.1), ρ_0 is the smooth unperturbed background density, $\dot{a} \equiv \frac{da}{dt}$ and c_s is the sound speed in the fluid and originates from the relation

$$\delta p = c_s^2\delta\rho \tag{3.15}$$

which applies to an *adiabatic* system where δp is the pressure perturbation and $\delta\rho$ is the density perturbation. Thus, equation (3.14) describes the linear time evolution of a small density perturbation in the cosmological fluid, i.e. how the density evolution was *before* the upcoming lumps got to be distinct gravitationally bound objects and *before* their density contrasts $\Delta(\boldsymbol{x}, t)$ became bigger than one (3.3). Note that from (3.15) zero pressure $p = 0$ implies zero sound speed $c_s = 0$ and then the second term on the right hand side disappears.

3.3 Nonlinear Perturbations in the Cosmic Fluid - The Spherical Collapse Model

The previous chapter 3.2 presented a way to describe the evolution of perturbations in the linear regime (3.14), i.e. when the density contrast $\Delta(\boldsymbol{x}, t)$ was greater than zero but less than one. When doing this, one of the tasks of cosmology is to confront the predictions with observational data, but a problem is that the objects observed today are the results of *nonlinear* evolution of perturbations. For example galaxy clusters are thousands of times denser than the background density ρ_b, and galaxies themselves have densities a million times this average. It is therefore critical to understand the evolution that continues *after* the linear description breaks down, i.e. when $\Delta(\boldsymbol{x}, t) > 1$ and $\Delta(\boldsymbol{x}, t) >> 1$.

So one needs to understand the process that created the structures of todays observed galaxies and galaxy clusters etc. to be able to test theories in the linear regime. This can only be done by *nonlinear* theories. The most realistic alternative among these are a brute force method called *N-body simulations* done on computers. This is done by numerical integration of the equations of motion for a large number of particles which are given small initial perturbations. Nevertheless, it is essential to develop other more intuitive nonlinear theories which are used for understanding the results of the N-body simulations and also to understand observational data. The simplest of these nonlinear theories is *The Spherical Collapse Model*.

3.3.1 The spherical collapse model

This subsection is based mainly on Padmanabhan [15] p. 273-277 and Peacock [14] p. 488. Nonlinear evolution of perturbations can be studied analytically if some simplifying assumptions are made, and the spherical collapse model is a theory that handles this.

Consider the density contrast $\Delta(\boldsymbol{x}, t_i)$ at some initial time $t = t_i$. It will divide the universe into overdense ($\Delta > 0$) and underdense ($\Delta < 0$) regions. The overdense mass concentrations are separated systems where each will generate a self-gravity which works *against* the expansion of the Universe and thus expand at a progressively slower rate compared to the background universe. At some point the density contrast of the system will be sufficiently big to generate a gravitational potential which *disentangling* it from the rest of the expanding universe. It has then made itself into a sort of a closed *sub-universe*.

Now, provided that this sub-universe is shaped as a sphere with *spherical symmetry*,

the following apply: According to the so called *Birkhoff theorem*[4] in GR, the metric and the equations of motion of a *freely falling test particle* (ch. 2.1.2) inside it are independent of what is happening outside it and the sub-universe are therefore itself a homogeneous isotropic universe, described by a FLRW metric (2.34). This is crucial to understand, because it means that this sub-universe can be described by the same set of equations of motion as the background universe, i.e. the same Friedmann equations (2.60) and (2.61), solved by its *own* scalefactor $a_s(t)$. Here the s-notation stands for 'sphere'. Note that the cosmic time t is still the same for both.

The details of the above collapsing process depends on the initial density profile which means - *how strong the initial density perturbation is decides how fast it will evolve.* For the spherical collapse model, the density distribution has a *spherical symmetry* about some point and this sphere is considered to be on scales much less than the particle horizon, i.e. much less than the observable Universe.

Derivation

Firstly, the derivation of the spherical collapse model is done by considering the sphere inside a universe with no dark energy. Secondly, as mentioned above, the sphere which is a sub-universe, is a universe in its own right and with its own scalefactor a_s. Analog with (3.9) the relation between its comoving coordinate $\boldsymbol{r}_s$ and physical coordinates $\boldsymbol{x}_s$ is

$$\boldsymbol{x}_s = a_s(t)\boldsymbol{r}_s \tag{3.16}$$

and its *physical radial* coordinate R, given as a *scalar* because of the spherical symmetry of the system, is defined as

$$R \equiv |\boldsymbol{x}_s| = a_s(t)|\boldsymbol{r}_s| = a_s(t)r_s \tag{3.17}$$

The sphere has an initial density (sub-notation 'i') distribution

$$\rho_s(R, t_i) = \rho_b(t_i) + \delta\rho(R, t_i) = \rho_b(t_i)[1 + \Delta_i(R)] \tag{3.18}$$

where $\rho_b(t_i)$ is the background density, $\delta\rho(R, t_i)$ is the density perturbation that gives the sphere its *additional* density, and $\Delta_i(R) \equiv \Delta(R, t_i)$ is the initial density contrast which is a function of the radius R.

[4] [16] p. 421.

Because $R = R(t_i)$ is taken to be much smaller than the observable universe and the gravity at work is still relatively small (though bigger than in the regime of linear evolution of perturbations), the dynamics of the sphere can be studied in the Newtonian limit and thus utilizing Newtonian physics, again not to be worried about GR. With this in mind the derivation can continue.

The *gravitational potential* ϕ_s of the sphere determines its dynamics and is given as

$$\begin{aligned}\phi_s(R,t) = \phi_b(R,t) + \delta\phi(R,t) &= -\tfrac{1}{2}\left(\tfrac{\ddot{a}}{a}\right)R^2 + \delta\phi(R,t) \\ &= \tfrac{2\pi}{3}G\rho_b(t)R^2 + \delta\phi(R,t)\end{aligned} \tag{3.19}$$

where $\phi_b(R,t)$ is the gravitational potential generated from the background density $\rho_b(t)$, $\delta\phi(R,t)$ is the gravitational potential generated by the additional density $\delta\rho(R,t)$, i.e. it is an effect of the density perturbation, and $a = a(t)$ is the background scale factor. The equality $-\frac{1}{2}\left(\frac{\ddot{a}}{a}\right) = \frac{2\pi}{3}G\rho_b$ is due to Friedmann's second equation (2.61) for the EdS universe.

The motion of a thin *shell* of particles located at a distance R from the center of the sphere is governed by the equation of motion

$$\frac{d^2\boldsymbol{R}}{dt^2} = -\nabla\phi_s \tag{3.20}$$

Because of the spherical symmetry, $\boldsymbol{R} \to R$ and $\nabla \to \frac{\partial}{\partial R}$, and thus when substituting (3.19) in (3.20) the result becomes

$$\frac{d^2R}{dt^2} = -\frac{\partial\phi_s}{\partial R} = -\frac{4\pi}{3}G\rho_b(t_i)R_i - \frac{\partial\delta\phi}{\partial R} = -\frac{GM_b(R_i,t_i)}{R_i^2} - \frac{G\delta M_b(R_i,t_i)}{R_i^2} \tag{3.21}$$

where $M_b(R_i,t_i)$ is the non-perturbed *part* of the mass inside the sphere given by the homogeneous background density $\rho_b(t_i)$ at a certain initial cosmic time $t = t_i$ and a certain initial physical radial coordinate $R(t_i) \equiv R_i$ of the sphere. Thus

$$M_b(R_i,t_i) = \frac{4\pi}{3}\rho_b(t_i)R_i^3 \equiv \frac{4\pi}{3}\rho_b(t_i)|\boldsymbol{x}_s(t_i)|^3 = \frac{4\pi}{3}\rho_b(t_i)a_s^3(t_i)|\boldsymbol{r}_s|^3 = constant \tag{3.22}$$

Before going further, one needs to specify the general expression for the density contrast (3.1) for this nonlinear model, and it is

$$\Delta(\boldsymbol{x},t) \;\longrightarrow\; \Delta(R_i,t_i) \equiv \frac{(\rho_b(R_i,t_i)+\delta\rho_b(R_i,t_i))-\rho_b(t_i)}{\rho_b(t_i)} = \frac{\rho_s(R_i,t_i)-\rho_b(t_i)}{\rho_b(t_i)} \quad (3.23)$$

which is for a specific initial cosmic time $t = t_i$. Note that the initial density of the sphere is $\rho_s(R_i,t_i) = \rho_b(R_i,t_i) + \delta\rho_b(R_i,t_i)$, where $\delta\rho_b(R_i,t_i)$ is a small initial density perturbation in the background density $\rho_b(R_i,t_i)$ such that $\rho_s(R_i,t_i) \gtrsim \rho_b(R_i,t_i)$. The density contrast for $t > t_i$ is then

$$\Delta(R,t) \equiv \frac{\rho_s(R,t)-\rho_b(t)}{\rho_b(t)} \quad (3.24)$$

where $R = R(t)$.

For a spherically symmetric density distribution, the gravitational force on *any* shell of the sphere depends only on the excess mass δM contained *inside* the shell. This mass is given as

$$\delta M(R,t) = 4\pi \int_0^R \delta\rho_b(q,t)q^2dq = 4\pi\rho_b(t)\int_0^R q^2\Delta(q,t)dq \quad (3.25)$$

where R is the physical radial coordinate (3.17), $\delta\rho_b$ is the excess density inside the shell (i.e. the density perturbation in the background density ρ_b), and Δ is the density contrast (3.24).

A simplification to this analytical derivation is an assumption that all the shells *do not cross* each other during their dynamical evolution. That is, if the shells are initially labeled with their corresponding physical radius, $R_1 < R_2 < R_3 \cdots R_{n-2} < R_{n-1} < R_n$, where R_1 is the distance to the center of the closest shell and R_n is the distance to the center of the farthest away shell, then the perturbed part δM of the total mass contained within a shell of radius R_j $(j = 1, 2, ..., n)$ does not change with time, i.e. $\delta M(R_j(t_i),t_i) = \delta M(R_j(t),t) = constant$.

One can now get some new expressions that unifies the two mass terms involved, $M_b(R_i,t_i)$ and δM. The *total* mass M_s of the whole sphere is given as

$$\begin{aligned} M_s &= M_b(R_i,t_i) + \bar{\Delta}_i M_b(R_i,t_i) = (1+\bar{\Delta}_i) M_b(R_i,t_i) \\ &= (1+\bar{\Delta}_i)\tfrac{4\pi}{3} R^3(t_i)\rho_b(t_i) = constant \end{aligned} \tag{3.26}$$

where

$$\bar{\Delta}_i \equiv \bar{\Delta}(R_i,t_i) \equiv \frac{\int_0^{R_i} \Delta(R,t_i) 4\pi R^2 dR}{\frac{4\pi}{3} R_i^3} \tag{3.27}$$

which is the *mean value* of the density contrast $\Delta(R,t_i)$, i.e. where $R \in [0,R_i]$, within the total sphere at the time $t = t_i$. By substituting (3.26) in the equation of motion (3.21) it can be written in a simpler manner as

$$\frac{d^2R}{dt^2} = -\frac{GM_s}{R^2} \tag{3.28}$$

and by integrating it one gets

$$\boxed{\frac{1}{2}\dot{R}^2 - \frac{GM_s}{R} = E} \tag{3.29}$$

where $\dot{R} \equiv \frac{dR}{dt}$, and E is a constant of integration and can be considered as the *total* energy of the sphere, that is, the sum of its *kinetic* energy K and *potential* energy U. This equation is useful and the sign of E holds important information which is

- If $E > 0$: $\dot{R}$ will never become zero and the shell will expand forever.
- If $E < 0$: As R increases $\dot{R}$ will eventually become zero and later negative, implying a contraction and collapse.

(3.30)

These conditions can be expressed in a more convenient form by considering the terms in (3.29) at an initial instant $t = t_i$, where t_i is chosen to be at a time which Δ_i is quite small so that the overdense region was expanding along with the *background*. By doing this implies that the peculiar velocity *part* of the spheres evolving velocity

$\dot{R}(t_i) \equiv \dot{R}_i$ can be neglected and thus, $\dot{R}_i = \left(\frac{\dot{a}}{a}\right) R_i \equiv H(t_i) R_i \equiv H_i R_i$ at this time t_i. Thus, the *initial* kinetic energy of the sphere will be

$$K(t_i) \equiv K_i = \frac{1}{2}\dot{R_i}^2 = \frac{1}{2} H_i^2 R_i^2 \tag{3.31}$$

and the potential energy is

$$\begin{aligned} |U(t_i)| \equiv |U_i| &= \left| \left(-\tfrac{GM_s}{R} \right)_{t=t_i} \right| = G\tfrac{4\pi}{3} \rho_b(t_i) R_i^2 (1 + \bar{\Delta}_i) \\ &= \tfrac{1}{2} H_i^2 R_i^2 \Omega_i (1 + \bar{\Delta}_i) = K_i \Omega_i (1 + \bar{\Delta}_i) \end{aligned} \tag{3.32}$$

where $\Omega_i = \frac{\rho_b(t_i)}{\rho_c(t_i)}$ denoting the initial value of the density parameter of the background universe, and $\rho_c(t_i) = \frac{3H_i^2}{8\pi G}$ is the critical density at this initial time t_i. The total energy E is therefore expressed as

$$E = K + U = K_i - K_i \Omega_i (1 + \bar{\Delta}_i) = K_i \Omega_i \Big[\frac{1}{\Omega_i} - (1 + \bar{\Delta}_i) \Big] \tag{3.33}$$

From this, one sees that the condition for the sphere to collapse ($E < 0$) becomes

$$\boxed{\bar{\Delta}_i > \left(\frac{1}{\Omega_i} - 1 \right)} \tag{3.34}$$

which then represents a critical value. By considering this condition the following can be stated:

- In a closed or flat universe ($\Omega_i^{-1} \leq 1$), any overdense region ($\Delta > 0$) will eventually collapse.
- In an open universe ($\Omega_i < 1$), any overdense region ($\Delta > 0$) has to be above a critical value Δ_{crit} to collapse.

(3.35)

Now, consider a sphere with total energy $E < 0$. It will expand to a maximum radius $R = R_{ta}$, the so called *turnaround* point (subnotation 'ta'), and then start to collapse.

The value of R_{ta} can be derived by noting that the expansion velocity of the sphere has to be zero at turnaround, i.e. $\dot{R}|_{R=R_{ta}} = 0$. By exploiting this in equation (3.29) and realize that (3.32) implies $GM_s = R_i K_i \Omega_i (1 + \bar{\Delta}_i)$ one gets

$$E = -\frac{GM_s}{R_{ta}} = -\frac{R_i}{R_{ta}} K_i \Omega_i (1 + \bar{\Delta}_i) \tag{3.36}$$

Now, by equating this expression for E with the one in (3.33) gives

$$\frac{R_{ta}}{R_i} = \frac{(1 + \bar{\Delta}_i)}{\bar{\Delta}_i - (\frac{1}{\Omega_i} - 1)} \tag{3.37}$$

This equation describes the fact that as *less* overdense a shell of the sphere is, compared to the critical value $(\frac{1}{\Omega_i} - 1)$ from (3.34), the *longer* time it will use before it reach the turnaround point and starts to collapse. This can be seen from the value of the sphere's maximal radius R_{ta} which it gets at turnaround, clearly $R_{ta} \gg R_i$ if $\bar{\Delta}_i \gtrsim \left(\frac{1}{\Omega_i} - 1\right)$. And if the density of the sphere is the same as the background density, that is $\bar{\Delta}_i = \left(\frac{1}{\Omega_i} - 1\right)$, then of course $R_{ta} \to \infty$ and it will never collapse.

Analytical solution

The time evolution of the shell can be described by *solutions* to equation (3.29). For the situations where $E < 0$, the solution is given in a *parametric* form[5] as

$$\boxed{\begin{array}{c} R = A(1 - \cos\theta) \\ t + T = B(\theta - \sin\theta) \\ A^3 = GM_s B^2 \end{array}} \tag{3.38}$$

where A and B are constants, the parameter θ increases with increasing time t, and the radius R increases to a maximum value before decreasing to zero. The constant T makes it possible to set the initial condition such that at $t = t_i$, the radius is $R = R_i$. The constant A can be determined as: At $\theta = \pi$, is $R(\pi) = 2A = R_{ta}$, and by substituting this R_{ta} in (3.37) gives

[5] [15] p. 276.

$$\boxed{A = \frac{R_i}{2}\frac{(1+\bar{\Delta}_i)}{\bar{\Delta}_i - (\frac{1}{\Omega_i} - 1)}} \tag{3.39}$$

The constant B can then be determined by utilizing the third equation of (3.38), substitute A with (3.39) and M_s with the expression from (3.26). After some standard algebraic calculations the result is

$$\boxed{B = \frac{1+\bar{\Delta}_i}{2H_i\Omega_i^{\frac{1}{2}}[\bar{\Delta}_i - (\frac{1}{\Omega_i} - 1)]^{\frac{3}{2}}}} \tag{3.40}$$

where H_i is the initial value of the Hubble parameter. Thus, the parametric form (3.38) describes a shell that encloses a mass M_s and is initially expanding *with* the background universe, with time it will progressively slow down, reach a maximum radius (turnaround point) at $\theta = \pi$, and then start to collapse inward toward its center. Because the density parameter Ω_i has not been given a specific value, this solution can be used in universe models which are either *closed*, *flat* or *open*. So it is a general solution for the situation where the shell has a total energy $E < 0$ and is contained in a universe with no dark energy.

3.4 The Origin of Cosmic Structure - A very short introduction

The two procedures discussed in chapter 3.2 and 3.3 which describes the evolution of an initial density perturbation in the linear regime and in the nonlinear regime, respectively, are both incomplete in one important aspect. They start out from an initial inhomogeneity without explaining its origin. That is, they describes the evolution of gravitational instabilities based on already existing density perturbations, but says nothing about where they came from. Despite that this thesis is not concerned about their origin, it is appropriate to have mentioned what possibly caused their existence in the first place.

Inflation and the uncertainty principle

None of the *established* physics today is capable of making perturbations[6]. However, there exists a mechanism that can, and one needs to go back to the early history of the Universe to see this.

It turns out that the very short epoch of *inflation*, from 10^{-36} to 10^{-32} seconds after the Big Bang, is capable of generating irregularities that serves as 'seeds' for initiating structure formation. This stems from the *uncertainty principle* in quantum mechanics which says that apparently empty space is a seething mass of *quantum fluctuations*, i.e. with particles continually popping in and out of existence. These processes happens at time and length scales so small which makes them easy to ignore, but during a period of inflation the Universe is expanding so rapidly that any fluctuations gets caught up in the expansion and *stretched*. That means, while one set of fluctuations is being stretched, new fluctuations are always being created which will then themselves be caught up in the expansion. Thus, by the end of this epoch, there has been created small irregularities, i.e. inhomogeneities in the cosmic fluid, on a wide range of different length scales.

From this point, the linear evolution of these perturbations starts, and eventually the nonlinear evolution takes over and ends up, much later, with the structures one observes today, such as galaxies and galaxy clusters (ch. 3.1). This inflationary mechanism is currently the most popular model for the origin of structure, mainly because so far it offers excellent agreement with the real Universe, such as with the *cosmic microwave background* spectrum. If it is a correct picture, a striking consequence is that *all* structures, including our own bodies, ultimately owe their existence to small quantum fluctuations.

[6] Based on [10] p. 157-158 and [15] p. 353.

Chapter 4

Spherical Collapse in the EdS Universe Model

In this chapter the mathematical framework of the spherical collapse model in the EdS universe will be derived. Also a condition for halting the inward collapse of this model will be given, and finally some important analytical values will be derived from it to be used in conjunction with numerical simulations in the following chapters.

4.1 The Equations of Motion of the Sphere in the EdS Universe Model

This section is bases on Padmanabhan [15] p. 277. When considering spherical collapse in the EdS universe model, the general solution (3.38) for spherical collapse presented in chapter 3.3.1 needs to be specified. In this model the universe is flat and that means the density parameter equals one ($\Omega_i = 1$). With this information, the constants A and B given in (3.39) and (3.40), respectively, is immediately given as

$$A = \frac{R_i}{2}\Big(\frac{1+\bar{\Delta}_i}{\bar{\Delta}_i}\Big) \qquad \text{and} \qquad B = \frac{1}{2H_i}\Big(\frac{1+\bar{\Delta}_i}{\bar{\Delta}_i^{\frac{3}{2}}}\Big) = \frac{3t_i}{4}\Big(\frac{1+\bar{\Delta}_i}{\bar{\Delta}_i^{\frac{3}{2}}}\Big) \tag{4.1}$$

where $H_i = \frac{2}{3t_i}$ in (2.75) for the EdS universe. Then, by substituting for A and B in the two first equation of (3.38), the conditions at time $t = t_i$ now have to satisfy

$$R_i = \frac{R_i}{2}\Big(\frac{1+\bar{\Delta}_i}{\bar{\Delta}_i}\Big)(1-\cos\theta_i) \tag{4.2}$$

and

$$t_i + T = \frac{1}{2H_i}\Big(\frac{1+\bar{\Delta}_i}{\bar{\Delta}_i^{\frac{3}{2}}}\Big)(\theta_i - \sin\theta_i) \tag{4.3}$$

where $\theta_i \equiv \theta(t = t_i)$. Equation (4.2) implies that $\cos\theta_i = \frac{1-\bar{\Delta}_i}{1+\bar{\Delta}_i} \approx 1 - 2\bar{\Delta}_i$ to first order since $\bar{\Delta}_i$ is expected to be small ($\bar{\Delta}_i \ll 1$). Then also $cos\theta_i$ can be expanded to first order, $cos\theta_i \simeq 1 - \frac{\theta_i^2}{2}$, and then by equating these two approximated expressions gives

$$1 - 2\bar{\Delta}_i = 1 - \frac{\theta_i^2}{2} \qquad \Rightarrow \qquad \theta_i^2 = 4\bar{\Delta}_i \qquad \Rightarrow \qquad \theta_i = 2\bar{\Delta}_i^{\frac{1}{2}} \tag{4.4}$$

Substituting (4.4) for θ_i in (4.3), and expanding $\sin(\theta_i) = \sin(2\bar{\Delta}_i^{\frac{1}{2}})$ to first order, that is, $\sin(2\bar{\Delta}_i^{\frac{1}{2}}) \simeq 2\bar{\Delta}_i^{\frac{1}{2}} - (2\bar{\Delta}_i^{\frac{1}{2}})^3/6$, and then do some standard algebra gives

$$H_i(t_i + T) = \frac{2}{3}(1 + \bar{\Delta}_i) \tag{4.5}$$

Since $H_i t_i = \frac{2}{3}$, then $H_i T = \frac{2}{3}\bar{\Delta}_i$ and thus this can be written as

$$H_i T = \Big(\frac{2}{3t_i}\Big)T = \frac{2}{3}\bar{\Delta}_i \qquad \Rightarrow \qquad \frac{T}{t_i} = \bar{\Delta}_i \ll 1 \tag{4.6}$$

Hence, T will be ignored in what follows. Note as long as $\bar{\Delta}_i \ll 1$ is assumed, similar conclusions hold for models with $\Omega_i \neq 1$.

For the sake of order, a collection of the equations (3.38) and (4.1) that describes a spherical collapse in the EdS universe is rewritten here:

$$\boxed{\begin{array}{c} R = A(1-\cos\theta), \qquad t = B(\theta - \sin\theta), \qquad A^3 = GM_s B^2 \\ \\ A = \frac{R_i}{2}\Big(\frac{1+\bar{\Delta}_i}{\bar{\Delta}_i}\Big) \qquad \text{and} \qquad B = \frac{3t_i}{4}\Big(\frac{1+\bar{\Delta}_i}{\bar{\Delta}_i^{\frac{3}{2}}}\Big) \end{array}} \tag{4.7}$$

where T has been ignored. These equations gives the complete information about how *each* perturbed mass shell of the sphere evolves. They can be used to work out all the characteristics of the evolution of a spherical perturbation in the nonlinear regime in the EdS universe model.

4.2 A Simplification - The whole sphere's density is homogeneous

This section is based on Padmanabhan [15] p. 277-279. The mass $M_s(R)$ within any shell with radius R, contained in a defined sphere, is at all times constant because of the assumption that no shells are crossing during the sphere's evolution. The *mean* density $\bar{\rho}_{sh}(R,t)$ within an arbitrary shell (subnotation 'sh') with radius R is therefore given as

$$\bar{\rho}_{sh}(R,t) \equiv \bar{\rho}_{sh}(t) = \frac{M_s(R)}{\frac{4}{3}\pi R^3(t)} = \frac{3M_s}{4\pi A^3(1-\cos\theta(t))^3} \tag{4.8}$$

where

$$M_s(R) = M_s(R(t_i)) \equiv M_s = constant \tag{4.9}$$

Note that $\bar{\rho}_{sh}(R,t) = \bar{\rho}_{sh}(t)$ because $R = R(t)$ given in (4.7). Now, in a *simplified* case one can consider the density of the total sphere at once and require it to be *homogeneous* at all times, i.e. for $t \geq t_i$. This simplified density will be represented as $\rho_s = \rho_s(R,t) = \rho_s(t)$. (Note that R is now the radius of the *whole* sphere and *not* the radius of a specific shell somewhere *within* the sphere.) This implies that $\bar{\rho}_{sh}(t)$ in (4.8) now represents the actual density of the whole sphere bounded by its radius $R = R(t)$. Thus

$$\bar{\rho}_{sh}(R,t) = \bar{\rho}_s(R,t) \equiv \rho_s(R,t) \equiv \rho_s(t) = \frac{M_s}{\frac{4}{3}\pi R^3(t)} = \frac{3M_s}{4\pi A^3(1-\cos\theta(t))^3} \tag{4.10}$$

So from now on and through the rest of this thesis:

$$\boxed{\rho_s = \rho_s(t) \textit{ represents the homogeneous density of the } \underline{\textit{whole}} \textit{ sphere.}} \tag{4.11}$$

This calls for an important clarification of the mean density contrast $\bar{\Delta}(R,t)$. So far, this has represented the *mean* density contrast inside a specific *shell* with radius R contained in the sphere. But now, in this simplified case, it should represent the density contrast of the *whole* sphere. That is, because the density of the total sphere now has been simplified to be homogeneous (4.11), the whole sphere will therefore also correspond to only *one* density contrast $\Delta = \Delta(t \geq t_i)$, i.e. with the same

quantity everywhere inside it at a specific time t. This simplified density contrast will be presented as

$$\Delta = \Delta(R,t) \equiv \Delta(t) = \frac{\rho_s(t) - \rho_b(t)}{\rho_b(t)} \tag{4.12}$$

One sees that it appears almost the same but with *no* bar on it. Note that this definition is the same as (3.24) but now, as just explained, corresponds to the whole sphere and not just a specific shell within the sphere. So from now on and through the rest of this thesis:

$\boxed{\Delta = \Delta(t) \text{ } \textit{represents the homogeneous density contrast of the } \underline{\textit{whole}} \textit{ sphere.}}$ (4.13)

To work out the time evolution of the density contrast $\Delta(t)$, one needs to know how the background density evolves. In this chapter the simplest case is considered, i.e. the sphere is evolving inside the EdS universe. The corresponding expansion factor $a(t)$ and density $\rho_b(t)$ of the background universe is given from the equations (2.74) and (2.67) in chapter 2.2 and reproduced here:

$$a(t) = \Big(\frac{t}{t_0}\Big)^{\frac{2}{3}} \quad \text{and} \quad \rho_b(t) = \rho_c(t) \equiv \frac{3H^2(t)}{8\pi G} \tag{4.14}$$

where the background density $\rho_b(t)$ is equal to the critical density $\rho_c(t)$ because the EdS universe is flat and required to contain only one component which here is CDM. Note that for ρ_b, compared with (2.67), the factor c^2 is removed to get the unit $[\rho_b] = \frac{kg}{m^3}$ instead of $\frac{J}{m^3} = \frac{kgm^2/s^2}{m^3}$. A more useful expression for $\rho_b(t)$ in the following, one gets by substitute the expression of $a(t)$ in $H(t)$ such that

$$\rho_b(t) = \frac{3H^2(t)}{8\pi G} \equiv \frac{3}{8\pi G}\Big(\frac{\dot{a}}{a}\Big)^2 = \frac{1}{6\pi G t^2} = \frac{1}{6\pi G[B(\theta(t) - \sin\theta(t))]^2} \tag{4.15}$$

where t is substituted by the expression in (4.7). Now, the density contrast $\Delta(t)$ of the total sphere (remember (4.13)), can be found by substituting for $\rho_s(t)$ and $\rho_b(t)$ in (4.12) which gives

$$\Delta(t) \equiv \frac{\rho_s(t) - \rho_b(t)}{\rho_b(t)} = \frac{\rho_s(t)}{\rho_b(t)} - 1 = \frac{9}{2}\frac{(\theta(t) - \sin\theta(t))^2}{(1 - \cos\theta(t))^3} - 1 \tag{4.16}$$

where the relation $A^3 = GM_sB^2$ from (4.7) has been used. Thus, this expression describes the cosmic time evolution of the *homogeneous density contrast* inside the whole sphere.

Growth law of Δ in the linear regime

Although this spherical model mainly describes evolution in the nonlinear regime, a correct growth law of the homogeneous density contrast $\Delta(t)$ in the *linear* regime (i.e. $\Delta(t) \longrightarrow \Delta_{lin}(t)$) can be derived from it. This description of linear evolution is recovered in the limit of *small* t. In this limit, t from (4.7) and $\Delta(t)$ from (4.16) becomes

$$t \approx \frac{B\theta^3}{6} \;\Leftrightarrow\; \theta \approx \Big(\frac{6t}{B}\Big)^{\frac{1}{3}} \quad \text{and} \quad \Delta(t) \approx \frac{3\theta^2}{20} \;\rightarrow\; \Delta_{lin}(t) = \frac{3\theta^2}{20} \tag{4.17}$$

where the subnotation 'lin' stands for linear. By substituting this approximated θ in $\Delta_{lin}(t)$ and also substitute B with (4.1) (note that now $\bar{\Delta}_i \longrightarrow \Delta_i$, see (4.13)) results in

$$\begin{aligned}
\Delta_{lin}(t) &= \frac{3}{20}\Big(\frac{6t}{B}\Big)^{\frac{2}{3}} = \frac{3}{20}(6t)^{\frac{2}{3}}\Big[\frac{4}{3t_i}\Big(\frac{\Delta_i^{\frac{3}{2}}}{1+\Delta_i}\Big)\Big]^{\frac{2}{3}} = \frac{3}{5}\Delta_i\Big(\frac{t}{t_i}\Big)^{\frac{2}{3}}(1+\Delta_i)^{-\frac{2}{3}} \\
&\approx \frac{3}{5}\Delta_i\Big(\frac{t}{t_i}\Big)^{\frac{2}{3}}(1-\frac{\Delta_i}{3})(1-\frac{\Delta_i}{3}) = \frac{3}{5}\Delta_i\Big(\frac{t}{t_i}\Big)^{\frac{2}{3}}(1-\frac{2}{3}\Delta_i+\frac{\Delta_i}{9}) \\
&\approx \frac{3}{5}\Delta_i\Big(\frac{t}{t_i}\Big)^{\frac{2}{3}} \quad \propto \quad a(t) = \Big(\frac{t}{t_0}\Big)^{\frac{2}{3}}
\end{aligned} \tag{4.18}$$

This is the correct growth law ($\Delta_{lin} \propto a \propto t^{\frac{2}{3}}$) for the purely growing mode in the linear regime if the initial peculiar velocity is zero, i.e. the initial expansion of the sphere is the same as the expansion of the background universe.

For the further discussion it is convenient to use two other variables which are

$$r_i \equiv r_s(t_i) = \frac{a(t_0)}{a(t_i)} R_i = constant$$
$$\Delta_{lin,0} \equiv \Delta_{lin}(t_0) \equiv \frac{3}{5}\Delta_i \Big(\frac{t_0}{t_i}\Big)^{\frac{2}{3}} = \frac{3}{5}\Delta_i \frac{\Big(\frac{t_0}{t_0}\Big)^{\frac{2}{3}}}{\Big(\frac{t_i}{t_0}\Big)^{\frac{2}{3}}} = \frac{3}{5}\Delta_i \frac{a(t_0)}{a(t_i)} = \frac{3}{5}\Delta_i(1+z_i) = constant \tag{4.19}$$

The first variable is the *comoving* radius of the sphere (see (3.16) and (3.17)) with the background universe at the initial time t_i of its evolution. Here it corresponds with the initial physical radius $R(t_i) \equiv R_i$. The second variable is defined from (4.18) and the last equality is taken from (2.26) where $z_i \equiv z(t_i)$ is the redshift at the *initial* time of evolution of the sphere. It represents the *present* value of the sphere's density contrast, predicted by the *linear* theory of the spherical collapse model, if the density contrast was Δ_i at the redshift z_i.

When considering the constants A and B from (4.7) again (remember $\bar{\Delta}_i \longrightarrow \Delta_i$), and utilizing these two new variables (4.19) together with the assumption that $\Delta_i \ll 1$, and retaining only the leading terms of Δ_i, results in two forms of simpler expressions for A and B, respectively. That is

$$\begin{aligned} A &= \frac{R_i}{2}\Big(\frac{1+\Delta_i}{\Delta_i}\Big) = \frac{R_i}{2}\Big(\frac{1}{\Delta_i}+1\Big) \approx \frac{R_i}{2\Delta_i} = \frac{1}{2\Delta_i}\Big(\frac{a(t_i)}{a(t_0)} r_i\Big) \\ &= \frac{1}{2}\left(\frac{1}{\frac{5}{3}\Delta_{lin,0}\frac{a(t_i)}{a(t_0)}}\right)\Big(\frac{a(t_i)}{a(t_0)} r_i\Big) = \frac{3r_i}{10\Delta_{lin,0}} \end{aligned} \tag{4.20}$$

and

$$\begin{aligned} B &= \frac{3t_i}{4}\left(\frac{1+\Delta_i}{\Delta_i^{\frac{3}{2}}}\right) = \frac{3t_i}{4}\left(\frac{1}{\Delta_i^{\frac{3}{2}}}+\frac{1}{\Delta_i^{\frac{1}{2}}}\right) \approx \frac{3t_i}{4\Delta_i^{\frac{3}{2}}} = \frac{3t_i}{4}\left(\frac{1}{\frac{5}{3}\Delta_{lin,0}\frac{a(t_i)}{a(t_0)}}\right)^{\frac{3}{2}} \\ &= \frac{3t_i}{4}\left(\frac{3}{5}\frac{1}{\Delta_{lin,0}}\frac{a(t_0)}{a(t_i)}\right)^{\frac{3}{2}} = \frac{3t_i}{4}\left(\frac{3}{5}\frac{1}{\Delta_{lin,0}}\frac{\Big(\frac{t_0}{t_0}\Big)^{\frac{2}{3}}}{\Big(\frac{t_i}{t_0}\Big)^{\frac{2}{3}}}\right)^{\frac{3}{2}} = \frac{3}{4}\Big(\frac{3}{5}\Big)^{\frac{3}{2}}\frac{t_0}{\Delta_{lin,0}^{\frac{3}{2}}} \end{aligned} \tag{4.21}$$

For the sake of order, collecting all the above results (4.7), (4.16), (4.20) and (4.21), the evolution of a spherical and homogeneous overdense region can be summarized by the following equations:

$$\boxed{\begin{aligned} R &= A(1-\cos\theta) = \frac{R_i}{2\Delta_i}(1-\cos\theta) = \frac{3r_i}{10\Delta_{lin,0}}(1-\cos\theta) \\ t &= B(\theta-\sin\theta) = \frac{3t_i}{4\Delta_i^{\frac{3}{2}}}(\theta-\sin\theta) = \frac{3}{4}\left(\frac{3}{5}\right)^{\frac{3}{2}}\frac{t_0}{\Delta_{lin,0}^{\frac{3}{2}}}(\theta-\sin\theta) \\ \Delta &\equiv \frac{9}{2}\frac{(\theta-\sin\theta)^2}{(1-\cos\theta)^3} - 1 \end{aligned}} \tag{4.22}$$

where R is the physical radius of the sphere, t is the cosmic time, $\theta \in [0, 2\pi]$ is a parameter, r_i and Δ_i are defined in (4.19), and Δ is given in (4.16).

4.3 Violent Relaxation and the Virial Theorem

This section is based mainly on Padmanabhan [15] p. 280-281. When the sphere has reached the turnaround point, it has ceased to expand and starts to contract towards its center. The expression for Δ in (4.22) implies that at $\theta = 2\pi$ all the mass will collapse to a point. However, long before this happens, this approximated model breaks down, because at some time during the collapse, it will no longer be realistic that matter is distributed in spherical shells and that random velocities of the particles are small. The collisionless component, i.e. CDM, that constitute the sphere will at some time reach at state of *virial equilibrium* by a process known as *violent relaxation*.

During a realistic collapse there will be large fluctuations in the gravitational potential, and thus individual particles will not follow orbits which conserves energy. This changes in energy depends in a complex way on the particles initial position and velocity, but the net effect will be to widen the range of energies available to the particles. Thus, a potential varying in time can provide a relaxation mechanism. This process will relax the collisionless component CDM to a configuration with physical radius $R = R_{vir}$ and density $\rho = \rho_{vir}$ ('*vir*' means virialization). Note that the behaviour of the baryonic component is more complicated. Such a virialized system can be used to model the structures which one observes in the universe today. The physical parameters of such a system are given by a well known theorem and which is very central in the spherical collapse model. This theorem is *The Virial Theorem*[1] and it says

$$\boxed{|U| = 2K} \tag{4.23}$$

where U is the potential energy of the sphere and K is its kinetic energy. *When* and *after* the sphere has virialized, this is the relation between its potential and kinetic energy. That is, the absolute value of the potential energy is twice as big as the kinetic energy.

The expression of the potential energy U, related to CDM, applies to a spherically symmetric system with *homogeneous* density and it is given as[2]

$$\boxed{U = -\frac{3}{5}\frac{GM_s^2}{R}} \tag{4.24}$$

where G is the gravitational constant, and

[1] A derivation of this theorem can be found in [17] p. 225-227.
[2] A derivation of this expression can be found in [17] p. 157-158.

$$M_s = \frac{4}{3}\pi R^3 \rho_s \tag{4.25}$$

is the total mass, R is the physical radius, and ρ_s is the homogeneous density of the sphere. The expression of the kinetic energy[3] K is

$$\boxed{K = \frac{1}{2}M_s v^2} \tag{4.26}$$

where M_s is the total mass and v is the *velocity dispersion*, i.e. the sphere's rate of expansion or collapse. One last equation is central in the spherical collapse model, and that is the one expressing *energy conservation*

$$\boxed{E = U + K} \tag{4.27}$$

where E is the *total* energy of the sphere. Now, with these last four equations (though one does not really need (4.26) in the following context), an important parameter can be derived which is the radius $R = R_{vir}$ of the sphere at virialization.

At the time $t = t_{ta}$ the sphere has reached its maximum expansion (the turnaround point) and *all* its energy E has to be in the form of potential energy $U = U(t_{ta})$, because then the expansion rate v is zero, i.e. $v = 0 \;\Rightarrow\; K(t_{ta}) = 0$. Thus

$$E(t_{ta}) = U(t_{ta}) + K(t_{ta}) = \underline{-\frac{3}{5}\frac{GM_s^2}{R_{ta}}}$$

$$|U(t_{vir})| = \frac{3}{5}\frac{GM_s^2}{R_{vir}} = 2K(t_{vir}) \qquad \text{(Virial theorem (4.23))}$$

$$E(t_{vir}) = U(t_{vir}) + K(t_{vir}) = U(t_{vir}) + \frac{1}{2}|U(t_{vir})| \tag{4.28}$$

$$= -\frac{3}{5}\frac{GM_s^2}{R_{vir}} + \frac{1}{2}\frac{3}{5}\frac{GM_s^2}{R_{vir}} = \underline{-\frac{1}{2}\frac{3}{5}\frac{GM_s^2}{R_{vir}}}$$

$$E(t_{ta}) \equiv E(t_{vir}) \quad \Longrightarrow \quad -\frac{3}{5}\frac{GM_s^2}{R_{ta}} = -\frac{1}{2}\frac{3}{5}\frac{GM_s^2}{R_{vir}} \quad \Longrightarrow \quad \underline{\frac{1}{R_{ta}} = \frac{1}{2}\frac{1}{R_{vir}}}$$

[3] A derivation of this expression can be found in [17] p. 227.

$$\Longrightarrow \qquad \boxed{R_{vir} = \frac{1}{2} R_{ta}} \tag{4.29}$$

where $t = t_{vir}$ is the time when the sphere has reached virial equilibrium, i.e. at the virialization point. So, the radius at virialization for a spherical collapse in the EdS universe is *half of the sphere's maximum radius*. This will be an important analytical value to compare numerical simulations with in the following chapters.

4.3.1 Virialization condition for the EdS universe

For the program code to be able to calculate when the sphere reaches its virial radius it needs a relation between the sphere's potential energy $U_{ta} \equiv U(t_{ta}) \equiv U(a_{s,ta})$ at turnaround, and the sphere's potential energy $U_{vir} \equiv U(t_{vir}) \equiv U(a_{s,vir})$ at virialization, where a_s is the sphere's scalefactor. This relation will now be derived.

Energy conservation (4.27) $\quad\Longrightarrow\quad$ $K(a_{s,ta}) + U(a_{s,ta}) = E(a_{s,ta}) < 0$

where K is the kinetic energy (4.26), U is the potential energy (4.24), and $a_{s,ta}$ is the scalefactor of the sphere at turnaround.

At turnaround, $K = K(a_{s,ta}) = 0$, and thus $\underline{E(a_{s,ta}) = U(a_{s,ta})}$.

Also, energy conservation (4.27) $\quad\Longrightarrow\quad$ $K(a_{s,vir}) + U(a_{s,vir}) = E(a_{s,vir}) < 0$

where $a_{s,vir}$ is the scalefactor of the sphere at virialization.

At virialization, (4.23) $\quad\Longrightarrow\quad$ $U(a_{s,vir}) = -2K(a_{s,vir})$, and thus
$-\frac{1}{2}U(a_{s,vir}) + U(a_{s,vir}) = E(a_{s,vir}) \quad\Longrightarrow\quad \underline{E(a_{s,vir}) = \frac{1}{2}U(a_{s,vir})}$

Because energy conservation demands $E(a_{s,vir}) = E(a_{s,ta})$, this implies that $\underline{U(a_{s,vir}) = 2U(a_{s,ta})}$.

Thus, the virialization condition implemented in the code is

$$\boxed{U(a_{s,vir}) = 2U(a_{s,ta})} \tag{4.30}$$

4.4 Analytical Calculations

This section[4] is important for the code developed for this thesis because of the analytical values that will be derived here can be compared with some of the simulated data.

The simplified model in section 4.2 serves as a way for the code to get *verified*, i.e. when the code simulates a spherical collapse of a homogeneous mass density distribution in the EdS universe, it will be doing it correctly if it is able to simulate data which is equal, or close to equal, to these analytical values. When this is in place, more credence can be given to the code when it gets modified to simulate spherical collapse in other types of universe models where it do not exists analytical values to compare with. These analytical values will now be derived.

From (2.26) one knows that the redshift and the scalefactor are related as $a = \frac{1}{1+z}$. By exploiting this fact one can derive the following useful relation

$$\frac{a(t)}{a(t_i)} = \frac{\left(\frac{t}{t_0}\right)^{\frac{2}{3}}}{\left(\frac{t_i}{t_0}\right)^{\frac{2}{3}}} = \frac{\left(\frac{1}{1+z}\right)}{\left(\frac{1}{1+z_i}\right)} \;\Rightarrow\; \frac{a(t)}{a(t_i)} = \left(\frac{t}{t_i}\right)^{\frac{2}{3}} = \frac{1+z_i}{1+z} \;\Leftrightarrow\; \frac{t}{t_i} = \left(\frac{1+z_i}{1+z}\right)^{\frac{3}{2}} \tag{4.31}$$

This can so be substituted for $\frac{t}{t_i}$ in the second equality of t in (4.22) which gives

$$\begin{aligned} \left(\frac{1+z_i}{1+z}\right)^{\frac{3}{2}} &= \frac{3}{4\Delta_i^{\frac{3}{2}}}(\theta - \sin\theta) \quad \Leftrightarrow \quad z = \left(\frac{4}{3}\right)^{\frac{2}{3}} \frac{\Delta_i(1+z_i)}{(\theta-\sin\theta)^{\frac{2}{3}}} - 1 \\ &= \left(\frac{4}{3}\right)^{\frac{2}{3}} \frac{\Delta_i\left(\frac{1}{a(t_i)}\right)}{(\theta-\sin\theta)^{\frac{2}{3}}} - 1 = \left(\frac{4}{3}\right)^{\frac{2}{3}} \frac{\Delta_i\left(\frac{t_0}{t_i}\right)^{\frac{2}{3}}}{(\theta-\sin\theta)^{\frac{2}{3}}} - 1 = \frac{5}{3}\left(\frac{4}{3}\right)^{\frac{2}{3}} \frac{\Delta_{lin,0}}{(\theta-\sin\theta)^{\frac{2}{3}}} - 1 \end{aligned} \tag{4.32}$$

where the last equality is given by (4.18), implying $\Delta_{lin}(t_0) \equiv \Delta_{lin,0} \approx \frac{3}{5}\Delta_i\left(\frac{t_0}{t_i}\right)^{\frac{2}{3}}$, which is the relation between the purely growing mode and the scalefactor $a(t) = (t/t_i)^{\frac{2}{3}}$ in the linear regime. This equation defines the parameter θ implicitly in terms of the redshift z, that is $\theta = \theta(z)$. Together with the definition of Δ from (4.22), they defines implicitly the function $\Delta(z)$ for $z > z_i$, i.e. the *nonlinear* evolution of the homogeneous density of the sphere as a function of the redshift z. In this manner, Δ from (4.22) is reproduced here,

[4] Based on Padmanabhan [15] p. 280-281.

$$\Delta = \Delta(z) = \Delta(\theta(z)) = \frac{9}{2}\frac{(\theta - \sin\theta)^2}{(1-\cos\theta)^3} - 1 \tag{4.33}$$

and for comparison, the linear evolution is given, implied by equation (4.19), as

$$\Delta_{lin} = \frac{3}{5}\Delta_i\Big(\frac{t}{t_i}\Big)^{\frac{2}{3}} = \frac{3}{5}\Delta_i\frac{a(t)}{a(t_i)} = \frac{3}{5}\Delta_i\frac{(1+z_i)}{(1+z)} = \frac{3}{5}\Big(\frac{3}{4}\Big)^{\frac{2}{3}}(\theta - \sin\theta)^{\frac{2}{3}} \tag{4.34}$$

where the last equality is given from (4.32). By using these last three equations, (4.32), (4.33) and (4.34), one can derive important analytical values and expressions:

Linear regime

When $z \gg 1$, then $\theta \ll 1$, and thus $\Delta \approx \Delta_{lin}$. (4.35)

Deviation from linearity

When $\theta = \big(\frac{\pi}{2}\big)$, then $\Delta_{lin} \approx 0.341$, but $\Delta \approx 0.466$, at $z \approx 1.761\Delta_i(1+z_i) - 1 = 2.934\Delta_{lin,0} - 1$.

Here the actual density contrast Δ is about 40% higher. (4.36)

The nonlinearity point

When $\theta = \big(\frac{2\pi}{3}\big)$, then $\Delta_{lin} \approx 0.568$, but $\Delta \approx 1.012 \approx 1$, at $z \approx 1.056\Delta_i(1+z_i) - 1 = 1.760\Delta_{lin,0} - 1$.

$\Delta \approx 1$ is interpreted as the *transition point to nonlinearity.* (4.37)

The turnaround point

When $\theta = \pi$, then $\Delta_{lin} \approx 1.062409652$, but $\Delta \approx 4.551652476$, at $z \approx 0.564753905\Delta_i(1+z_i) - 1 = 0.941256509\Delta_{lin,0} - 1$.

The sphere reaches its *maximum* radius $R = R_{ta}$ of expansion, which is $R(\theta = \pi) \equiv R_{ta} = \frac{R_i}{\Delta_i} = \frac{3r_i}{5\Delta_{lin,0}}$ from (4.22). This is called the *turnaround* point. (4.38)

Note that the reason for all the numbers in use after the decimal point is to get as close to the analytical values as possible. Then when these values are compared with their corresponding numerical values the comparison will be as precise as possible. See appendix C for details.

The box (4.38) contains particular important information and corresponds to the epoch of *turnaround*, and some more explanation is appropriate. If for example the initial density contrast is $\Delta_i \approx 3 \cdot 10^{-3}$ at the corresponding initial redshift $z_i \approx 1100$, such a perturbation would have turned around at $z = z_{ta} \approx 0.565\Delta_i(1 + z_i) - 1 = 0.565 \cdot 3 \cdot 10^{-3} \cdot (1 + 1100) - 1 \approx 0.866$. The actual density contrast, i.e. the nonlinear density contrast Δ, is here given as $\Delta \approx 4.5517$. This shows that the sphere at turnaround is nearly six times denser than the background universe, i.e. $\frac{\rho_s}{\rho_b} = 1 + \Delta = 1 + 4.552 \approx 6$. Note also how far of the linear prediction Δ_{lin} is from the actual value of the density contrast.

The time t_{vir} is essentially the time corresponding to $\theta = 2\pi$. Thus, it no longer makes sense of finding the nonlinear density contrast Δ by using the equation (4.33), because $\Delta(\theta = 2\pi) = \infty$. But still, $\Delta(t_{vir}) \equiv \Delta_{vir}$ can be determined, by first expressing the sphere's homogeneous density $\rho_s(t_{vir})$ at virialization and then exploiting (4.29) so that

$$\rho_s(t_{vir}) = \frac{M_s}{V_{vir}} = \frac{M_s}{\frac{4}{3}\pi R_{vir}^3} = \frac{M_s}{\frac{4}{3}\pi\left(\frac{R_{ta}}{2}\right)^3} = 8 \cdot \frac{M_s}{\frac{4}{3}\pi R_{ta}^3} = 8\frac{M_s}{V_{ta}} = 8\rho_s(t_{ta}) \tag{4.39}$$

where $V(t_{vir}) \equiv V_{vir}$ and $V(t_{ta}) \equiv V_{ta}$ are the sphere's volume at virialization and at turnaround, respectively. Now, from (4.38), $\Delta(t_{ta}) \approx 4.551652476$ and thus

$$\begin{aligned} \frac{\rho_s(t_{ta}) - \rho_b(t_{ta})}{\rho_b(t_{ta})} \equiv \Delta(t_{ta}) = \frac{\rho_s(t_{ta})}{\rho_b(t_{ta})} - 1 = 4.551652476 \\ \Leftrightarrow \quad \rho_s(t_{ta}) = 5.551652476\rho_b(t_{ta}) \end{aligned} \tag{4.40}$$

Then an expression for the background density at turnaround $\rho_b(t_{ta})$ is needed,

$$\rho_b(t_{ta}) = \frac{\rho_{b0}}{a_{ta}^3} \quad \text{and} \quad \rho_b(t_{vir}) = \frac{\rho_{b0}}{a_{vir}^3} \quad \text{gives}$$
$$\rho_b(t_{ta}) = \frac{\rho_b(t_{vir}) a_{vir}^3}{a_{ta}^3} = \rho_b(t_{vir}) \frac{(1+z_{ta})^3}{(1+z_{vir})^3} \tag{4.41}$$

and the fraction here is a constant from equation (4.32) because

$$(1+z_{ta}) = \frac{5}{3}\Big(\frac{4}{3}\Big)^{\frac{2}{3}} \frac{\Delta_{lin,0}}{(\pi - \sin(\pi))^{\frac{2}{3}}} \approx 0.941256509 \Delta_{lin,0}$$
$$(1+z_{vir}) = \frac{5}{3}\Big(\frac{4}{3}\Big)^{\frac{2}{3}} \frac{\Delta_{lin,0}}{(2\pi - \sin(2\pi))^{\frac{2}{3}}} \approx 0.592954444 \Delta_{lin,0} \tag{4.42}$$
$$\longrightarrow \qquad \frac{(1+z_{ta})^3}{(1+z_{vir})^3} \approx 4.000000011$$

Now, substituting (4.42), (4.41) and (4.40) in (4.39) gives

$$\rho_s(t_{vir}) = 8 \cdot 5.551652476 \rho_b(t_{ta}) = 8 \cdot 5.551652476 \cdot \rho_b(t_{vir}) \frac{(1+z_{ta})^3}{(1+z_{vir})^3}$$
$$= 8 \cdot 5.551652476 \cdot \rho_b(t_{vir}) \cdot 4.000000011$$
$$\Rightarrow \quad \frac{\rho_s(t_{vir})}{\rho_b(t_{vir})} \approx 177.6528797 \quad \Rightarrow \quad \frac{\rho_s(t_{vir})}{\rho_b(t_{vir})} - 1 \approx 176.6528797 \tag{4.43}$$
$$\Leftrightarrow \quad \frac{\rho_s(t_{vir}) - \rho_b(t_{vir})}{\rho_b(t_{vir})} \equiv \Delta(t_{vir}) \approx 176.6528797$$

Again, by using the equations (4.32), (4.33) and (4.34), one can derive the following important analytical values and expressions for the *virialization* point which corresponds to $\theta = 2\pi$:

The virialization point

When $\theta = 2\pi$, then $\Delta_{lin} \approx 1.6864702$ and $\Delta \approx 176.6528797$ at $z \approx 0.355772667\Delta_i(1+z_i) - 1 = 0.592954444\Delta_{lin,0} - 1$.

The sphere reaches its *virial* radius $R = R(\theta = 2\pi) \equiv R_{vir} = \frac{1}{2}R_{ta}$ from (4.23), where $R_{ta} = \frac{R_i}{\Delta_i} = \frac{3r_i}{5\Delta_{lin,0}}$ from (4.38).
This is called the *virialization* point. (4.44)

The five boxes, (4.35), (4.36), (4.37), (4.38) and (4.44), contains the essential analytical values and analytical expressions for the spherical collapse model inside the EdS universe.

In the following two chapters 5 and 6 the focus will be on three of the values now derived which is the density contrast $\Delta = \Delta_{ta}$ at turnaround, the density contrast $\Delta = \Delta_{vir}$ at virialization, and the radius at virialization given as R_{vir}/R_{ta}.

4.5 Chapter Summary

In section 3.3 the spherical collapse model was introduced and derived in general. Then in section 4.1 this model got specified for the EdS universe, and a set of equations for describing the evolution of each shell of the sphere was derived from the general equations in section 3.3. These specified equations was given in the box (4.7). So forth in section 4.2 a simplification of the spherical collapse model for the EdS universe were made. It was required that the whole sphere was homogeneous at all times, and a set of new equations (4.22) describing its evolution was derived. In section 4.3 the virial theorem for the sphere in the EdS universe were introduced and it was derived that the sphere's radius at virialization is *half* of its radius at the epoch of turnaround. Then in subsection 4.3.1 a virialization condition was derived. It was a mechanism to halt the collapse. It implicitly gave the correct virialization radius and it was stated that this condition was used in the code. Finally in section 4.4 central analytical values for the spherical collapse model in the EdS universe were derived, and the importance of these in conjunction with numerical simulations was pointed out.

Now the whole theoretical framework for the spherical collapse model describing the evolution of a homogeneous spherical overdensity in the EdS universe has been introduced and derived. The task for the code in the following chapters will be to reproduce this model correctly, and then based on this, also be able to get modified correctly so to simulate spherical collapse in the other types of universe models considered in this thesis. Note that in the appendix B all the implemented Friedmann equations which the code uses to simulate these models are presented and derived, and in the appendix C a verification that the code are able to simulate the analytical values relevant for this thesis is shown.

To end this chapter, from the simulations are two plots shown in figure 4.1 with the purpose of illustrating spherical collapse in the EdS universe for different values of initial density contrasts $\Delta(t = t_i) \equiv \Delta_i \ll 1$, which are "planted" at the initial redshift $z(t = t_i) \equiv z_i = 1100$ and then starts to evolve. It shows how the evolving spheres with time (i.e. when approaching $z = 0$) starts to disentangle from the expanding background, then halt their expansion completely at the epoch of turnaround, and finally collapse towards its center (i.e. $a_s \to 0$). A closer explanation is given in the figure text.

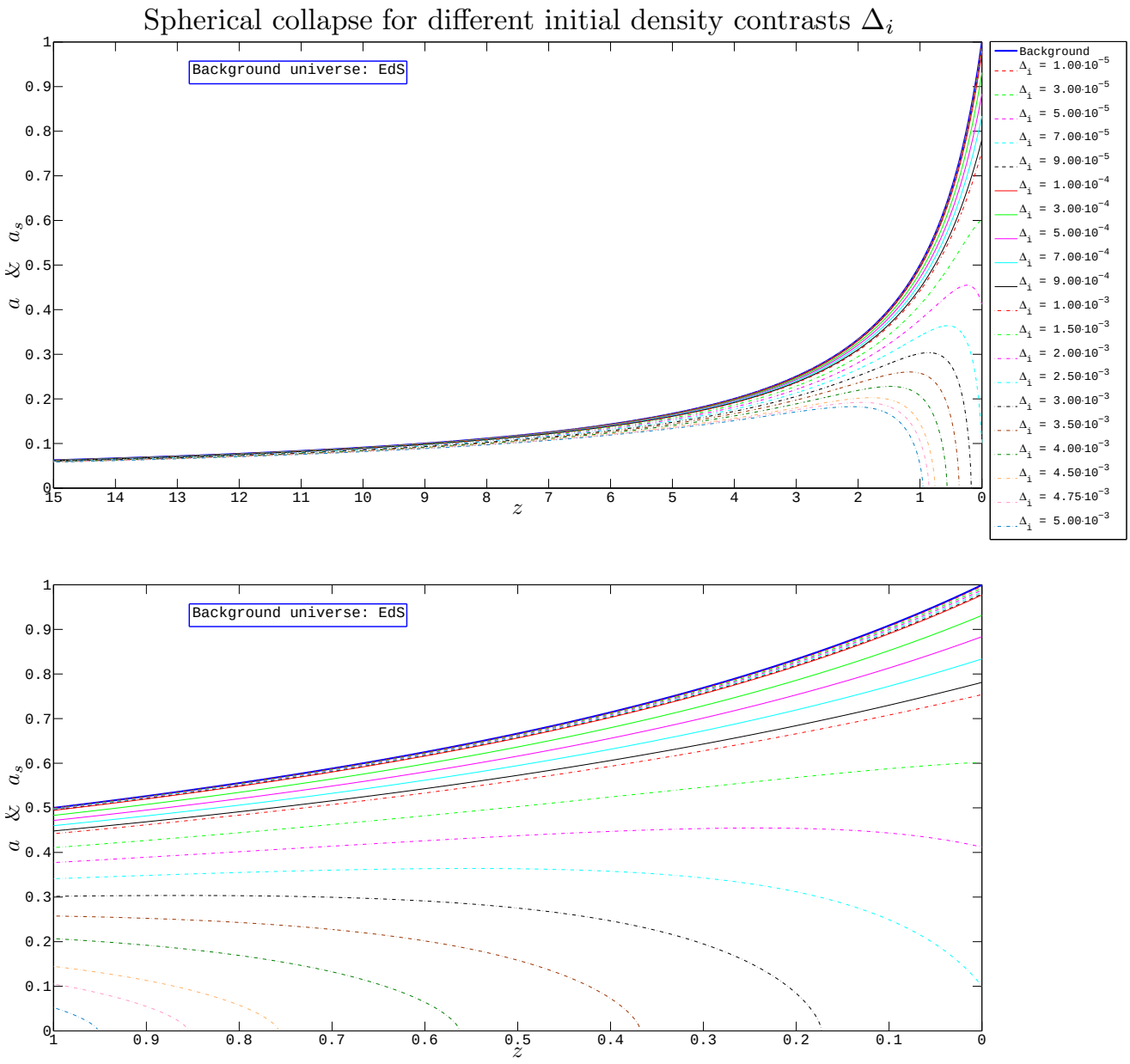

Figure 4.1: Spherical collapses in the EdS universe for initial density perturbations corresponding to different initial density contrasts Δ_i which starts their evolution at an initial redshift $z_i = 1100$. Note that these two plots are the same, but given in two different redshift intervals. Also note that they both only shows the last part of the evolutions, i.e. from $z = 15$ and $z = 1$, respectively. However, one sees, especially from the top plot, that the perturbed spheres expands closer to the background as further back in time (i.e. increasing redshifts z) one consider. This is to be expected because the spheres has the same initial expansion rate $\dot{a}_s(t_i)$ as the expansion rate $\dot{a}(t_i)$ of the background universe at the same time t_i, i.e. $\dot{a}(t_i) = \dot{a}_s(t_i)$. In the interval approximately $z \in [0, 2]$, eight of the strongest perturbed spheres, i.e. those with the strongest initial density contrasts Δ_i, reaches turnaround and starts to collapse, i.e. $a_s \to 0$. The rest do not reach turnaround and starts to collapse because they have not been able to generate a sufficiently gravitational potential given by a high enough density ρ_s (i.e. CDM density).

Chapter 5

Spherical Collapse in the ΛCDM Universe Model

The ΛCDM universe model was presented in subsection 2.2.9. It was mentioned that observational data indicates that approximately 70% of the Universe consist of dark energy, named the cosmological constant Λ, and the rest is approximately 30% CDM. Λ is considered to have a significant different nature than CDM and is yet to be understood. One of its effects is that the Universe have had an accelerated expansion for approximately the last 3.7 billion years and which is consistent with observations. In section 2.2.8 the EdS universe model was presented and by comparing it with the ΛCDM model one realize that there are several significantly different properties between these two models, such as their differences in energy contents and their different expansion history. In section 2.2.6 it was pointed out that one needs to know all the energy contents of the Universe to be able to describe how it evolves. With these three sections in mind one should expect to see some different results of how the spherical collapse model evolves in the ΛCDM universe compared to its evolution in the EdS universe.

In this chapter it will be shown how a spherical collapse evolves in the ΛCDM universe, and then compare this result to a similar spherical collapse in the EdS universe.

5.1 Dynamics in the ΛCDM Universe Model

In the appendix B.1, an equivalent form of the two Friedmann equations (2.60) and (2.61) from section 2.2.6 is derived for the ΛCDM universe model. These are (B.18) and (B.19) and are reproduced here:

$$\frac{\dot{a}^2}{a^2} = \frac{8\pi G}{3}\rho \tag{5.1}$$

$$\frac{\ddot{a}}{a} = -\frac{4\pi G}{3}\Big(\rho + \frac{3p}{c^2}\Big) \tag{5.2}$$

where

$$\rho = \rho_m + \rho_\Lambda \equiv \rho_{m0}a^{-3} + \rho_{\Lambda 0} \quad \text{and} \quad p = p_m + p_\Lambda \equiv 0 + (-\rho_{\Lambda 0}c^2) \tag{5.3}$$

The second Friedmann equation (5.2) shows an additional term on the RHS compared to the corresponding Friedmann equation (B.2) for the EdS universe model. When substituting the expression for the pressure p in (5.3) it is easy to see that the pressure $p = p_\Lambda = -c^2\rho_{\Lambda 0}$, generated by the density $\rho = \rho_\Lambda = \rho_{\Lambda 0}$ of the cosmological constant, contributes with a positive term to the acceleration of the scalefactor $\ddot{a}$. Explicitly this is given as

$$\frac{\ddot{a}}{a} = -\frac{4\pi G}{3}\Big(\rho_m + \rho_{\Lambda 0} + \frac{3}{c^2}(-\rho_{\Lambda 0}c^2)\Big) = -\frac{4\pi G}{3}\Big(\rho_m - 2\rho_{\Lambda 0}\Big) \tag{5.4}$$

which implies that when $\rho_{\Lambda 0} > \frac{1}{2}\rho_m$ the expansion will have a positive acceleration, i.e. $\ddot{a} > 0$. This relation can be illustrated in the two plots (A.1) and (6.1) when considering $w = -1$ and rewriting the two densities ρ_m and $\rho_{\Lambda 0}$ to their respective density parameters Ω_m and Ω_Λ. It appears that $\ddot{a} > 0$ at a redshift $z \leq 0.67$.

With only this information of the background universe one can do some speculations on how a sphere would evolve from an initial time t_0, corresponding to an initial redshift $z_i = 1100$, in this universe compared to the same situation in the EdS universe. Intuitively one should expect that a sphere evolving in the ΛCDM universe would need more time to collapse than an identical sphere in the EdS universe. That is because the accelerated expansion which the ΛCDM universe have had for the last ~ 3.7 billion years (i.e. since $z \approx 0.67$) should have a sort of braking effect on the collapse and thus work *against* the spheres' force of gravity.

These two situations have been simulated by the code. The evolution of twenty different initial density contrasts $\Delta_i \in [10^{-5}, 9 \cdot 10^{-5}]$ has been described from an initial time

corresponding to the redshift $z_i = 1100$. Their evolution is illustrated in figure 5.1 below where the top plot shows the evolutions in the EdS universe and the bottom plot shows the evolutions of the same initial density contrasts in the ΛCDM universe. The plots in figure 5.1 has then been analyzed further in the figures 5.2, 5.3, and 5.4. These will be discussed in the following.

Figure 5.1 reinforces the resent speculation. It shows that any density contrasts Δ_i evolving in the ΛCDM universe will need more time to collapse compared to the same density contrast evolving in the EdS universe. For example the greatest density contrast $\Delta_i = 5 \cdot 10^{-3}$ will collapse (i.e. reach $a_s = 0$) approximately at a redshift $z \approx 1$ in the EdS universe, but the same density contrast evolving in the ΛCDM universe will collapse at $z \approx 0.8$. This means it needs more time to collapse because it reaches $a_s = 0$ closer to $z = 0$ (which corresponds to the present time t_0). Another example to consider is the initial density contrast $\Delta_i = 3 \cdot 10^{-3}$. Its evolution in the EdS universe ends with a collapse at $z \approx 0.2$ but the same density contrast evolving in the ΛCDM universe has not yet reached collapse at present time t_0 (i.e. $z = 0$).

Figure 5.2 shows these collapses in more details by zooming into the redshift interval $z \in [0, 1]$ and only include the strongest part of the initial density contrasts, i.e. $\Delta_i \in [1.00 \cdot 10^{-3}, 5.00 \cdot 10^{-3}]$. Thus, the top plot is the same plot as in figure 5.1 but zoomed into the interval $z \in [0, 1]$, only $\Delta_i \in [1.00 \cdot 10^{-3}, 5.00 \cdot 10^{-3}]$ are included, and the lines from both the EdS and the ΛCDM universe is in it. This makes it is easier to compare. The bottom plot shows the percentage deviations of the corresponding collapses of these particular Δ_i in the EdS and ΛCDM universe so to also quantify the deviations. Note that most of these percentage deviations blows up on the y-axis because the scale factors of the spheres in the EdS universe always reaches zero before their corresponding scale factors in the ΛCDM universe (i.e. one ends up dividing with zero). In the top plot two equal initial density contrasts Δ_i in each of the universe models share the same color but has a different line styles. An example of how to read this top plot is: The density contrast $\Delta_i = 3 \cdot 10^{-3}$ (also considered in figure 5.1) has black color. One sees that for the one evolving in the EdS universe (dotted line) it reaches collapse at the redshift $z \approx 0.18$, and the one evolving in the ΛCDM universe has not yet reached collapse at present time (i.e. $z = 0$). That is, at $z = 0$ the sphere corresponding to this density contrast in the ΛCDM universe has a scalefactor $a_s \approx 0.23$, i.e. it is about 23% of the scalefactor a of the background ΛCDM universe. In the bottom plot (of figure 5.2) one can follow the increasing deviation of these two equal initial density contrasts (the black graph) and one realize that in this redshift interval the difference between these two are significant. For example, at the redshift $z \approx 0.5$, the scalefactor of the sphere evolving in the ΛCDM model is about 19% bigger than the corresponding sphere evolving in the EdS universe.

Figure 5.3: The same considerations as done in figure 5.2 with the strongest part of the Δ_i can be done with the weakest part of the Δ_i as shown in figure 5.3. In figure 5.1

it is hard to see if there are any deviations of the similar spheres evolving in each of their models when these spheres corresponds to the weakest part of the initial density contrasts $\Delta_i \in [1.00 \cdot 10^{-5}, 9.00 \cdot 10^{-5}]$. If there are any deviations then of course they would be smaller than the ones considered in figure 5.2. To be able to separate the graphs for these weak density contrasts it was necessary to zoom in to a redshift interval of approximately $z \in [0, 0.33]$ and a scalefactor interval of $a \in [0.75, 1.00]$. The results are shown in figure 5.3. To avoid the same explanation again, as done for figure 5.2, it should be sufficient to say that the same explanation goes for this figure. The top plot shows deviations, but they are much less significant than what was shown in figure 5.2. This appears also clearly in the bottom plot which for example shows that 'the strongest of the weakest' initial density contrast $\Delta_i = 9 \cdot 10^{-5}$ corresponds to a sphere with a scalefactor a_s only about 0.46% bigger than the scalefactor of the sphere of the same Δ_i evolving in the EdS universe. So this indicates that the same weak initial density contrasts evolving in the two considered universe models basically has the same scalefactor a_s as the background scalefactor a. This is no surprise because spheres with densities close to the background density is *not* able to put up a gravitational potential that generates a significant gravitational force making the sphere to collapse in on itself.

Figure 5.4 shows the evolution of the last part of the collection of initial density contrasts Δ_i from figure 5.1. This part is the intermediate part of the Δ_i shown in the figures 5.2 and 5.3. The top plot (in figure 5.4) has the same zoom as figure 5.2. It shows no final collapses (i.e. no $a_s = 0$) but indicates greater deviations of two equal Δ_i evolving in each their universe model when compared to the top plot of figure 5.3. For example, by considering the 'strongest of these intermediate density contrasts', i.e. $\Delta_i = 9 \cdot 10^{-4}$, one sees in the top plot that it collapses the most in the EdS universe. The bottom plot shows that at present time (i.e. z = 0) the scalefactor of this particular density contrast (black color) has a scalefactor a_s about 6.7% greater in the ΛCDM universe than its corresponding density contrast in the EdS universe. So the same effect applies here as in the consideration of the two other figures 5.2 and 5.3, which shows the evolution of greater and smaller Δ_i, respectively.

Before going further in this discussion of spherical collapse in the ΛCDM universe, a way to know how and when these spherical systems virializes is needed. This is the subject for the next section 5.2.

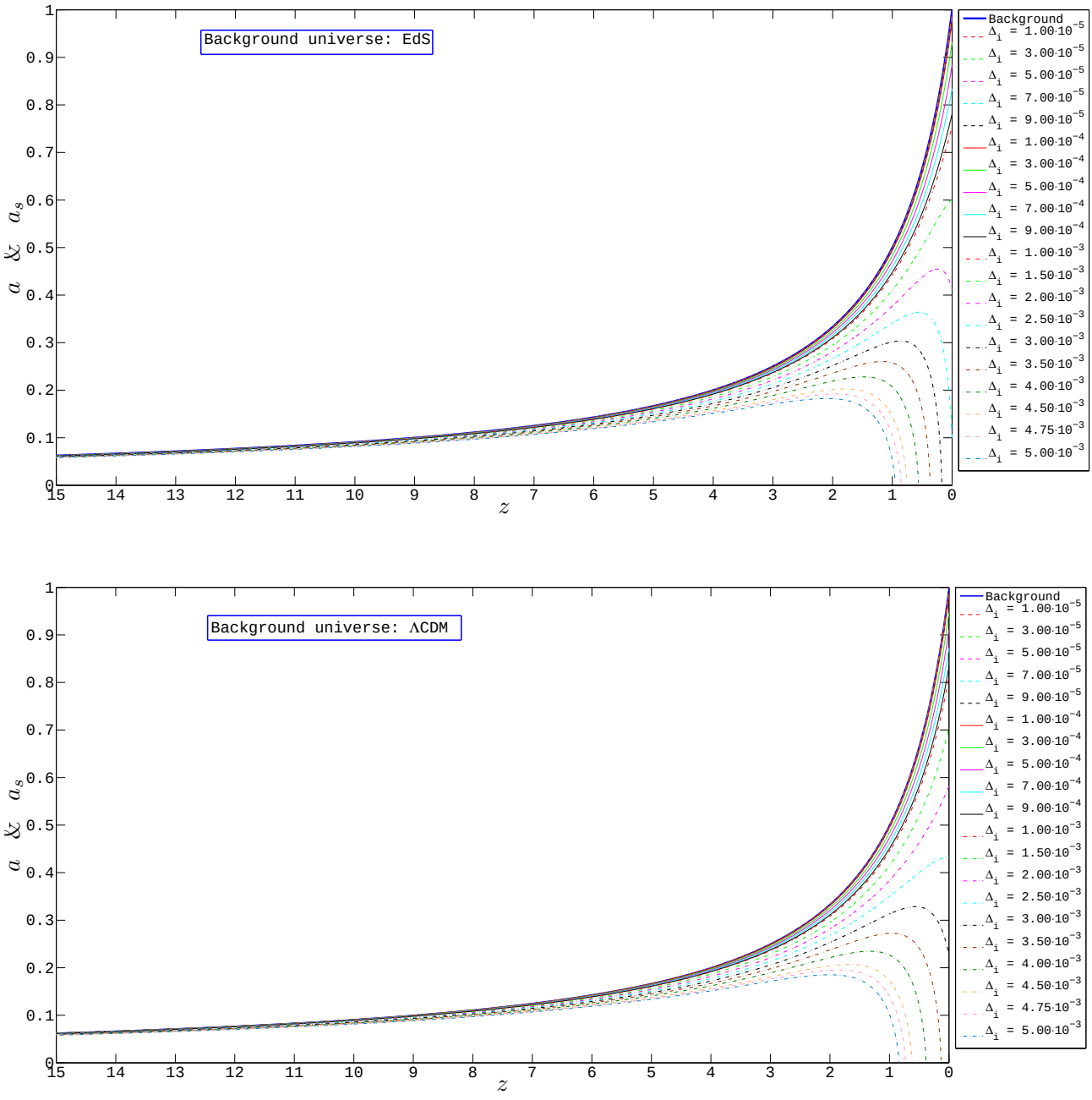

Figure 5.1: The evolution of twenty different initial density contrasts $\Delta_i \in [10^{-5}, 5 \cdot 10^{-3}]$ shown over the redshift interval $z \in [0, 15]$. The top plot is in the EdS universe and the bottom plot is in the ΛCDM universe. Note that the evolution of $\Delta_i \in [10^{-5}, 9 \cdot 10^{-5}]$ can hardly be seen because their evolution is close to equal to the evolution of the background universes. This is because these spheres' gravitational potential, generated by the additional perturbed densities, are too small to put up a gravitational force which can dominate over the expanding background universe. Also note that the collapse has only been shown over the redshift interval $z \in [0, 15]$ because as closer the description reach $z_i = 1100$ the more closer are all of the spheres' evolutions to the background universe. Both plots shows this trend. A third thing to be aware of is that the evolutions of the two background universes appear to be identical. This is not the case but the reason it is so here is because their scale factors are here functions of the redshift z and not cosmic time t. So both are given as $a = \frac{1}{1+z}$.

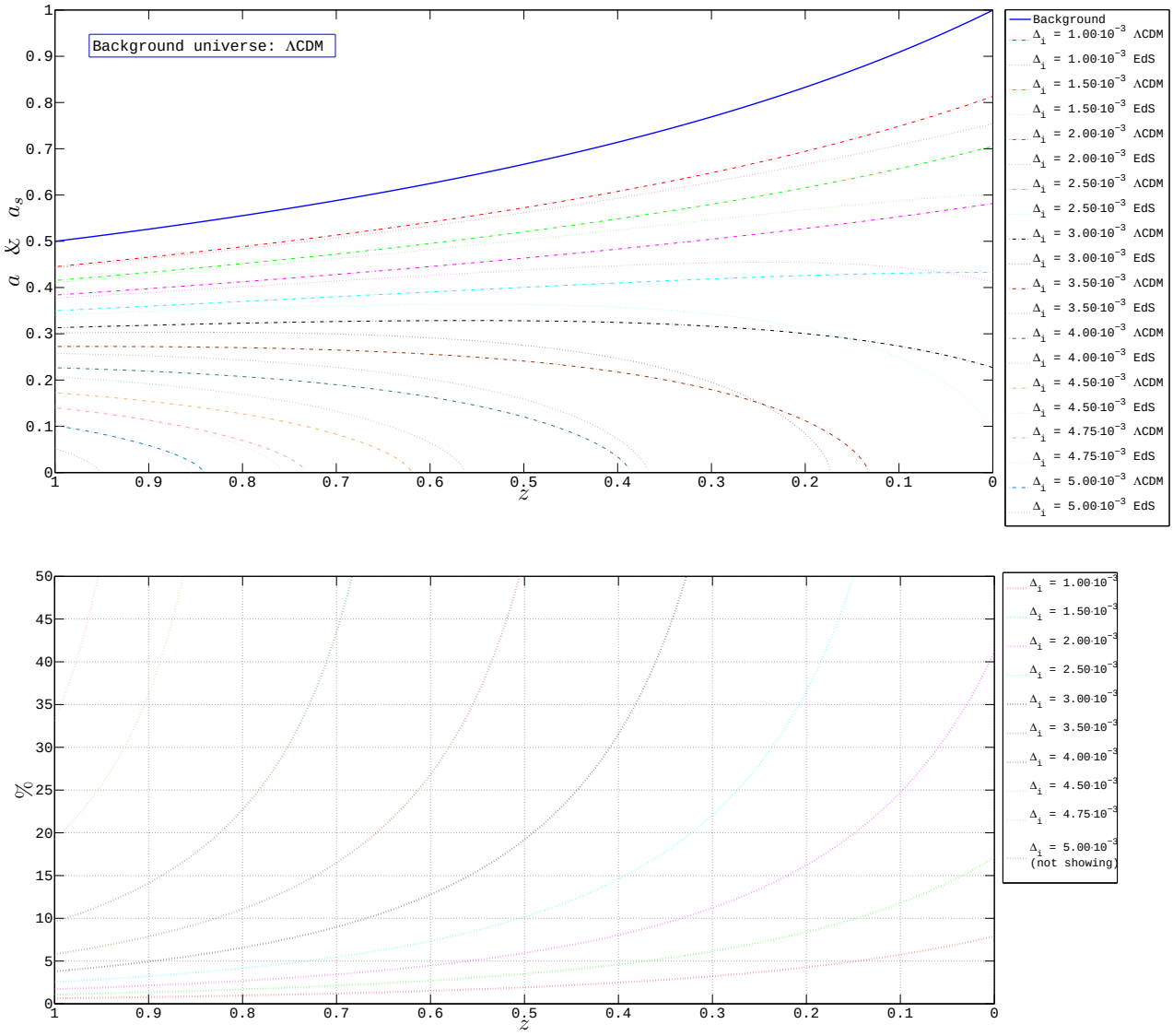

Figure 5.2: Top plot: This is the same plot as in figure 5.1 but with some changes. It is zoomed in to the redshift interval $z \in [0, 1]$, only the strongest initial density contrast $\Delta_i \in [1.00 \cdot 10^{-3}, 5.00 \cdot 10^{-3}]$ are included, and the lines of these Δ_i from both the EdS and the ΛCDM universe are included. This makes it easier to compare two equal initial density contrasts Δ_i evolving in each of the universe models. One specific Δ_i in each universe has the same color, but their line style are different (i.e. dotted or dashed). Bottom plot: It shows the percentage deviations between two *equal* initial density contrasts evolving in each of the two different models. That is, it represents how much, in percent, the scalefactor of a sphere deviates in the ΛCDM universe compared to the corresponding scalefactor of a sphere that evolves in the EdS universe. Note that the colors here represents the same Δ_i as in the top plot.

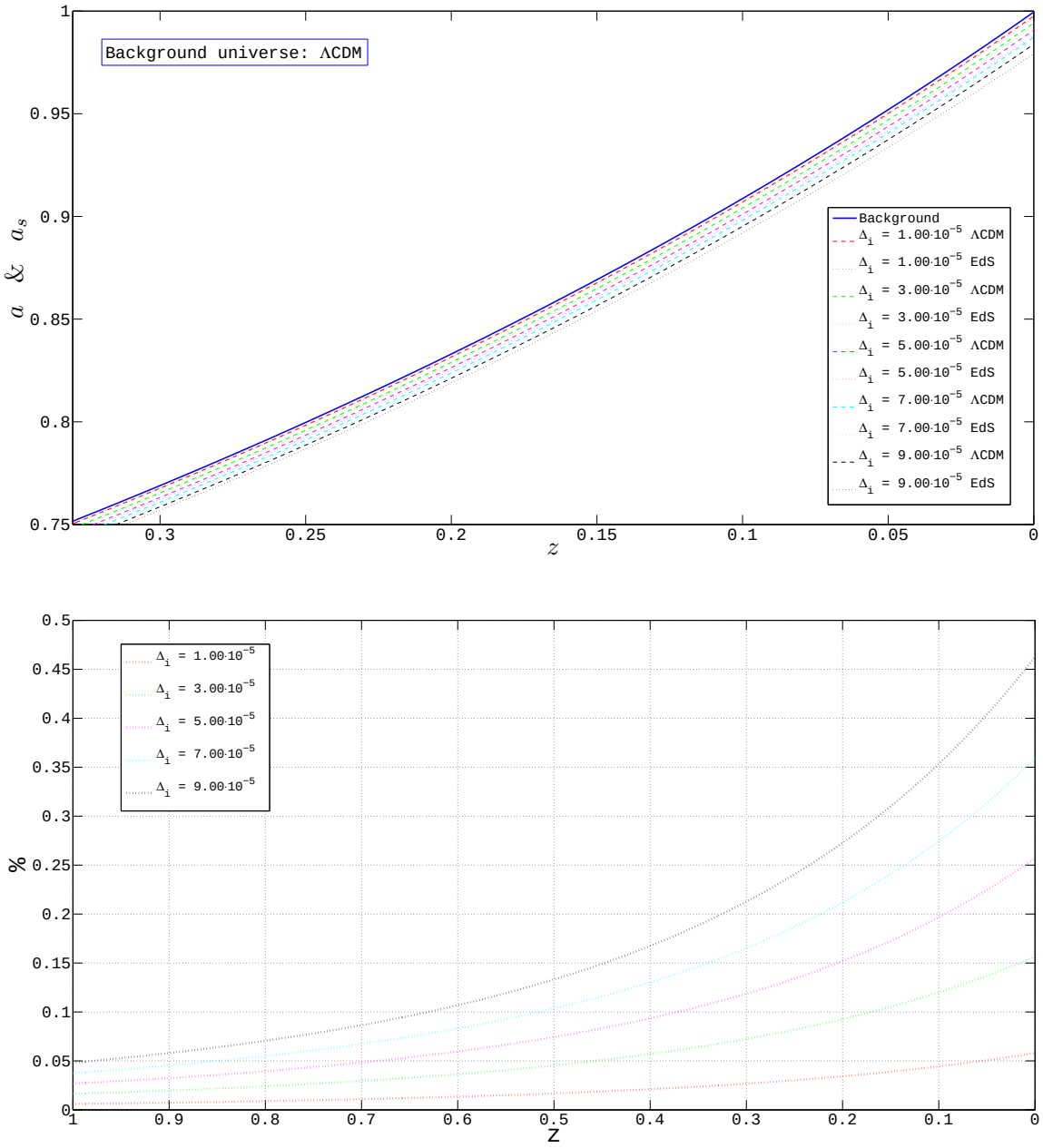

Figure 5.3: The same explanation applies here as given in the text of figure 5.2. The difference is the closer zoom on both the x-axis and the y-axis because here is weaker initial density contrasts Δ_i in considerations. One sees that all of these spheres (i.e. the evolving density contrasts) evolves almost equal to the background, something which is quite different from what was shown in the plots of figure 5.2. Top plot: It shows small deviations of the scale factors a_s for the evolving density contrasts in the EdS and the ΛCDM background universe. Bottom plot: It shows the percentage differences of the deviations from the top plot. Note that it shows the deviations for $z \in [0, 1]$ even though the top plot is only given for approximately $z \in [0, 0.33]$.

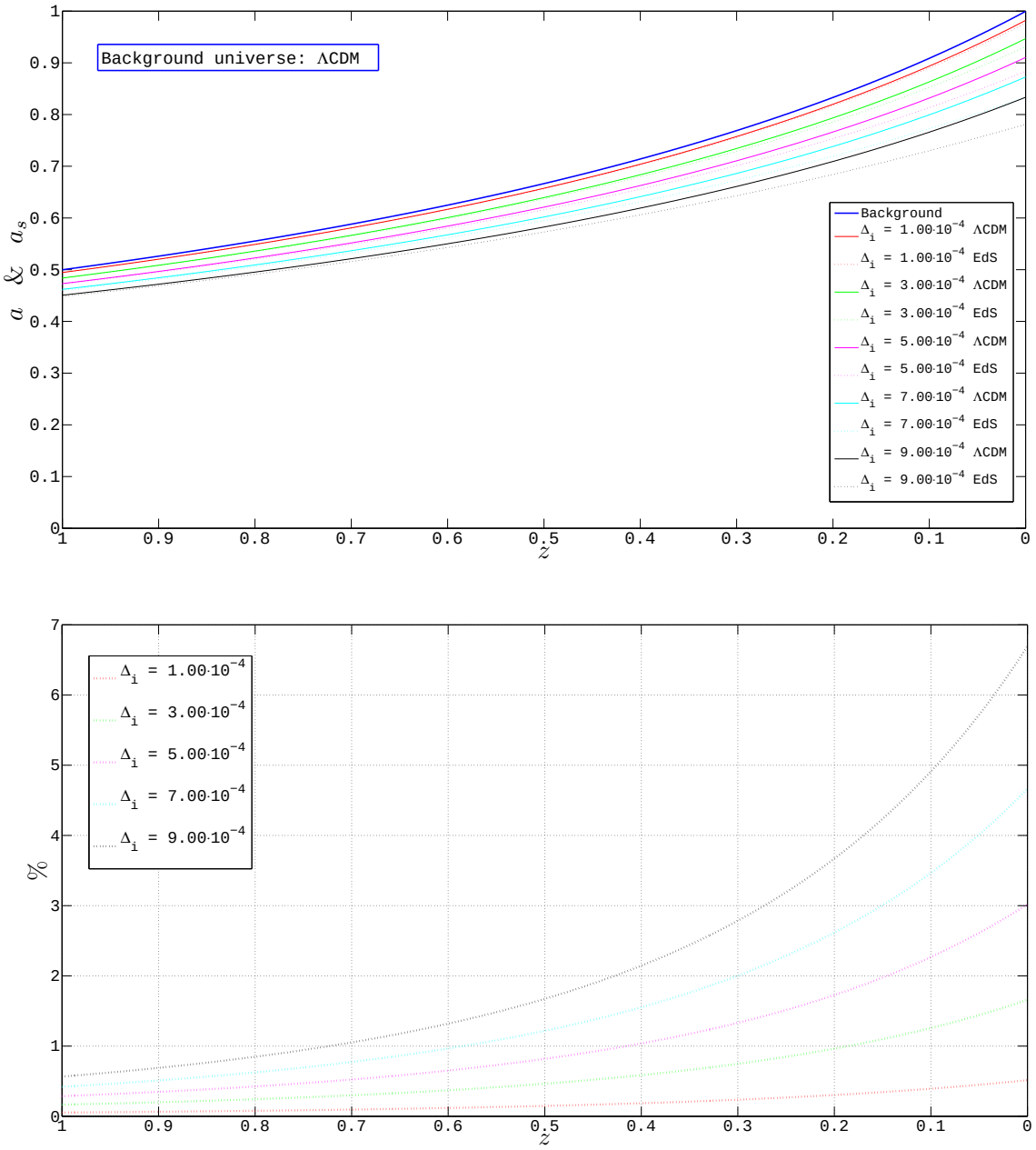

Figure 5.4: As said in the figure text of figure 5.3, the same explanation applies here as given in the figure text of figure 5.2. The only difference, compared to figure 5.2, is the weaker initial density contrasts Δ_i in considerations. Top plot: It shows the small deviations of the scale factors a_s for the evolving initial density contrasts Δ_i in the EdS and the ΛCDM background universe. Bottom plot: It shows the percentage differences of these deviations from the top plot. One sees that the results here lies in between the results of the bottom plots in the figures 5.2 and 5.3.

5.2 Virialization Condition

Compared to the EdS model, the ΛCDM model consist of one more energy component, namely the cosmological constant Λ. Because it is a true constant, its only contribution to the dynamics of the CDM inside the sphere (beside accelerating the background universe when $z < 0.67$) is that it sets up an extra potential U_Λ 'felt' by the CDM. Thus, in addition to the CDM's own gravitational potential U_m, it is also submerged in a potential field U_Λ generated by Λ.

The gravitational potential energy U_m generated by the CDM itself was introduced in the equation (4.24) in section 4.3 and reproduced here:

$$\boxed{U_m = -\frac{3}{5}\frac{GM_s^2}{R}} \tag{5.5}$$

In the article [2] by Lahav and Lilje et al. the *Tolman-Bondi equation* for 'the energy ϵ *per unit mass* for a shell enclosing the mass m' was considered in the case of a universe with Λ. This equation is reproduced here as

$$\epsilon = \frac{1}{2}\dot{R}^2 - \frac{GM_s}{R} - \frac{c^2}{6}\Lambda R^2 \tag{5.6}$$

where G is the gravitational constant, and R is the physical radius of a particular shell. Note that as stated in section 4.2, in this thesis it represents the physical radius of the *total* sphere. Therefore also note that 'm' which was explained just prior to the equation, has been rewritten to $m = M_s$ which represents the total mass of the sphere. This equation shows that the classical potential $\phi_m = -\frac{GM_s}{R}$ has been modified by an extra potential term[1] $\phi_\Lambda = -\frac{c^2}{6}\Lambda R^2$.

Now, to derive the additional part U_Λ of the potential energy of the CDM generated by the potential ϕ_Λ, this term needs to be integrated over a sphere. Thus

$$U_\Lambda = \frac{M_s}{V}\int \phi_\Lambda dV = \frac{3M_s}{4\pi R^3}\int_0^R \Big(-\frac{c^2}{6}\Lambda R'^2\Big)4\pi R'^2 dR' = -\frac{c^2}{2}\frac{M_s\Lambda}{R^3}\frac{R^5}{5}$$

$$\iff \quad \boxed{U_\Lambda = -\frac{c^2}{10}M_s\Lambda R^2} \tag{5.7}$$

[1] Note that the light speed c has been included explicit so that all four terms in the equation is consistent with the dimension $\frac{m^2}{s^2}$.

The additional potential energy U_Λ is derived and then a crucial thing to realize is that the virialization theorem (4.23) needs to be modified. It needs to include U_Λ and thus the virialization theorem for the ΛCDM universe model says[2]

$$\boxed{K = -\frac{1}{2}U_m + U_\Lambda} \tag{5.8}$$

Now that both of the potentials for the ΛCDM universe are given, (5.5) and (5.7), and the virialization theorem has been modified, the specific virialization condition for this model can be derived. Note that in this derivation, the sphere's scalefactor a_s has been used instead of its physical radius R.

Energy conservation (4.27) $\quad\Longrightarrow\quad$ $K(a_{s,ta}) + U(a_{s,ta}) = E(a_{s,ta}) < 0$

where K is the kinetic energy (4.26) and $U(a_{s,ta}) = U_m(a_{s,ta}) + U_\Lambda(a_{s,ta})$ is the total potential energy and $a_{s,ta}$ is the scalefactor of the sphere at turnaround.

At turnaround, $K = K(a_{s,ta}) = 0$, and thus $\underline{E(a_{s,ta}) = U_m(a_{s,ta}) + U_\Lambda(a_{s,ta})}$.

Modified virialization theorem (5.8): $\quad K(a_{s,vir}) = -\frac{1}{2}U_m(a_{s,vir}) + U_\Lambda(a_{s,vir})$

where $a_{s,vir}$ is the sphere's scalefactor at virialization. Thus, at virialization

$$E(a_{s,vir}) = K(a_{s,vir}) + U_m(a_{s,vir}) + U_\Lambda(a_{s,vir}) = \underline{\frac{1}{2}U_m(a_{s,vir}) + 2U_\Lambda(a_{s,vir})}$$

Energy conservation (4.27) then implies $E(a_{s,ta}) = E(a_{s,vir}) \quad\Longrightarrow$

$$\boxed{\frac{1}{2}U_m(a_{s,vir}) + 2U_\Lambda(a_{s,vir}) = U_m(a_{s,ta}) + U_\Lambda(a_{s,ta})} \tag{5.9}$$

which is the virialization condition in the ΛCDM universe[3].

[2] [2] p. 134.
[3] As used in [2].

An important thing to note about this virialization condition is that it is based on the properties imposed to the cosmological constant Λ. In the ΛCDM model the dark energy (i.e. Λ) is considered to be *passive*. That means, as already said, its influence on how the sphere and the background universe evolves is by setting up an extra potential ϕ_Λ that the CDM 'feels'. Though for example *if* the dark energy could be considered as particles and which interacted with the CDM, it would be reasonable to consider it to participate in the virialization process. This implies that the dark energy have a *dynamical* nature and is *not* passive. It would thus call for a modification of the virialization condition (5.9). Then a particular sphere would evolve differently than what it would have if the dark energy had a passive nature. That is, its radius and density at virialization etc. would most likely have been different. This is something that will be studied in chapter 6.

5.3 Numerical Simulations

In section 5.1 the dynamics of different evolving spheres, with different initial density contrasts Δ_i, was studied inside the ΛCDM universe. It was considered how they behaved differently from corresponding spheres which evolved inside the EdS universe. It was pointed out several important differences in the spheres scale factors a_s within the redshift interval under consideration. That is, the scale factors of the spheres evolving in a ΛCDM universe was always greater than its corresponding similar spheres which evolved inside the EdS universe. For redshifts $z > 1$ it appeared that all of these spheres evolved increasingly similar to the background universe as $z \to 1100$. Then in section 5.2 the virialization condition (5.9) for spheres evolving in the ΛCDM universe was derived. It was explained that this virialization condition was based on certain characteristic properties which the cosmological constant Λ is perceived to have. With these two sections in mind it should be possible to interpret, to a certain extent, the numerical data generated by the code when this gets simulated. The simulations are presented in figure 5.5 and 5.6.

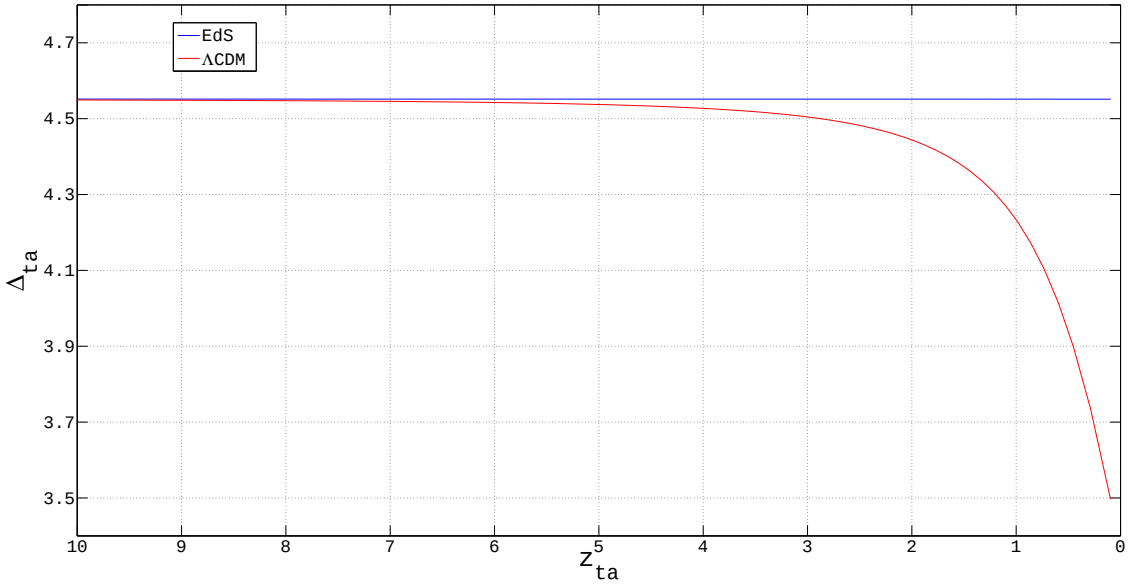

Figure 5.5: The density contrast Δ_{ta} at turnaround simulated for a spherical collapse in the EdS and the ΛCDM universe.

Figure 5.5
This plot shows the simulation of the density contrast Δ_{ta} at turnaround over a redshift interval $z_{ta} \in [0, 15]$ for spherical collapse in the EdS and the ΛCDM universe. For the EdS universe one sees that the code simulates the correct constant value of Δ_{ta}, i.e.

$\Delta_{ta} = \Delta_{ta}(EdS) \approx 4.55$ as stated in (4.38). This has also been pointed out in the appendix C.

The red line represents the density contrast simulated in the ΛCDM universe and it behaves quite differently for small redshifts z_{ta}. The first to note is that it appear to move toward the same Δ_{ta} as for the EdS universe when $z_{ta} \to 1100$. This makes sense based on the fact that the ΛCDM universe is basically equal to the EdS universe at high redshifts. That is because then the density $\rho_m \propto a^{-3}$ of the CDM dominates fully over the constant density ρ_Λ of the cosmological constant Λ and thus it can be neglected.

The reason why the density contrast $\Delta_{ta} = \Delta_{ta}(\Lambda CDM)$ in the ΛCDM universe gets weaker when the redshift z_{ta} goes towards zero seems to have an intuitive explanation. That is, if the turnaround radius gets bigger, then the CDM density $\rho_{m,s}$ inside the sphere gets smaller, and therefore the density contrast Δ_{ta} also needs to be weaker. But one must be careful when interpreting density contrasts because there exists more than one way of defining it. The general definition of the density contrast was introduced in (3.1). By first starting with the density contrast $\Delta = \Delta(EdS)$ in the EdS universe this definition implies (at turnaround)

$$\Delta_{ta}(EdS) \equiv \frac{\rho_s - \rho}{\rho} = \frac{\rho_{m,s,init}\left(\frac{a_{s,init}}{a_{s,ta}}\right)^3 - \rho_{m0}a_{ta}^{-3}}{\rho_{m0}a_{ta}^{-3}} = \frac{\rho_{m,s,init}\left(\frac{a_{s,init}}{a_{s,ta}}\right)^3}{\rho_{m0}a_{ta}^{-3}} - 1 \tag{5.10}$$

where ρ_s is the density of the sphere, ρ is the background density, $\rho_{m,s,init}$ is the initial CDM density of the sphere, $a_{s,init}$ is the initial scale factor of the sphere, $a_{s,ta}$ is the scale factor of the sphere at turnaround, $\rho_{m,s,init}\left(\frac{a_{s,init}}{a_{s,ta}}\right)^3 = \rho_{m,s,ta}$ is the sphere's CDM density at turnaround, ρ_{m0} is the CDM density of the background at present, and a_{ta} is the background scale factor when the sphere reach turnaround.

However in the ΛCDM universe one can choose to include or not include the density ρ_Λ of Λ in the definition and this has big consequences of how the density contrast $\Delta = \Delta(\Lambda CDM)$ behaves in plots. The definition selected for this thesis is

$$\begin{aligned}\Delta_{ta}(\Lambda CDM) \equiv \frac{\rho_s - \rho}{\rho} &= \frac{(\rho_{m,s,init}\left(\frac{a_{s,init}}{a_{s,ta}}\right)^3 + \rho_\Lambda) - (\rho_{m0}a_{ta}^{-3} + \rho_\Lambda)}{\rho_{m0}a_{ta}^{-3} + \rho_\Lambda} \\ &= \frac{\rho_{m,s,init}\left(\frac{a_{s,init}}{a_{s,ta}}\right)^3 + \rho_\Lambda}{\rho_{m0}a_{ta}^{-3} + \rho_\Lambda} - 1\end{aligned} \tag{5.11}$$

where ρ is the total background density, ρ_s is the total density of the sphere, $\rho_{m,s,init}$ is the initial CDM density of the sphere, $\rho_{m,s,init}\left(\frac{a_{s,init}}{a_{s,ta}}\right)^3 = \rho_{m,s,ta}$ is the sphere's CDM density at turnaround, $a_{s,ta}$ is the scale scactor of the sphere at turnaround, ρ_{m0} is the density of the background CDM at present, a_{ta} is the background scale factor when the sphere reach turnaround, and $\rho_\Lambda = constant$ is the density of the cosmological constant.

Another thing to note is that ρ_{m0} are not equal in the EdS and ΛCDM universe. That is because the density parameter Ω at present and any other time in the EdS universe is $\Omega = \Omega_m = \Omega_{m0} = 1$ for CDM, but in the ΛCDM universe $\Omega_{m0} = 0.3$ and $\Omega_{\Lambda 0} = 0.7$ at present. Then by recalling the critical density ρ_{c0} from (2.67) one realize that $\frac{\rho_{m0}}{\rho_{c0}} = \Omega_{m0} \Rightarrow \rho_{m0} = \rho_{c0}$ for the EdS universe, but $\rho_{m0} = 0.3\rho_{c0}$ in the ΛCDM universe.

Also both $a_{s,ta}$ and a_{ta} is affected differently by the accelerated expansion compared to the same ones in the EdS universe so there are many things to take into consideration when comparing $\Delta_{ta}(EdS)$ and $\Delta_{ta}(\Lambda CDM)$. I will leave the interpretation with these two expressions (5.10) and (6.36), and their explanation and trust the simulation.

Figure 5.6 - top plot
This plot shows the virialization radius, given as R_{vir}/R_{ta}, is simulated for the EdS and the ΛCDM universe. For the EdS universe one sees that the code simulates R_{vir} as it should because, as stated in (4.44), $R_{vir}/R_{ta} = 0.5$ is the analytical value.

For the ΛCDM universe one sees again that it behaves in the same way as the EdS universe when $z_{vir} \to 1100$ for the same reasons as stated about figure 5.5. By considering the virialization condition (5.9) together with the expression (5.7) for the potential energy U_Λ of Λ one also realize that it can be neglected compared to the potential energy (5.5) of CDM when $z_{vir} \to 1100$ because then $R \propto a_s \to 0$ and the virialization condition (5.9) is reduced to the virialization condition (4.28) for the EdS universe. To explain why $R_{vir}/R_{ta} < 0.5$ when z_{vir} moves towards zero one needs to take two things into consideration. The first one is that R_{ta} is in general *greater* in the ΛCDM universe and then contributes to reduce R_{vir}/R_{ta}. The second is that, by looking at the virialization condition (5.9), one realize that R_{vir} for U_m on the LHS needs to get *smaller* than in the EdS universe to compensate for the U_Λ term on the RHS. That is, the sphere in the ΛCDM universe needs to collapse longer towards its center to achieve virialization for approximately $z_{vir} \in [0, 10]$ which is what this plot shows.

Figure 5.6 - bottom plot
Before starting with the interpretation there is one important thing to note about this plot. In section 4.4 the analytical values for parameters regarding the spherical collapse model in the EdS universe was derived and in the box (4.44) the analytical value for

the density contrast Δ at virialization was derived to be $\Delta \approx 176.65$. Still there exists another constant analytical value also referring to the density contrast Δ. This value[4] is $\Delta = \Delta_{vir}(EdS) \approx 145.84$ and will through the rest of the thesis be related to the constant analytical value of Δ_{vir} in the EdS universe. It is only a matter of definition. This exchange has its origin from a problem in the program code, not intended to go into here.

Now, the bottom plot of figure 5.6 shows the density contrast Δ_{vir} at virialization. One sees that the code simulates the correct density contrast for the EdS, that is ≈ 145.84.

The density contrast $\Delta_{vir} = \Delta_{vir}(\Lambda CDM)$ for the ΛCDM universe might appear to be wrong. Because intuitively a smaller R_{vir} should mean a higher density ρ_s of the sphere and thus a stronger density contrast $\Delta_{vir}(\Lambda CDM)$ (compared with the EdS universe). As for figure 5.5, one needs to be careful when interpreting this plot, so one should instead look at the two expressions which defines these two quantities and which has the same form as (5.10) and (5.11). They are given as

$$\Delta_{vir}(EdS) = \frac{\rho_{m,s,init}\left(\frac{a_{s,init}}{a_{s,vir}}\right)^3 - \rho_{m0}a_{vir}^{-3}}{\rho_{m0}a_{vir}^{-3}} = \frac{\rho_{m,s,init}\left(\frac{a_{s,init}}{a_{s,vir}}\right)^3}{\rho_{mo}a_{vir}^{-3}} - 1 \tag{5.12}$$

and

$$\begin{aligned}\Delta_{vir}(\Lambda CDM) &= \frac{(\rho_{m,s,init}\left(\frac{a_{s,init}}{a_{s,vir}}\right)^3 + \rho_\Lambda) - (\rho_{m0}a_{vir}^{-3} + \rho_\Lambda)}{\rho_{m0}a_{vir}^{-3} + \rho_\Lambda} \\ &= \frac{\rho_{m,s,init}\left(\frac{a_{s,init}}{a_{s,vir}}\right)^3 + \rho_\Lambda}{\rho_{m0}a_{vir}^{-3} + \rho_\Lambda} - 1\end{aligned} \tag{5.13}$$

The quantities are the same as for (5.10) and (5.11), except for the scale factors which now are given at virialization, $a = a_{vir}$ and $a_s = a_{s,vir}$. Again there are many things to take into consideration so I will leave the interpretation with these two last expressions for the density contrasts and trust the simulation.

[4] For a closer explanation see John A. Peacock [14] p. 489.

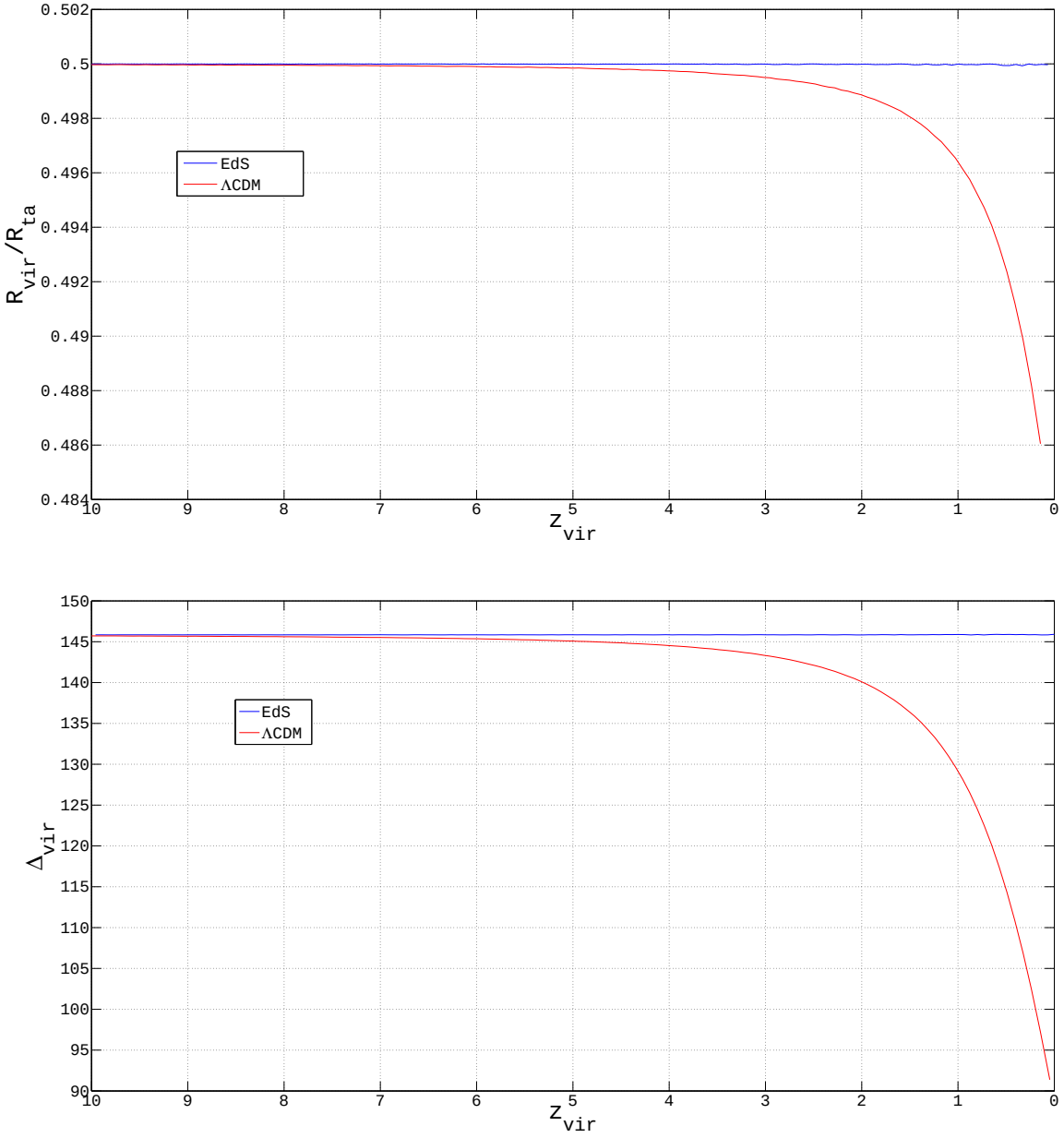

Figure 5.6: Top plot: The radius given as R_{vir}/R_{ta} at virialization simulated for a spherical collapse in the EdS and the ΛCDM universe. Bottom plot: The density contrast Δ_{vir} at virialization simulated for a spherical collapse in the EdS and the ΛCDM universe.

Chapter 6

Spherical Collapse in Dark Energy Universe Models

This chapter will have the same structure as chapter 5. It begins with a section that studies only the dynamics of the sphere, i.e. without any virial conditions to halt the collapse. This will be done in several types of dark energy models which will be compared with each other, and also compared with the same situations in the ΛCDM model. In the next section three new types of virialization conditions will be introduced and derived. These conditions takes into account different types of imposed properties to the dark energy component. In the third section these new virial conditions are included in the spherical collapse simulation inside many different dark energy models with a constant equation of state. These simulations are presented in plots and one realizes that the different types of properties imposed to the dark energy have significant impact to the evolution of the spherical collapse.

6.1 Dynamics in Dark Energy Universe Models

The Friedmann equations for universe models which includes certain types of dark energy components X is given in the appendix B.1. These types of dark energies are characterized by *constant* values of $-1 < w < 0$ in the models' equation of state. The equations (B.29), (B.30) and (B.31), implies

$$\frac{\dot{a}^2}{a^2} = \frac{8\pi G}{3}\Big(\rho_m + \rho_X\Big) \tag{6.1}$$

$$\frac{\ddot{a}}{a} = -\frac{4\pi G}{3}\Big(\rho_m + (1+3w)\rho_X\Big) \tag{6.2}$$

$$\rho_m = \rho_{m0}a^{-3} \quad \text{and} \quad \rho_X = \rho_{X0}a^{-3(1+w)} \tag{6.3}$$

where ρ_{m0} and ρ_{X0} are the densities of CDM and X, respectively, at present time. As noted in the appendix B.1.3, for $w = -1$, these two Friedmann equations gives the same Friedmann equations (B.18) and (B.19) which describes the ΛCDM universe. Not mentioned is that, for $w = 0$, they also gives the Friedmann equations (B.4) and (B.5) for the EdS universe because then X behaves equal as CDM and 'adds itself to' CDM such that $\rho_m + \rho_X = \rho_{m0}a^{-3} + \rho_{X0}a^{-3(1+0)} \longrightarrow \rho_m$. A third thing to note is that, when considering (6.2), the second term on the RHS contributes with a *positive* value to $\ddot{a}$ *only* for $w < -\frac{1}{3}$. Thus to simulate a universe model which achieve a positive accelerated expansion at some time before present (or in the future) its equation of state needs to have $w < -\frac{1}{3}$.

In section (5.1), the dynamics of the ΛCDM universe where discussed, and some of its effects on collapsing spheres where considered and compared with similar collapsing spheres in the EdS universe. Because the ΛCDM universe have had an accelerating expansion for the last 3.7 billion years, it was speculated that a sphere evolving in this universe should need more time to collapse than its corresponding collapsing sphere evolving in the EdS universe. This was later shown to be supported by the numerical data generated by the program code which simulated these two different systems, and the data was presented in the figures (5.1) and (5.2) etc.

One can now continue these speculations and ask how a sphere would behave within a background universe, described by (6.1), (6.2) and (6.3), when w is still a constant but somewhere *in between* the values -1 and 0. From the acceleration equation (6.2) one realize that the expansion rate is fully dependent on the equation of state, i.e. the value of w. Therefore, for a representative sample of these w-values, a relation between $\ddot{a}$ and w are illustrated in figure 6.1 below. It shows how $\ddot{a}$ changes from an early time corresponding to a redshift $z = 1100$ and until the present, i.e. at $z = 0$.

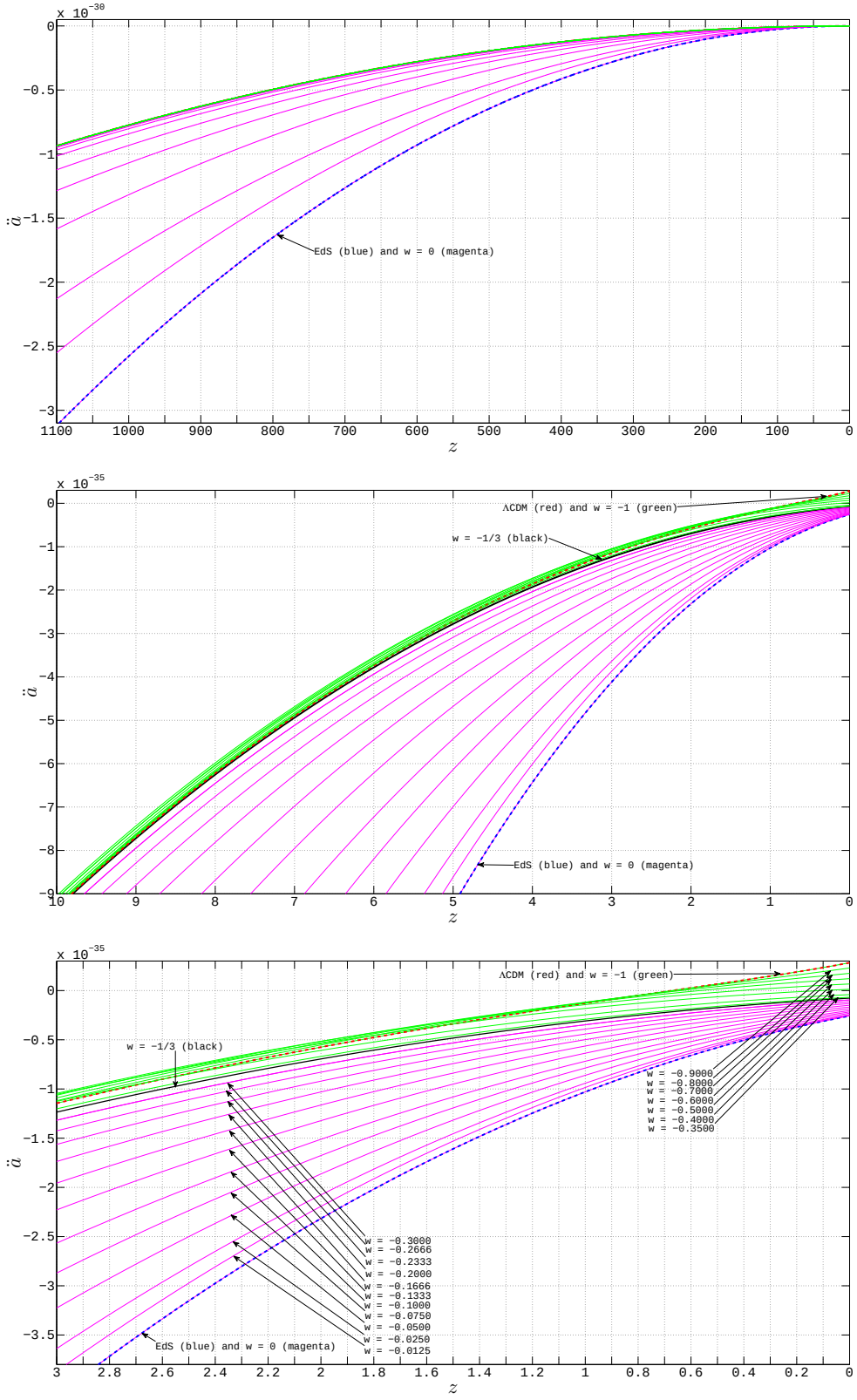

Figure 6.1: Evolution of the expansion acceleration in the EdS model, ΛCDM model, and dark energy models with -1 ≤ w ≤ 0. Note that in appendix A there is also a related figure A.1 showing the evolution of the energy density parameters for these universe models.

Important to note about the many accelerations $\ddot{a}$ in figure (6.1) is that they obviously evolves differently during this redshift interval $z \in [0, 1100]$. Particularly interesting is it to compare these different evolutions of $\ddot{a}$ with the acceleration $\ddot{a} = \ddot{a}_\Lambda$ for the ΛCDM universe represented by the red dashed line. It appears that the ΛCDM universe is the first model to get a positive acceleration (at $z \approx 0.67$), and for the rest, only the models with approximately $-1 < w \leq -0.5$ gets a positive acceleration *before* present time ($z = 0$). And as already stated, one also sees an indication that those $\ddot{a}$ corresponding to $w > -\frac{1}{3}$ never will be positive. That is, the black line representing the $\ddot{a}$ for $w = -\frac{1}{3}$ appears to move asymptotically to zero in the future.

For the $-1 < w \leq -0.5$ models it might be intuitive to conclude that spheres evolving inside them must collapse *faster* than similar spheres in the ΛCDM universe since the ΛCDM universe have had the longest ongoing *positive* acceleration, and therefore have generated the longest 'breaking' effect, which thus retards the collapse the most. But when studying figure 6.1 a bit closer, one sees that toward greater redshifts, all of the $\ddot{a}$ of the universe models corresponding to $-1 < w \leq -0.5$, has a greater $\ddot{a}$ than $\ddot{a}_\Lambda$. This can be seen for $z \approx 10$ in the middle plot of the figure. So for $z > 10$ all these now considered $\ddot{a}$'s have been greater than $\ddot{a}_\Lambda$ (not so easy to see from the top plot, unfortunately) which then *maybe* have the effect that a collapsing sphere still needs *longer* time to collapse in these universe models, compared to a similar sphere in the ΛCDM universe.

Another essential thing to take into consideration when describing how a particular sphere evolves within a particular dark energy model is how the contents that constitute the sphere behaves. For the density $\rho_{m,s}$ of the CDM inside the sphere it has already been stated that

$$\rho_{m,s} \propto a_s^{-3} \tag{6.4}$$

where a_s is the scalefactor of the sphere. For the dark energy X it is here considered to be either homogeneous at all times, i.e. its density $\rho_{X,s}$ *inside* the sphere only depends on the scalefactor a of the background universe, or the X is fully clustering, which means that the density of X inside the sphere depends on the scalefactor a_s of the sphere in a specific way decided by the constant value of w. That is,

$$\begin{aligned} &\rho_{X,s} \propto a^{-3(1+w)} \quad \text{for non-clustering } X, \text{ or} \\ &\rho_{X,s} \propto a_s^{-3(1+w)} \quad \text{when } X \text{ is clustering.} \end{aligned} \tag{6.5}$$

With these statements (6.4) and (6.5) in mind, the expression of the acceleration $\ddot{a}_s$ of the sphere's scalefactor is important to understand. This equation is basically telling

how the sphere shall evolve in a specific background universe model with some specific properties of the dark energy. From the appendix B.1.3 (when not stated as a function of the redshift z), $\ddot{a}_s$ is implied from (B.36) as

$$\boxed{\ddot{a}_s = -\frac{4\pi G}{3}\Big(\rho_{m,s} + (1+3w)\rho_{X,s}\Big)a_s} \tag{6.6}$$

where, more specifically,

$$\boxed{\rho_{m,s} = \rho_{m,s,init}\Big(\frac{a_{s,init}}{a_s}\Big)^3} \tag{6.7}$$

and

$$\boxed{\begin{array}{ll} \rho_{X,s} = \rho_{X0}a^{-3(1+w)} & \text{for non-clustering } X, \text{ or} \\ \\ \rho_{X,s} = \rho_{X,s,init}\Big(\frac{a_{s,init}}{a_s}\Big)^{3(1+w)} & \text{when } X \text{ is clustering.} \end{array}} \tag{6.8}$$

Here ρ_{X0} is the present density of the background dark energy, and $\rho_{X,s,init}$ is dark energy density inside the sphere at the initial time for the calculation of the sphere's evolution.

As for the background universe, when considering $\ddot{a}_s$ in (6.6) it is crucial to note that for $w < -\frac{1}{3}$ the dark energy density $\rho_{X,s}$ inside the sphere contributes with a *positive* term. This can be interpreted as a form of pressure or vacuum energy etc. However, the important thing here is that this effect acts as an opposite force to gravity, i.e. it works *against* the gravitational collapse of the sphere. Also important to note for the $w \in [-1, 0]$, is that as closer w is to zero, the faster the density $\rho_{X,s}$ of the clustering version of X, *increases* with decreasing a_s, as the equation in (6.8) shows. This implies some kind of 'trade of' between the values of w and $\rho_{X,s}$ which one should be aware of especially when one wish to explain those cases where $\rho_{X,s}$ contributes with a positive term in (6.6) and thus making the collapse go slower because of the additional force it generates which works against the gravitational force.

6.1.1 Collapsing sphere with non-clustering dark energy

By first consider the four plots in figure 6.2, where the dark energy is homogeneous, the recent speculations, that sphere's needs *longer* time to collapse in universe models with

approximately $-1 < w \leq -0.5$ compared with similar spheres in the ΛCDM universe model, gets supported by the numerical data when simulating collapses in the three different background universe models for $w = -0.8$, $w = -0.6$ and $w = -0.4$. Note that the trend continues for $w > -0.5$, even though $\ddot{a}$ for the $w = -0.4$ universe has not reach a positive accelerated expansion at present time, as discussed in figure (6.1). The reason for this is that the homogeneous dark energy density $\rho_{X,s}$ inside the sphere (which in this case only depends on the background) gets diluted by a slower rate than the homogeneous dark energies in the $w = -0.6$ and $w = -0.8$ universes. Thus, because $\rho_{X,s}(w = -0.4) > \rho_{X,s}(w = -0.6) > \rho_{X,s}(w = -0.8)$ for any background scalefactor a it means that $\rho_{X,s}(w = -0.4)$ contributes with the greatest positive term on the RHS of (6.6) and thus it generates the greatest outward pressure which slows down the collapse the most. This means that the spheres with $\rho_{X,s}(w = -0.4)$ is the ones reaching $a_s = 0$ closest to $z = 0$, compared with the other considered spheres. This is just what the last plot in figure 6.2 shows. Also note that all the spheres in the three last plots in this figure collapses toward zero ($a_s \to 0$) closer to $z = 0$ compared to the corresponding spheres in the ΛCDM plot at the top.

To make a specific example, one can consider the more detailed figure 6.3 which basically shows the same plots as figure 6.2, but the redshift interval has been zoomed in to $z \in [0, 1]$. Note that the top plot in this figure 6.3 shows collapses for both the EdS and the ΛCDM universe, and it only shows the lines which represents the strongest initially perturbed spheres, i.e. $\Delta_i \in [1 \cdot 10^{-3}, 5 \cdot 10^{-3}]$ because those are the most interesting. One can start out by consider only the blue line in the ΛCDM plot which represents the evolution of a sphere with the strongest initial density contrast $\Delta_i = 5 \cdot 10^{-3}$. This sphere reaches $a_s = 0$ at $z = z_\Lambda \approx 0.84$. For the same sphere evolving in the $w = -0.8$ model it reaches $a_s = 0$ at $z = z_{-0.8} \approx 0.74$. By doing the same inspections for the last two plots one sees that the similar sphere reaches $a_s = 0$ at $z = z_{-0.6} \approx 0.54$ for the $w = -0.6$ model, and $a_s = 0$ at $z = z_{-0.4} \approx 0.075$ for the $w = -0.4$ model. So the relation is

$$\begin{gathered} z_\Lambda(a_s = 0) > z_{-0.8}(a_s = 0) > z_{-0.6}(a_s = 0) > z_{-0.4}(a_s = 0) \\ \Longleftrightarrow \\ 0.840 > 0.740 > 0.540 > 0.075 \end{gathered} \tag{6.9}$$

for when the similar collapses happens in the considered models. That is, at least for universe models with $-1 < w \leq -0.4$ and a passive dark energy component which now have been simulated.

This example now performed can be applied for all the considered collapsing spheres presented in the figures 6.2 and 6.3. That is, for those lines which by inspection are possible to distinguish. All the plots shows the same set of initially perturbed spheres which evolves in a specific way fully determined by the acceleration equation (6.6) which again is fully dependent on the evolution of the specific background universe and also how its energy content CDM and X evolves.

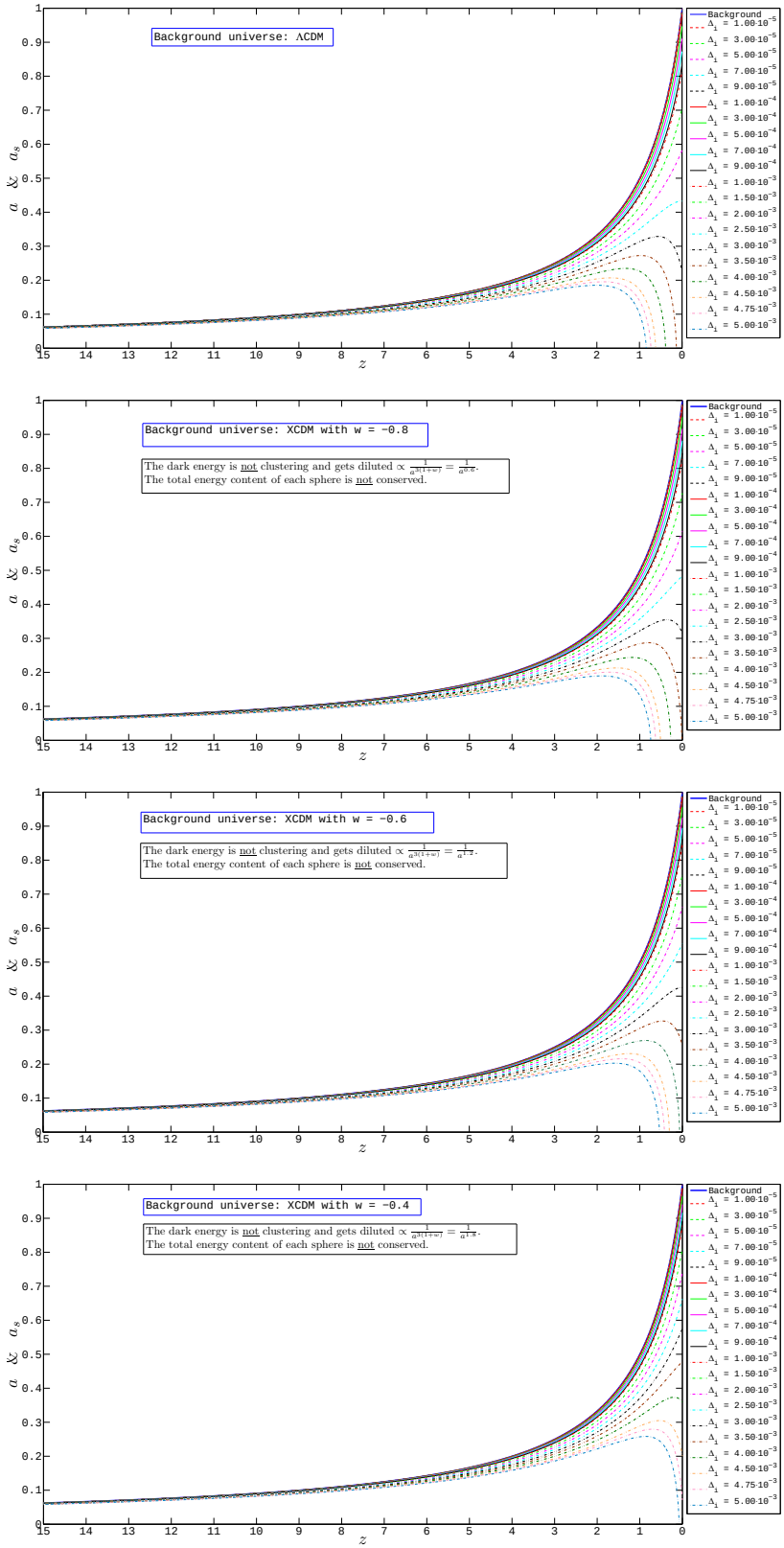

Figure 6.2: The evolution of initial density contrasts $\Delta_i \in [10^{-5}, 5 \cdot 10^{-3}]$ over the redshift interval $z \in [0, 15]$ in dark energy models with $w = -0.8$, $w = -0.6$ and $w = -0.4$. The dark energy is homogeneous and only dependent on the background, thus the energy within each of these spheres is not conserved.

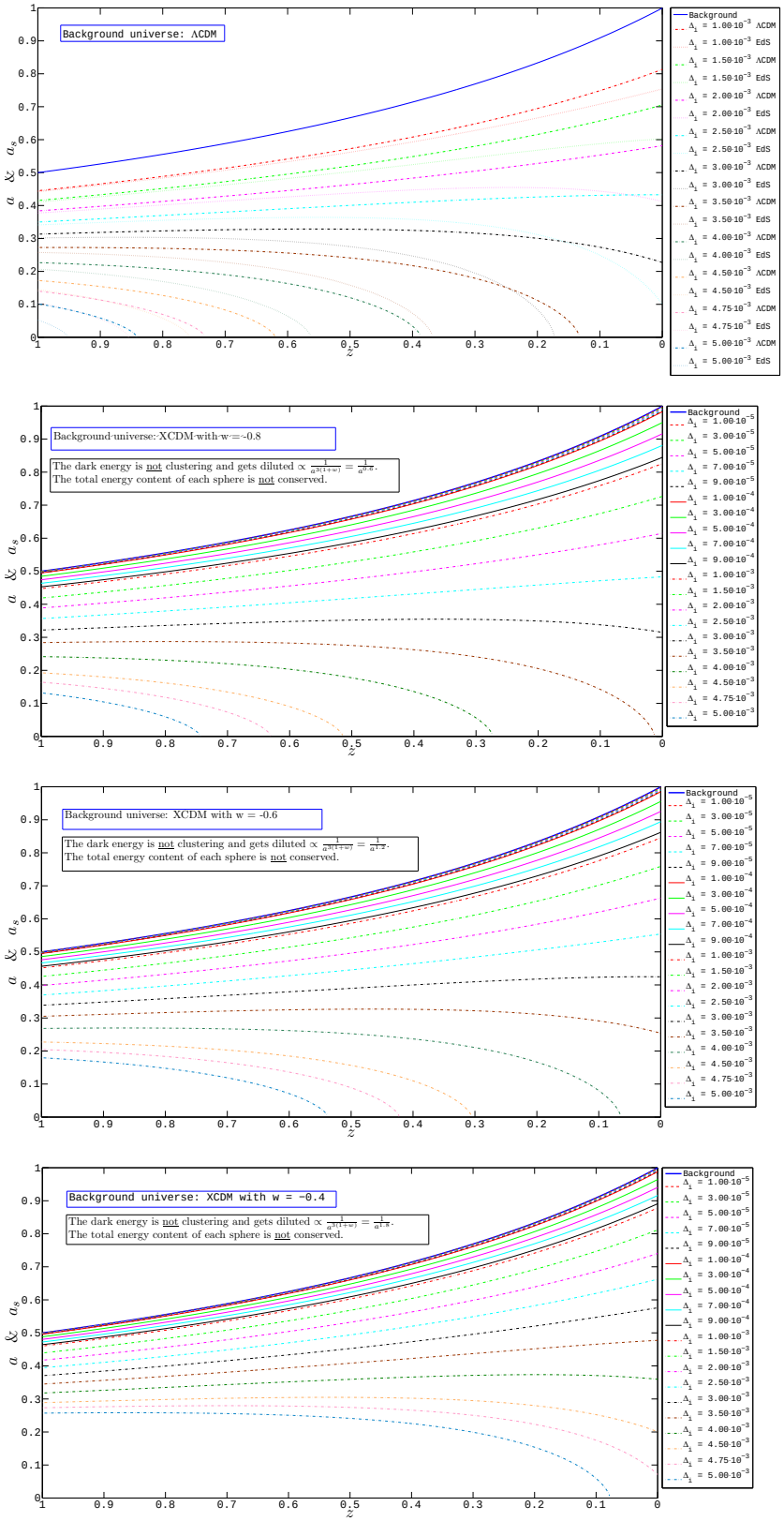

Figure 6.3: The evolution of initial density contrasts $\Delta_i \in [10^{-5}, 5 \cdot 10^{-3}]$ over the redshift interval $z \in [0, 1]$ in dark energy models with $w = -0.8$, $w = -0.6$ and $w = -0.4$. The dark energy is homogeneous and only dependent on the background, thus the energy within each of these spheres is not conserved.

6.1.2 Collapsing sphere with clustering dark energy

In this subsection figure 6.4 and 6.5 will be discussed. They show plots with some other results than their similar plots in figure 6.2 and 6.3, i.e. they all collapse *later*. The reason is that X in these situations is required to fully cluster inside the sphere as described in (6.5). This means

$$\rho_{X,s}(clustering) > \rho_{X,s}(homogeneous) \tag{6.10}$$

at any time in the sphere's evolution. By considering the sphere's acceleration equation (6.6) again one realize that $\rho_{X,s}(clustering)$ will contribute to a greater positive term on the right side compared with $\rho_{X,s}(homogeneous)$ when this comparing is done with the same $w < -\frac{1}{3}$.

To also make a specific example for this property of the dark energy, one can consider the more detailed figure 6.5 within the redshift interval $z \in [0, 1]$. Again, start out by consider only the blue line in the ΛCDM plot which represents the evolution of a sphere with the strongest initial density contrast $\Delta_i = 5 \cdot 10^{-3}$. Its line reaches $a_s = 0$ at $z = z_\Lambda \approx 0.84$. For the same sphere evolving in the $w = -0.8$ model it reaches $a_s = 0$ at $z = z_{-0.8} \approx 0.725$. The same inspections for the last two plots shows that the similar sphere reaches $a_s = 0$ at $z = z_{-0.6} \approx 0.465$ for the $w = -0.6$ model, and it have not yet reached $a_s = 0$ at present time for the $w = -0.4$ model. The relation is

$$\begin{gathered} z_\Lambda(a_s = 0) > z_{-0.8}(a_s = 0) > z_{-0.6}(a_s = 0) > z_{-0.4}(a_s = 0) \\ \Longleftrightarrow \\ 0.84 > 0.725 > 0.465 > z_{-0.4}(a_s = 0) \end{gathered} \tag{6.11}$$

where $z_{-0.4}(a_s = 0) < 0$, i.e. the sphere in the $w = -0.4$ model reach $a_s = 0$ some time in the future.

When comparing this relation (6.11) with the similar relation in (6.9) it becomes obvious that clustering dark energy has the effect of slowing down the evolution of collapsing spheres in the types of cosmological fluids now considered

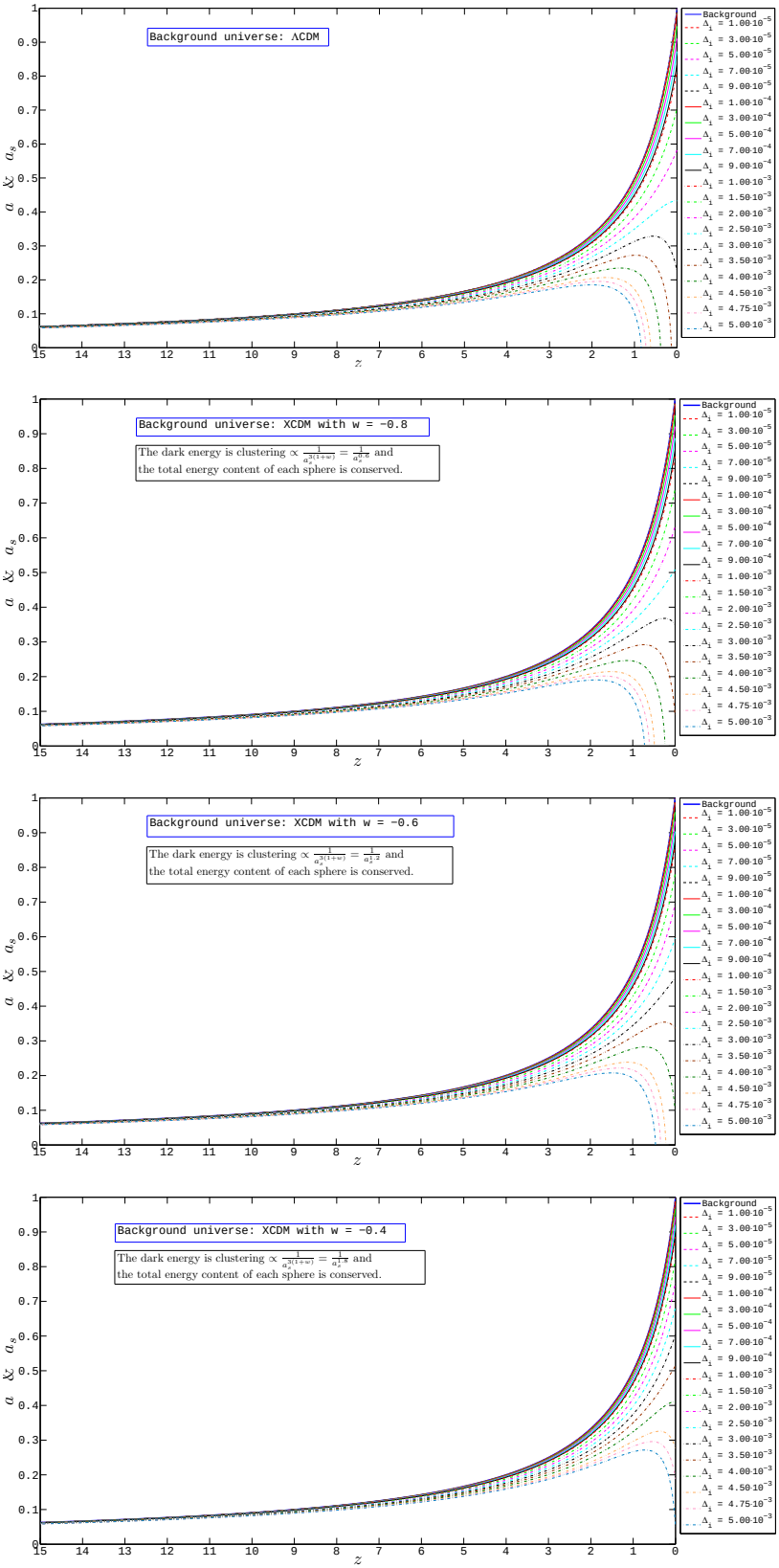

Figure 6.4: The evolution of initial density contrasts $\Delta_i \in [10^{-5}, 5 \cdot 10^{-3}]$ over the redshift interval $z \in [0, 15]$ in dark energy models with $w = -0.8$, $w = -0.6$ and $w = -0.4$. The dark energy is fully clustering and dependent on the scalefactor of the sphere. Thus the energy within each of these spheres is conserved.

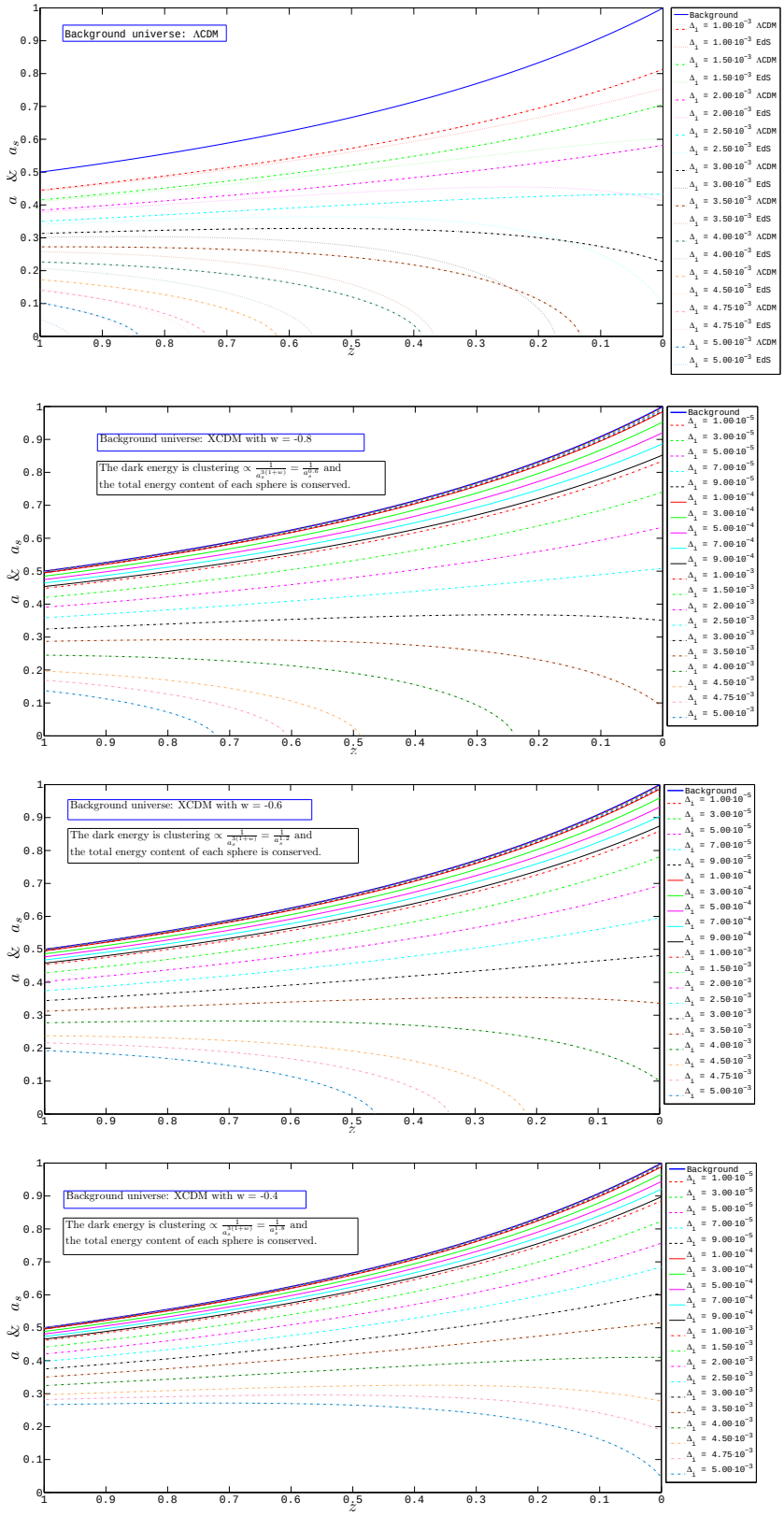

Figure 6.5: The evolution of initial density contrasts $\Delta_i \in [10^{-5}, 5 \cdot 10^{-3}]$ over the redshift interval $z \in [0, 1]$ in dark energy models with $w = -0.8$, $w = -0.6$ and $w = -0.4$. The dark energy is fully clustering and dependent on the scalefactor of the sphere. Thus the energy within each of these spheres is conserved.

6.2 Virialization Conditions

So far in this chapter's discussion of dynamics in dark energy models - no mechanism to stop the sphere's collapse towards $a_s = 0$ have been considered. This mechanism is handled by the virialization conditions and have already been derived for the EdS universe (4.30) and for the ΛCDM universe (5.9). Because spherical collapse is now considered in other types of universe models, new virialization conditions needs to be introduced.

The virialization conditions depends on the specific backgrounds and the properties being imposed to the dark energy. In this section, three different virialization conditions will be derived. The first condition require the dark energy to be *passive* and *non-clustering*, the second condition require the dark energy to be *dynamical* and *clustering*, and the third condition require the dark energy to be *dynamical* and *non-clustering*.

6.2.1 Virialization condition for passive and non-clustering dark energy

This virialization condition includes a passive dark energy component X with a density ρ_X inside the sphere that is dependent on the evolution of the background. That is, $\rho_X \propto a^{-3(1+w)}$ where a is the scalefactor of the background universe. It is applied in the article [4] by Horellou and Berge where also the potential energy U_X associated with X is given.

The Poisson equation, in spherical coordinates, with the pressure term $p_X = w\rho_X$, is given as[1]

$$\begin{aligned} \nabla^2\Phi_X = \frac{1}{r^2}\frac{d}{dr}\Big(r^2\frac{d\Phi_X}{dr}\Big) = 4\pi G\rho = 4\pi G(\rho_X + 3p_X) \\ \iff \quad \nabla^2\Phi_X = 4\pi G(1+3w)\rho_X \end{aligned} \tag{6.12}$$

where Φ_X is the potential of X, R is the radius of the sphere, G is the gravitational constant, and ρ_X is the density of the dark energy. By integration this yields[2]

$$\Phi_X = (1+3w)\rho_X\frac{2\pi G}{3}R^2 \tag{6.13}$$

and then by using the same form of integration as in (5.7) done for U_Λ, gives

[1] [8] p. 199.
[2] [8] p. 199-200.

$$U_X = \frac{M_s}{V}\int \Phi_X dV = \frac{3M_s}{4\pi R^3}(1+3w)\rho_X \frac{2\pi G}{3}\int_0^R r^2 4\pi r^2 dr \quad \text{i.e.}$$

$$\boxed{U_X = (1+3w)\rho_X \frac{2\pi G M_s}{5}R^2} \tag{6.14}$$

where M_s is the total mass (CDM) of the sphere, V is the total volume of the sphere, and $dV = 4\pi r^2 dr$. Note that this expression for U_X has the limit for the potential energy U_Λ of the cosmological constant Λ, i.e. when $w = -1$ and $\rho_X = \rho_\Lambda = \frac{c^2\Lambda}{8\pi G}$ it reproduces the potential energy $U_\Lambda = -\frac{c^2}{10}\Lambda M_s R^2$ derived in (5.7).

The virialization condition including this type of X has the same form as for the ΛCDM universe. The derivation is the same as the one in (5.9) only with the replacement of $U_\Lambda \to U_X$. Thus, the virialization condition for a passive X which do not cluster is:

$$\boxed{\frac{1}{2}U_m(a_{s,vir}) + 2U_X(a_{s,vir}) = U_m(a_{s,ta}) + U_X(a_{s,ta})} \tag{6.15}$$

where $U_m = -\frac{3GM_s}{5R}$ is the potential energy of the CDM from (4.24). Note that the physical radius R of the sphere have been replaced with the sphere's scalefactor a_s which has an equivalent meaning in this context.

6.2.2 Virialization condition for dynamical and clustering dark energy

This virialization condition includes a dynamical dark energy component X with a density $\rho_{X,s}$ inside the sphere that is fully clustering in the same way as CDM, the only difference being its equation of state which dictates a different energy conservation, i.e.

$$\rho_{X,s} \propto a_s^{-3(1+w)} \tag{6.16}$$

where a_s is the scalefactor of the sphere. However, energy is conserved, and since the dark energy is dynamical and thus active in the dynamics of the system, it is reasonable to imagine that it takes part in the virialization process. This virialization condition is applied in the article [3] by Maor and Lahav where also the expression of the potential

energy U_X associated with X is stated. A slightly more detailed derivation of these two equations will now follow, but it is fully based on [3].

When the full system virializes, the virial theorem should relate the full kinetic and potential energies of the system. The total potential energy is

$$U = \frac{1}{2}\int (\rho_{m,s} + \rho_{X,s})(\Phi_m + \Phi_X)dV \tag{6.17}$$

where Φ_m and Φ_X are the potentials induced by each energy component in a spherical homogeneous configuration given by[3]

$$\Phi_y(r) = -2\pi G(1+3w_y)\rho_{y,s}\Big(R^2 - \frac{r^2}{3}\Big) \tag{6.18}$$

where the subnotation y stands for m or X, and $r \in [0, R]$. The total kinetic energy K at virialization is

$$K = \frac{1}{2}R\frac{\partial U}{\partial R} \tag{6.19}$$

With the two equations (6.17) and (6.18), the expression for the total potential energy U can be derived. From (6.18) the potential for the CDM ($w = 0$) and X ($-1 \leq w < 0$) is

$$\Phi_m(r) = -2\pi G\rho_{m,s}\Big(R^2 - \frac{r^2}{3}\Big) \quad \text{and} \quad \Phi_X(r) = -2\pi G(1+3w)\rho_{X,s}\Big(R^2 - \frac{r^2}{3}\Big), \tag{6.20}$$

respectively, and with some standard algebra, the integrand of the total potential energy U in (6.17) yields

$$(\rho_{m,s}+\rho_{X,s})(\Phi_m+\Phi_X) = -2\pi\Big(\rho_{m,s}^2+(2+3w)\rho_{m,s}\rho_{X,s}+(1+3w)\rho_{X,s}^2\Big)\Big(R^2-\frac{r^2}{3}\Big) \tag{6.21}$$

Then by substituting this into (6.17) gives

[3] [8] p. 200.

$$
\begin{aligned}
U &= -\frac{1}{2}2\pi\Big(\rho_{m,s}^2 + (2+3w)\rho_{m,s}\rho_{X,s} + (1+3w)\rho_{X,s}^2\Big)\int_0^R \Big(R^2 - \frac{r^2}{3}\Big)4\pi r^2 dr \\
&= -\frac{3GM_s^2}{5R} - (2+3w)\frac{4}{5}\pi G M_s \rho_{X,s} R^2 - (1+3w)\frac{16\pi^2 G}{15}\rho_{X,s}^2 R^5
\end{aligned}
\tag{6.22}
$$

where $dV = 4\pi r^2 dr$. To end up with the expression of U implemented in the program code for this thesis, one now have to consider how $\rho_{m,s}$ and $\rho_{X,s}$ acts. They depend on the scalefactor a_s of the sphere as

$$
\rho_{m,s} = \rho_{m,s,ta} a_s^{-3} \quad \text{and} \quad \rho_{X,s} = \rho_{X,s,ta} a_s^{-3(1+w)} \tag{6.23}
$$

where $\rho_{m,s,ta}$ and $\rho_{X,s,ta}$ is the density of CDM and X inside the sphere, respectively, at turnaround. By substituting (6.23) into (6.22) and continue to use the physical radius R, and not the scalefactor a_s, gives the following equivalent expression for (6.22) after some more standard algebra:

$$
\boxed{
\begin{aligned}
U = -\frac{16\pi^2 G}{15}\Bigg[&\rho_{m,s,ta}^2 R_{ta}^6 R^{-1} + (2+3w)\rho_{m,s,ta}\rho_{X,s,ta} R_{ta}^{3(2+w)} R^{-(1+3w)} \\
&+ (1+3w)\rho_{X,s,ta}^2 R_{ta}^{6(1+w)} R^{-(1+6w)}\Bigg]
\end{aligned}
}
\tag{6.24}
$$

where $R_{ta} = constant$ is the physical radius at turnaround. Then by substituting this final expression for U into the expression for the total kinetic energy K in (6.19) the implemented expression for K follows:

$$
\boxed{
\begin{aligned}
K = \frac{8\pi^2 G}{15}\Bigg[&\rho_{m,s,ta}^2 R_{ta}^6 R^{-1} + (1+3w)(2+3w)\rho_{m,s,ta}\rho_{X,s,ta} R_{ta}^{3(2+w)} R^{-(1+3w)} \\
&+ (1+6w)(1+3w)\rho_{X,s,ta}^2 R_{ta}^{6(1+w)} R^{-(1+6w)}\Bigg]
\end{aligned}
}
\tag{6.25}
$$

Then finally, by utilizing energy conservation between turnaround and virialization, i.e.

$$U_{vir} + K_{vir} = U_{ta} + K_{ta} \tag{6.26}$$

the virialization condition follows as

$$\boxed{U(a_{s,vir}) + K(a_{s,vir}) = U(a_{s,ta})} \tag{6.27}$$

which implicitly state the radius at virialization $R_{vir} \Leftrightarrow a_{s,vir}$ when it is fulfilled. That is, when $U(a_{s,vir})$ and $K(a_{s,vir})$ have been substituted by (6.24) and (6.25), respectively, and $U(a_{s,ta})$ have been determined. Note that the kinetic energy at turnaround must be zero, i.e. $K_{ta} = 0$, and R_{ta} and R_{vir} has once again been replaced with its corresponding $a_{s,ta}$ and $a_{s,vir}$ so to have the same form as the virialization condition (6.15).

6.2.3 Virialization condition for dynamical and non-clustering dark energy

Often are spatial perturbations in the dark energy neglected, i.e. it is considered to be non-clustering (i.e. homogeneous), only dependent on the background universe. This implies that the system of spherical collapse does not conserves energy. Because the virialization condition (6.27) is based on energy conservation (6.26) between turnaround and virialization, a problem arises of how to define the right radius of virialization. Again referring to the article [3] by Maor and Lahav, a correction to equation (6.27) that will take into account the loss of energy, will now be presented.

A new function $\tilde{U}$ is defined as the sphere's potential energy *had* it conserved energy. Thus the energy lost by the sphere can be expressed as

$$\Delta U \equiv \tilde{U} - U \quad \Rightarrow \quad \Delta U_{vir} \equiv \tilde{U}_{vir} - U_{vir} \tag{6.28}$$

where U is the potential energy of the sphere which do *not* conserve energy. Firstly, the equation stating energy conservation (6.26), where $K_{ta} = 0$, can be rewritten as

$$\Big[U + \frac{R}{2}\frac{\partial U}{\partial R}\Big]_{vir} = U_{ta} \tag{6.29}$$

where $K_{vir} = \left[\frac{R}{2}\frac{\partial U}{\partial R}\right]_{vir}$ implied by equation (6.19). Now, accounting for the lost energy ΔU, equation (6.29) can be corrected such that

$$\begin{aligned} &\Big[U + \frac{R}{2}\frac{\partial U}{\partial R}\Big]_{vir} + \Delta U_{vir} = U_{ta} \\ \iff \quad &\boxed{\Big[\tilde{U} + \frac{R}{2}\frac{\partial U}{\partial R}\Big]_{vir} = U_{ta}} \end{aligned} \tag{6.30}$$

where $\tilde{U}_{vir} = U_{vir} + \Delta U_{vir}$ from (6.28). This is the virialization condition which take into account the loss of energy inside the sphere. This needs some further explanation.

By looking at (6.22), and remembering that it is equivalent with (6.24), one realize that $U = U(\rho_{m,s}, \rho_{X,s}, R)$. Then in order to calculate $\tilde{U} = \tilde{U}(\rho_{m,s}, \rho_{X,s}, R)$, one needs to replace $\rho_{X,s}$ with $\tilde{\rho}_{X,s} \propto a_s^{-3(1+w)}$. That is, when calculating $\tilde{U}$, one need to use the density $\tilde{\rho}_{X,s}$ which is the density of the dark energy inside the sphere *had* it been fully clustering. Thus

$$\tilde{U}(\rho_{X,s}, \rho_{m,s}, R) = U(\tilde{\rho}_{X,s}, \rho_{m,s}, R) \tag{6.31}$$

where in *this* subsection

$$\rho_{X,s} \propto a^{-3(1+w)} \quad \text{but} \quad \tilde{\rho}_{X,s} \propto a_s^{-3(1+w)} \tag{6.32}$$

Note that the relation (6.31) shall <u>not</u> be used for the U when calculating the kinetic al energy $K = \frac{R}{2}\frac{\partial U}{\partial R}$ in the virialization condition (6.30). For this expression of K the potential energy is the non-corrected $U = U(\rho_{X,s}, \rho_{m,s}, R)$ which means it is using the U which do not corrects the loss of energy.

Finally, it is important to be aware of the boundary conditions $\tilde{\rho}_{X,s,ta} = \rho_{X,s,ta}$, which states that the two densities are equal at turnaround. That is

$$\tilde{\rho}_X(a_{s,ta})\Big(\frac{R_{ta}}{R_{vir}}\Big)^{3(1+w)} = \rho_X(a_{s,ta})\Big(\frac{R_{ta}}{R_{vir}}\Big)^{3(1+w)} \tag{6.33}$$

i.e. $\tilde{\rho}_X(a_{s,ta}) = \rho_X(a_{s,ta})$.

This was the end of the presentation for the last three virialization conditions considered in this thesis. The next section will present the simulations when including these conditions to spherical collapse in the dark energy models now introduced, and in addition to many more.

6.3 Numerical Simulations

In this section, three parameters will be presented in plots:

- Density contrast at turnaround Δ_{ta}
- Radius at virialization R_{vir}
- Density contrast at virialization Δ_{vir}

(Note that appendix A contains additional plots for these parameters given as functions of initial density contrasts Δ_i.)

These are the numerical data generated by the code when it simulates the evolution of overdense spheres inside the dark energy models presented in section 6.1 and in additional models with other constant values of $w \in [-1, 0]$. Regarding the two latter parameters they are a result by adopting the virialization conditions presented in section 6.2 into these simulations. The effects of each of the three properties of X will be considered in separated plots.

Mainly eight plots will be discussed and each of these contains 21 lines which represents the relevant parameter given for 21 different dark energy models which corresponds to a constant equation of state, i.e. a constant $w \in [-1, 0]$. Note that a discussion of each one of these lines will be much too extensive. The interpretation will therefore focus on the models with an equation of state given with $w = 0$, $w = -1/3$, and $w = -1$. This will give an impression of how the same parameters in the rest of the models evolve by comparison.

6.3.1 Short description of the program code

Before getting to the results it is appropriate to explaine, to a certain extent, how these numerical data are generated, and now that all the relevant analytical equations are presented and mostly derived throughout the thesis, this is thus possible to do. Note that this description will only be given qualitatively.

The program code can roughly be divided into three main levels [4]. In the bottom is the simulation of the background universe described by the Friedmann equations (6.1) and (6.2), and the density evolution of the energy components (6.3). In the second level runs the simulation of the evolution of the initial overdensity given as the homogeneous sphere - which interact with the background. This sphere is basically described by its own second Friedmann equation (6.6), and the density evolution of its energy components given in the equations (6.7) and (6.8). These two levels of the

[4] Even though the following description refers only to equations in chapter 6, it also applies for the parts of the code describing spheres in the EdS and ΛCDM models presented earlier.

code are able to simulate a spherical collapse. But if the sphere ever reach turnaround, then its scalefactor a_s will end up at zero which is non physical. That is, they miss out the most important part of this physical system which is when the sphere reaches virialization. This is where the third level enters. It calculates all the terms in the equation which represents the current virialization condition given by one of them presented in the subsections 6.2.1, 6.2.2 and 6.2.3. Then it compares each side of this equation, and eventually ends the simulation when the condition is met, i.e. when each side are equal. Finally the desired data is written to file, i.e. R_{vir} and Δ_{vir}.

This is the essence of how the code developed for this thesis works, and thus its procedure for generating the data which have so far been presented, and for the remaining which will be presented in the three subsections 6.3.3, 6.3.4, and 6.3.5.

6.3.2 How to read the plots

At first glance of the plots in the figures (6.6), (6.7) and (6.8), they appear messy. But yet there exists a kind of order among all the lines. These lines have different colors relating to how they evolve as functions of redshift z. Lines with the same color evolve in a similar way which should be obvious when observing them. With this in mind, one should read each plot by starting with the line corresponding to $w = -1$ and then continue to look at the other lines corresponding to w-values in *ascending order* all the way to $w = 0$. By doing this one sees that there are a form of continuity between all of them. That is, they all appear to be only *one* line moving through the plot. When this is incorporated it will be easyer to focus on only one line among all the other.

6.3.3 Density contrast Δ_{ta} at turnaround

As emphasized in section 5.3 it is important to know how the density contrast Δ is defined. It has the same definition here but one need to account for the dark energy X which is no longer a constant. In this context the density contrast Δ_{ta} at turnaround is thus defined as

$$\begin{aligned}\Delta_{ta} \equiv \frac{\rho_s - \rho}{\rho} &= \frac{\left(\rho_{m,s,init}(\frac{a_{s,init}}{a_{s,ta}})^3 + \rho_{X,s}\right) - (\rho_{m0}a_{ta}^{-3} + \rho_X)}{\rho_{m0}a_{ta}^{-3} + \rho_X} \\ &= \frac{\rho_{m,s,init}(\frac{a_{s,init}}{a_{s,ta}})^3 + \rho_{X,s}}{\rho_{m0}a_{ta}^{-3} + \rho_X} - 1\end{aligned} \tag{6.34}$$

where

$$\begin{aligned} \rho_{X,s} \equiv \rho_X = \rho_{X0} a^{-3(1+w)} \qquad & \text{for non-clustering } X, \text{ and} \\ \rho_{X,s} = \rho_{X,s,init} \Big(\frac{a_{s,init}}{a_s} \Big)^{3(1+w)} \qquad & \text{for clustering } X. \end{aligned} \tag{6.35}$$

Here ρ_s is the total density of the sphere, ρ is the total background density, $\rho_{m,s,init}$ is the initial CDM density of the sphere, $\rho_{m,s,init}(\frac{a_{s,init}}{a_{s,ta}})^3 = \rho_{m,s,ta}$ is the sphere's CDM density at turnaround, $a_{s,init}$ is the scale factor of the sphere when it starts to evolve, $a_{s,ta}$ is the scale factor of the sphere at turnaround, $\rho_{X,s}$ is the density X inside the sphere, ρ_{m0} is the density of the background CDM at present, a_{ta} is the background scale factor when the sphere reach turnaround, ρ_{X0} is the background density of X at present, and ρ_X is the background density of X at any time.

In figure 6.6, two plots are presented for the density contrast Δ_{ta} at turnaround over a redshift interval approximately $z \in [0, 17]$. The top plot applies to non-clustering dark energy X, and the bottom plot applies to clustering X.

Top plot
The line marked $w = 0$ have a constant value $\Delta_{ta}(w = 0) \approx 3.6$ and by recalling the constant analytical value $\Delta_{ta}(EdS) \approx 4.55$ given in (4.38) for the EdS model one realize that this dark energy model is describing a system which is similar to the EdS model. That is, the *background* has become the EdS model and X has gotten *some* of the same properties as CDM, i.e. $p_X = p_m = 0$ because $w = 0$. However, this system do not have all the same properties as the EdS model because X is required to depend on the background. Thus, even though X has $p_X(w = 0) = p_m = 0$ it gets diluted with the evolution of the background. From the initial time (i.e. z = 1100) 70% of the energy content of the sphere (which in this case is X) is $\propto a^{-3(1+w)} = a^{-3}$ and therefore the sphere loses energy.

The line marked $w = -1$ represents a reproduction of the background ΛCDM model and also of the particular features of its dark energy $X = \Lambda$, i.e. $p_X(w = -1) = p_\Lambda = -\rho_\Lambda c^2 = constant$, because $\rho_X(w = -1) = \rho_\Lambda \propto a^{-3(1+w)} = 1$ when recalling the evolution of X given in (6.5). It is equal to the line in figure 5.5 of section 5.3 which presented the results for the parameters in the ΛCDM model. When $z_{ta} \approx 0$ one sees that $\Delta_{ta}(w = -1) \approx 3.5$, which means that $\Delta_{ta}(w = -1) < \Delta_{ta}(w = 0)$. This is the effect of the accelerating background of the ΛCDM model (from $z \approx 0.67$) which do not exists in the EdS model. When $z_{ta} \to 1100$ one sees that $\Delta_{ta}(w = -1) \to \Delta_{ta}(EdS) \approx 4.55$, i.e. the conditions in the ΛCDM model goes asymptotically towards the EdS model. This is because at these early times the density of CDM dominates completely over the density of Λ and thus Λ is reduced to a negligible energy component.

The rest of the lines, with labels marked $-1 < w < 0$, can be seen to have a behaviour somewhere in between the two w-limits now discussed. They illustrate how dependent

the density contrast Δ_{ta} of an evolving sphere is of the equation of state, and also the property imposed to the X component (non-clustering in this case). For all the blue lines (i.e. $w \in [-0.6, 0]$) one interesting common behaviour to note is that they all are crossing, and they are also crossing the black lines (i.e. $w \in [-1, -0.7]$). This means that one particulary value of Δ_{ta} can correspond to several of these dark energy models.

Bottom plot
The line marked $w = 0$ has a constant value $\Delta_{ta}(w = 0) \approx 4.55$. Again by recalling the constant analytical value $\Delta_{ta}(EdS) \approx 4.55$ given in (4.38) one realize that this system is the result of the simulated dark energy model reproducing the EdS model completely. In this case, the dark energy component X has both of the properties of CDM, which was not the case in the top plot. That is, $p_X(w = 0) = p_m = 0$ and $\rho_X(w = 0) \propto a_s^{-3(1+w)} = a_s^{-3}$. Thus X is clustering identically as CDM.

The line marked $w = -1$ represents a complete reproduction of the ΛCDM model with the same explanation as given for the top plot.

The line marked $w = -1/3$ stands out here compared to its corresponding line in the top plot. When $z_{ta} \approx 0$ it has the strongest density contrast $\Delta_{ta}(w = -1/3) \approx 6.55$. To explain this, one need to consider the second Friedmann equation for both the background universe and the sphere, i.e. the equations (6.2) and (6.6), respectively. These equations (which describes their respective accelerations) shows that for an equation of state with $w = -1/3$, none of them is getting a contribution from the X-term. Thus, the background universe gets *no* contribution from X to 'brake' the collapse, and the X-component inside the sphere do *not* contribute to an outward pressure which works against the force of gravity.

The rest of the lines (i.e. $-1 < w < -1/3$ and $-1/3 < w < 0$) can be seen to have a behaviour somewhere in between these three w-limits now discussed. As said for the top plot, they illustrate how dependent the density contrast Δ_{ta} of an evolving sphere is of the equation of state, and also the property required to the X component (clustering in this case). As for the lines in the top plot, the lines in this bottom plot are also crossing. Thus one needs to be aware of that one particular value of Δ_{ta} are not necessarily enough to decide the equation of state. Another interesting observation in this bottom plot is the line (not shown) corresponding to a value of w somewhere in between $w = -0.8$ and $w = -0.7$. Because all these lines appear to have a continuous connection there should exist a particular value of w which have the same density contrast $\Delta_{ta}(z_{ta} \approx 0)$ as the line corresponding to $w = 0$. Thus, for $z_{ta} \approx 0$ there exist a dark energy model with $-0.8 < w < -0.7$ which mimics the EdS model.

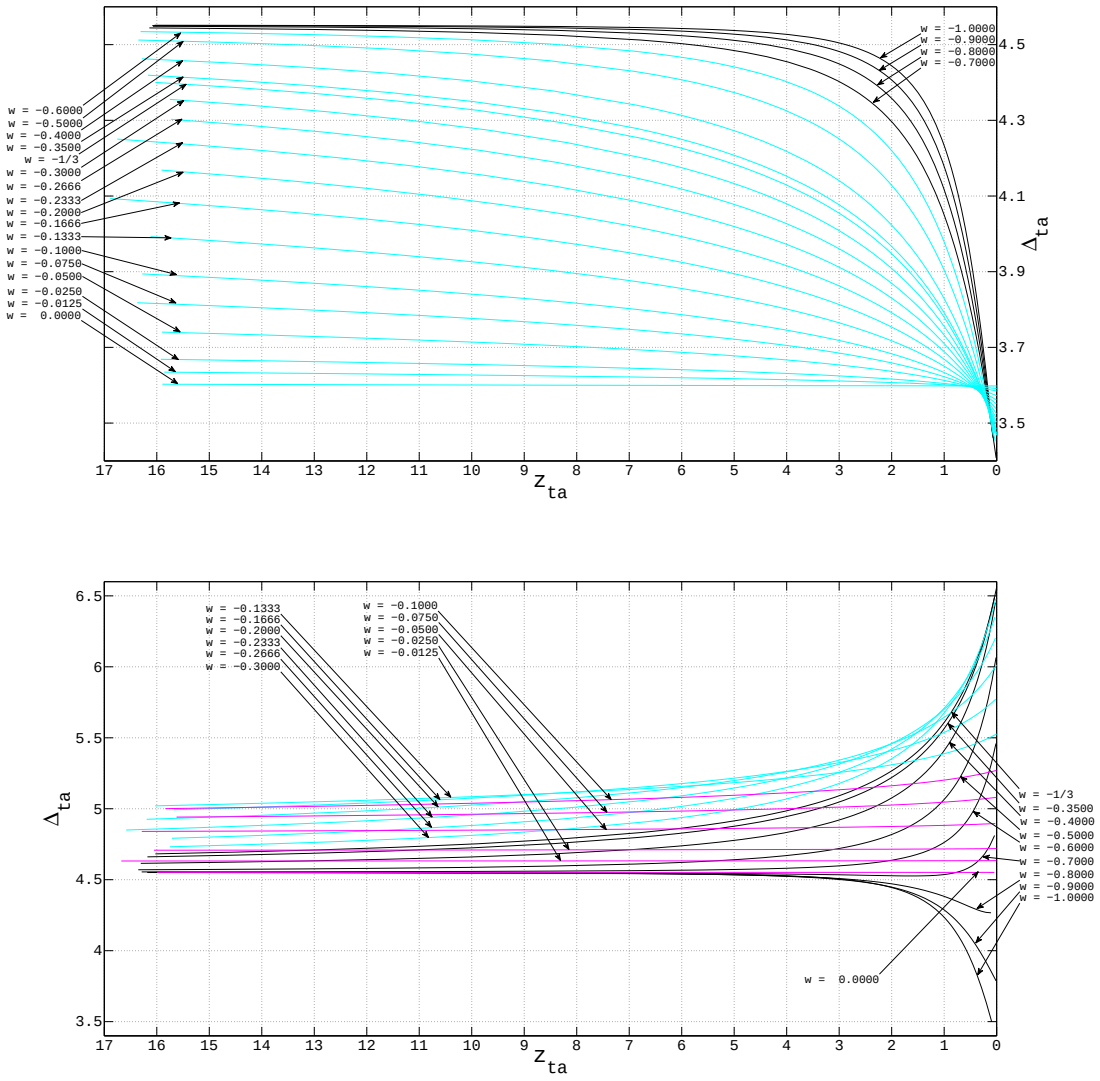

Figure 6.6: Both plots shows the density contrast Δ_{ta} at turnaround as a function of redshift z_{ta}. Top plot: The dark energy is not clustering, i.e. total energy of the sphere is not conserved. Bottom plot: Dark energy is clustering, i.e. total energy of the sphere is conserved.

6.3.4 Radius R_{vir} at virialization

In figure 6.7, three plots are presented for the radius R_{vir} at virialization in the redshift interval $z \in [0, 10]$. The top plot applies to a non-clustering and passive X, the middle plot applies to a non-clustering and dynamical X, and the bottom plot applies to a clustering and dynamical X. These three properties of X was presented in section 6.2.

Top plot

The line marked $w = 0$ shows a constant value $R_{vir}/R_{ta} \approx 0.541$. As explained for the top plot in figure 6.6, the background is the EdS model, but X is a function of the background and thus the sphere loses energy. Then because the conditions in this system is not identical to all the conditions in the EdS model one should expect to see another constant value of R_{vir} than the constant analytical value (i.e. 0.5) given in the derivation (4.29).

The line marked $w = -1/3$ is interesting. This dark energy model mimics the EdS model because the line has the constant value $R_{vir}/R_{ta} = 0.5$. As for the bottom plot in 6.6 one need to consider the second Friedmann equation for both the background universe and the sphere, i.e. the equations (6.2) and (6.6), respectively. For $w = -1/3$, none of them is getting any contribution from the X-term. That is, the background universe gets *no* contribution from X to 'brake' the collapse, and the X-component inside the sphere do *not* contribute to an outward pressure which works against the force of gravity. This can also be explained by the fact that X can not contribute with any force if it is not able to generate any potential, i.e. if $\Phi_X = 0$. When looking at the expression for Φ_X in equation (6.13) one realize that this is the case. Another important thing to consider is that the density $\rho_{X,s}$ of X inside the sphere do not evolve equally as the density $\rho_{m,s}$ of the CDM inside the sphere. That means, even though this dark energy model generates the same R_{vir} as the EdS model, its cosmological fluid has not the same properties as the fluid of the EdS model. Thus, what this line represents is a 'trade of' between how the equation of state tells the fluid of X to evolve, and how it tells X to affect the acceleration of the background and of the sphere.

The line marked $w = -1$ represents a complete reproduction of the ΛCDM model with the same explanation as given for the top plot in figure 6.6. As stated in subsection 6.2.1, this virialization condition (applied to the current plot) reduces to the virialization condition for the ΛCDM model. This line is the the same as the one presented in figure 5.6 of section 5.3 for the ΛCDM model.

The rest of the lines (i.e. $-1 < w < -1/3$ and $-1/3 < w < 0$) can be seen to have a behaviour somewhere in between these three w-limits now discussed. Note that only the lines $-1 \leq w < -1/3$ which refers to models that already have a positive acceleration at $z_{vir} = 0$ *or* are able to achieve it some time in the future (as mentioned in section 6.1 when discussing figure 6.1) is the ones crossing each other. This means, if we happen to live in a universe which we know for sure has $-1 \leq w < -1/3$, and we also happen to know for sure that the virialization condition for this particular plot is the correct one, then we can conclude that there are more than one equation of state which can generate the same virial radius R_{vir} as a consequence of these intersecting lines. To be sure of pointing out the correct w, one needs to observe R_{vir} at more than one redshift z_{vir}.

Middle plot

The line marked $w = 0$ shows a constant value $R_{vir}/R_{ta} \approx 0.574$. As noted in the top plot, $w = 0$ implies that the background universe is described by the EdS model. The difference in this model is that of the new property of X where it is imposed to be dynamical despite its density $\rho_{X,s}$ inside the sphere is dependent of the background. Thus the sphere still loses energy. Because X has this dynamical nature it will participate in the virialization process and therefore it will contribute with a force working against the gravitational force. This implies that $R_{vir}(dynamical\ X)$ have to be greater compared with $R_{vir}(passive\ X)$ for $w = 0$ in the top plot. This conclusion is consistent with what these two plots shows, i.e. $(R_{vir}/R_{ta})_{top\,plot} \approx 0.541 < (R_{vir}/R_{ta})_{middle\,plot} \approx 0.574$.

The line marked $w = -1/3$ is again interesting. One sees a dark energy model mimicing the EdS model because the line has the constant value $R_{vir}/R_{ta} = 0.5$. At first glance this behaviour is maby unexpected because in this context X has a dynamical nature which was not the case when discussing the $w = -1/3$ line in the top plot. Still, here the sphere virializes with radius $R_{vir} = 0.5R_{ta}$. Now, because $\Phi_X = 0$ as explained for the top plot, this new virialization condition (derived in subsection 6.2.2) which takes into consideration a dynamical nature of X, will be reduced to the virialization condition which was applied for the top plot. That is, the equation of state with $w = -1/3$ will impose X to have a passive nature, even though X in genereal for $w \in [-1, 0]$ do not have a passive nature in context with this middle plot.

The line marked $w = -1$ has a significant different behaviour than the line with the same label in the top plot. For the same value of $z_{vir} \approx 0$ one sees that in the top plot $(R_{vir}/R_{ta})_{top\,plot} \approx 0.484$ and in the middle plot $(R_{vir}/R_{ta})_{middle\,plot} \approx 0.520$. That is, $(R_{vir}/R_{ta})_{top\,plot} < (R_{vir}/R_{ta})_{middle\,plot}$. This means that if one impose the cosmological constant Λ to have a dynamical nature instead of a passive nature this has a fundamental impact on how structures in the Universe virializes.

The last line of this middle plot which stands out is the line marked $w = -0.6$. For $z_{vir} \approx 0$ it is the line corresponding to the shortest virialization radius $R_{vir} \approx 0.474$. Thus, even though X is dynamical there are dark models which still give values of $R_{vir} < 0.5R_{ta}$. This includes the models with $-0.8 \lesssim w < -1/3$. With the interpretations of the three previous w-values this result will be left whith no further interpretation. This is what the numerical data implies based on the somewhat complex connection between the equations involved and how the equation of state ($w = -0.6$) imposes them to behave. By inspection there is obviously a continuity between all these lines.

Bottom plot

The lines marked $w = 0$ and $w = -1/3$ are both giving the constant analytical value $R_{vir}/R_{ta} = 0.5$ as for the EdS model. The $w = 0$ line has the simple explanation that the dark energy model here simulated is reduced to the EdS model. When $w = 0$ the Friedmann equations which describes the background becomes the Friedmann equa-

tions which describe the EdS model. Also, when $w = 0$ together with the requirement that X is clustering, X inside the sphere has the identical properties as CDM. That is, $\rho_{X,s}(w = 0) \propto a_s^{-3(1+w)} = a_s^{-3}$ and $p_X(w = 0) = w\rho_X = p_m = 0$. For the $w = -1/3$ the explanation given for the same marked line in the middle plot applies here. That is, in this system the virialization condition will get reduced to the one applied for the top plot as a consequence of $\Phi_X(w = -1/3) = 0$. Still, there is one main difference which demands explanation. Here X is imposed to cluster which is not the case in the middle plot. This means that at any equal redshift z_{vir} for the two $w = -1/3$ lines in the middle and the bottom plot, the line in this bottom plot will correspond to a sphere with a stronger density contrast Δ_{vir}. This is consistent with the middle and bottom plot in figure 6.8 which corresponds to the middle and bottom plot discussed here.

As for the middle plot, the line marked $w = -1$ has a significant different behaviour than the line with the same label in the top plot. Again the reason is the dynamical nature imposed on X through the virialization condition in use for this bottom plot (and the middle plot). This $w = -1$ line is equal to the same marked line in the middle plot. The reason is that even though X for this bottom plot in general is imposed to cluster as $\propto a_s^{-3(1+w)}$ one realize that $X = \Lambda$ also for this bottom plot because $\rho_X(w = -1) \propto a_s^{-3(1+w)} = 1$ and therefore $\rho_X(w = -1) = \rho_\Lambda = constant$.

With the interpretations of these three w-values in mind the rest of the lines will be left with no further interpretation. As said about the $w = -0.6$ in the middle plot, this is what the numerical data implies based on the somewhat complex connection between the equations involved and how the rest of these equation of state imposes them to behave. By inspection there is obviously a continuity between all these lines which have a behaviour determined by the equation of state.

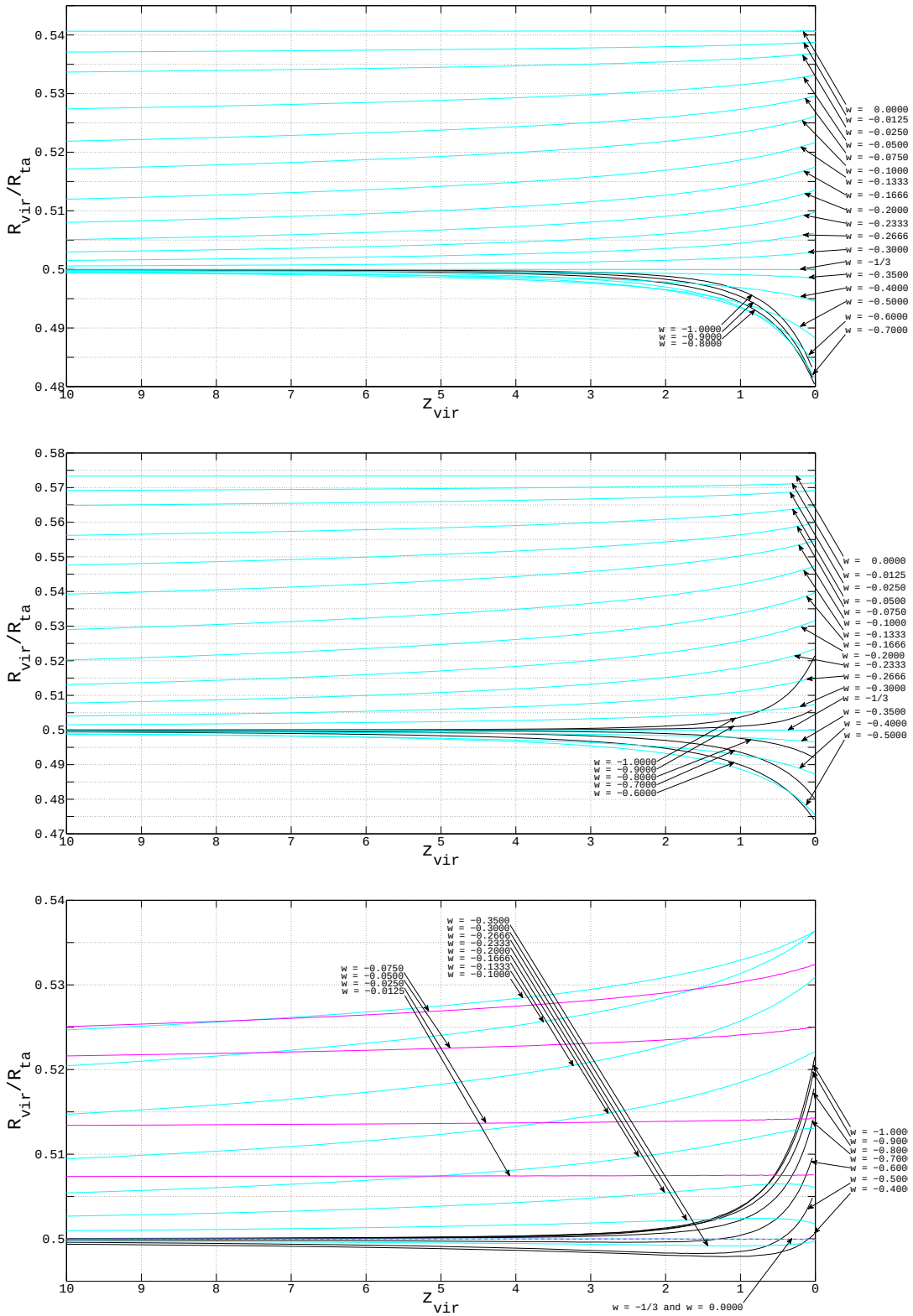

Figure 6.7: All three plots shows the radius R_{vir} at virialization (presented as the ratio R_{vir}/R_{ta} where R_{ta} is the radius at turnaround) at virialization as a function of redshift z_{vir}. Top plot: The dark energy is not clustering and it is passive. Middle plot: The dark energy is not clustering but it is dynamical, i.e. total energy of the sphere is not conserved. Bottom plot: The dark energy is clustering and it is dynamical, i.e. total energy of the sphere is conserved.

6.3.5 Density contrast Δ_{vir} at virialization

The density contrast Δ_{vir} at virialization has the same definition as Δ_{ta} in subsection 6.3.3. The only difference is that the scale factors for the sphere and the background are given at viriralization, i.e. $a_s = a_{s,vir}$ and $a = a_{vir}$. The density contrast Δ_{vir} at virialization is thus

$$\begin{aligned}\Delta_{vir} &= \frac{\left(\rho_{m,s,init}(\frac{a_{s,init}}{a_{s,vir}})^3 + \rho_{X,s}\right) - (\rho_{m0}a_{vir}^{-3} + \rho_X)}{\rho_{m0}a_{vir}^{-3} + \rho_X} \\ &= \frac{\rho_{m,s,init}(\frac{a_{s,init}}{a_{s,vir}})^3 + \rho_{X,s}}{\rho_{m0}a_{vir}^{-3} + \rho_X} - 1\end{aligned} \tag{6.36}$$

where still

$$\begin{aligned}&\rho_{X,s} \equiv \rho_X = \rho_{X0}a^{-3(1+w)} && \text{for non-clustering } X, \text{ and} \\ &\rho_{X,s} = \rho_{X,s,init}\Big(\frac{a_{s,init}}{a_s}\Big)^{3(1+w)} && \text{for clustering } X.\end{aligned} \tag{6.37}$$

In figure 6.8, three plots are presented for the density contrast Δ_{vir} at virialization in the redshift interval $z_{vir} \in [0, 10]$. The top plot applies to a non-clustering and passive X, the middle plot applies to a non-clustering and dynamical X, and the bottom plot applies to a clustering and dynamical X. These three properties of X was presented in section 6.2. Also these three plots are related to the three plots in figure 6.7, i.e. the two top plots are related, the two middle plots are related etc. Therefore the same interpretation as given for the w-lines in the plots in 6.7 applies for the w-lines in each related plot in figure 6.8.

Top plot
The line marked $w = 0$ has a constant value $\Delta_{vir}(w = 0) \approx 89$. Based on the constant value $R_{vir}/R_{ta} \approx 0.541$ from the corresponding top plot in figure 6.7, *and* the fact that the density $\rho_{X,s}(w = 0)$ of X inside the sphere gets diluted (with the background) in the same way as the CDM density $\rho_{m,s}(w = 0)$ inside the sphere is clustering, a constant value of $\Delta_{vir}(w = 0)$ is to be expected. That is, $\rho_{X,s}(w = 0) \propto a^{-3(1+w)} = a^{-3}$ and $\rho_{m,s}(w = 0) \propto a_s^{-3(1+w)} = a_s^{-3}$. Also note the relation that $R_{vir}/R_{ta} \approx 0.541$ represents the greatest R_{vir}/R_{ta} and $\Delta_{vir}(w = 0) \approx 89$ is the weakest density contrast in the current plot.

The line marked $w = -1/3$ shows a behaviour which is consistent with the explanation for the same marked line in the top plot of figure 6.7. It was here pointed out that even though this $w = -1/3$ model virialized with the same constant value of R_{vir}/R_{ta} it still did not have all of the same properties as the EdS model because their respective cosmological fluids did not evolve equally. That is, in the beginning of this subsection 6.3.5 it was explained that the density contrast at virialization for the EdS model was a constant value $\Delta = \Delta_{vir}(EdS) \approx 145.84$. This is not the case for the line representing $\Delta_{vir}(w = -1/3)$ in this top plot. $\Delta_{vir}(w = -1/3)$ is not a constant as a consequence of $\rho_{m,s} \propto a_s^{-3(1+w)} = a_s^{-3}$ but $\rho_{X,s} \propto a^{-3(1+w)} = a^{-2}$. That is, these two components evolves in two significant different ways.

For the $w = -1$ line one observes that the density contrast $\Delta_{vir}(w = -1)$ appears to move asymptotically to $\Delta_{vir}(EdS) \approx 145.84$ towards greater redshifts z_{vir}. This is consistent with its corresponding top plot in figure 6.7 where the value of $R_{vir}/R_{ta} \to 0.5$ towards greater redshifts.

The lines with the w-values now discussed have been considered to be consistent with the top plot in 6.7. The apparent continuity between all the lines should therefore reinforce the assumption that the rest of the lines in this plot also is consistent with their corresponding lines in the top plot of 6.7.

Middle plot

The $w = 0$ line has a constant density contrast $\Delta_{vir}(w = 0)|_{middle\ plot} \approx 72.5$. That means it is weaker than $\Delta_{vir}(EdS) \approx 145.84$. One of the reasons for this is that the density $\rho_{X,s}$ of X is dependent on the background. Thus the evolution of the X component makes this fluid not to cluster as the fluid in the EdS model. The second reason is that the virialization condition used for this plot takes into account the requirement that X has a dynamical nature and therefore participate in the virialization process. This indicates that the sphere should virialize with a greater value of R_{vir}/R_{ta} because of the additional outward force generated by X. This was shown to be the case for the $w = 0$ line in the corresponding middle plot of figure 6.7. Then it is also reasonable to conclude that the density contrast in this case should be weaker than $\Delta_{vir}(w = 0)|_{top\ plot} \approx 89$ where X is passive. This is what the top and middle plot shows, i.e. $\Delta_{vir}(w = 0)|_{top\ plot} > \Delta_{vir}(w = 0)|_{middle\ plot}$.

The $w = -1/3$ line is identical to the same marked line in the top plot. The first part of the explanation for this is referred to the interpretation of the same marked line in the middle plot of figure 6.7 which pointed out that when $w = -1/3$ then the virialization condition reduces to the one used for passive X in the top plot. The last part of the explanation for this current $w = -1/3$ line is the interpretation given for the same marked line in the top plot.

The $w = -1$ line goes asymptotically to the value $\Delta_{vir}(EdS) \approx 145.84$ as in the top

plot, and which also is consistent with the same marked line in the middle plot of figure 6.7. Compared with the same marked line in the top plot one realize that $\Delta_{vir}(w = -1)$ in general is weaker in this middle plot. The reason is the greater R_{vir}/R_{ta} as an effect of X participating in the virialization process.

The lines with the w-values now discussed have been considered to be consistent with the middle plot in 6.7. The apparent continuity between all the lines should therefore reinforce the assumption that the rest of the lines in this plot also is consistent with their corresponding lines in the middle plot of 6.7.

Bottom plot
The $w = 0$ line has the constant analytical value $\Delta_{vir}(w = 0) = \Delta_{vir}(EdS) \approx 145.84$. This is consistent with the same marked line in the bottom plot of figure 6.7. The interpretation for this will be reffered to the interpretation done for this same marked line in the bottom plot of figure 6.7.

For the $w = -1/3$ line one sees that it represents a stronger density contrast $\Delta_{vir}(w = -1/3)$ at any z_{vir} compared to the same marked lines in the middle plot. The reason is that X in this case is clustering and thus contribute more to the total density ρ_s which generates a stronger density contrast. A second reason is that $\Phi_X(w = -1/3) = 0$ and then X is not dynamical in this case for the same reason as explained for the $w = -1/3$ line in the bottom plot of figure 6.7.

For the $w = -1$ line it is equal to the same marked line in the middle plot. The reason is that the density $\rho_{X,s}$ of X has become a constant similar to the cosmological constant Λ. Still its nature is different than Λ because it is consider to be dynamical. That means the properties of X in this case is the same as for X in the middle plot. Thus, the two lines needs to be equal and they are.

The lines with the w-values now discussed have been considered to be consistent with the bottom plot in 6.7. The apparent continuity between all the lines should therefore again reinforce the assumption that the rest of the lines in this plot also is consistent with their corresponding lines in the middle plot of 6.7.

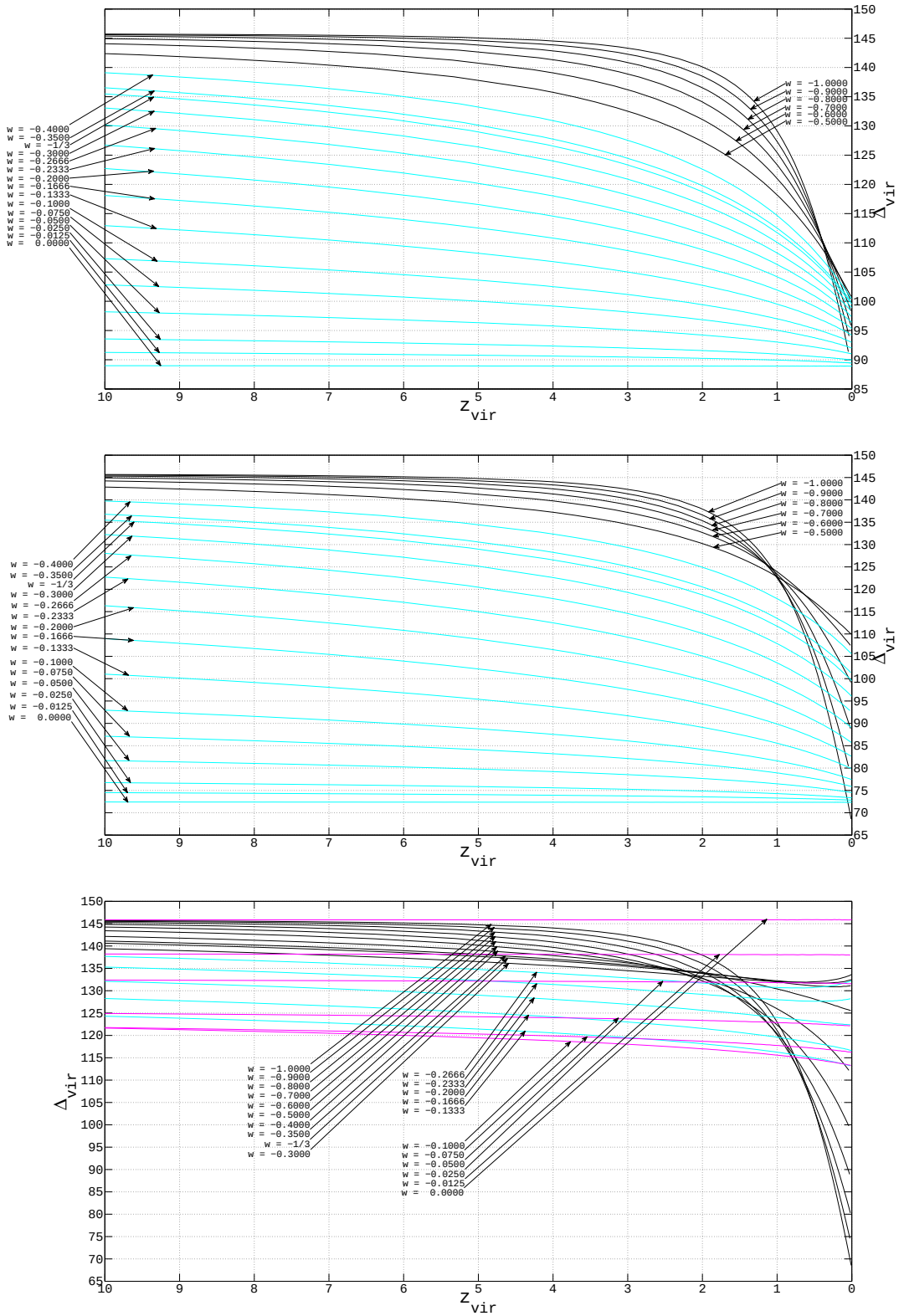

Figure 6.8: All three plots shows the density contrast Δ_{vir} at virialization as a function of redshift z_{vir}. Top plot: The dark energy is <u>not</u> clustering and it is passive. Middle plot: The dark energy is <u>not</u> clustering but it is dynamical, i.e. total energy of the sphere is <u>not</u> conserved. Bottom plot: The dark energy <u>is</u> clustering and it is dynamical, i.e. total energy of the sphere <u>is</u> conserved.

6.4 Chapter Summary

In this chapter it have been studied the evolution of spherical collapse in many different dark energy models with a constant equation of state. In section 6.1 we saw how the sphere evolved when starting with a set of initial density contrasts Δ_i in the ΛCDM model, and then compared this with how it evolved, starting with the same set of Δ_i, in three other types of dark energy models. In each of these three models we first considered the sphere's evolution when the dark energy component was non-clustering, and then compared this with how the sphere evolved when the dark energy was clustering. It was obvious that all three conditions had a fundamental impact of the sphere's evolution. That is, the sphere's evolution depended fully of

- the initial density contrast Δ_i
- the equation of state w
- non-clustering or clustering dark energy

These conditions decided how fast the sphere disentangled from the background and at which redshift it fully collapsed. In section 6.2 three types of virialization conditions was introduced and derived. They decided at which radius the sphere would virialize depending on what type of properties the dark energy was imposed to have. These properties were

- non-clustering and passive dark energy
- non-clustering and dynamical dark energy
- clustering and dynamical dark energy

Then in section 6.3 these different virialization conditions were included in the simulations of the evolving sphere in a total of 21 different dark energy models with a constant equation of state within $w \in [-1, 0]$. Three differenet parameters, i.e. Δ_{ta}, R_{vir}/R_{ta} and Δ_{vir}, of the sphere were calculated. These three parameters were each presented in three different figures which each contained three plots reffering to the three different virialization conditions. It was shown that these parameters in general where fully dependent of the above points.

To end this chapter is a figure consisting of three plots. All three are related to a dark energy model with an equation of state $w = -0.9$. Their content have already been shown in figure (6.6), (6.7) and (6.8), but here they appear in the same plot and thus are easier to compare. This figure (6.9) is an illustration of the importance of what cosmological structures can tell us about the nature of the dark energy and the equation of state of the Universe. One realize that different properties imposed to the dark energy has significant impact to how structures evolves and how they eventually virializes to a final shape. By comparing observational data with simulations based on theoretical studies these plots serves as an indication of the importance the spherical collapse model has in the quest for revealing the true nature of dark energy.

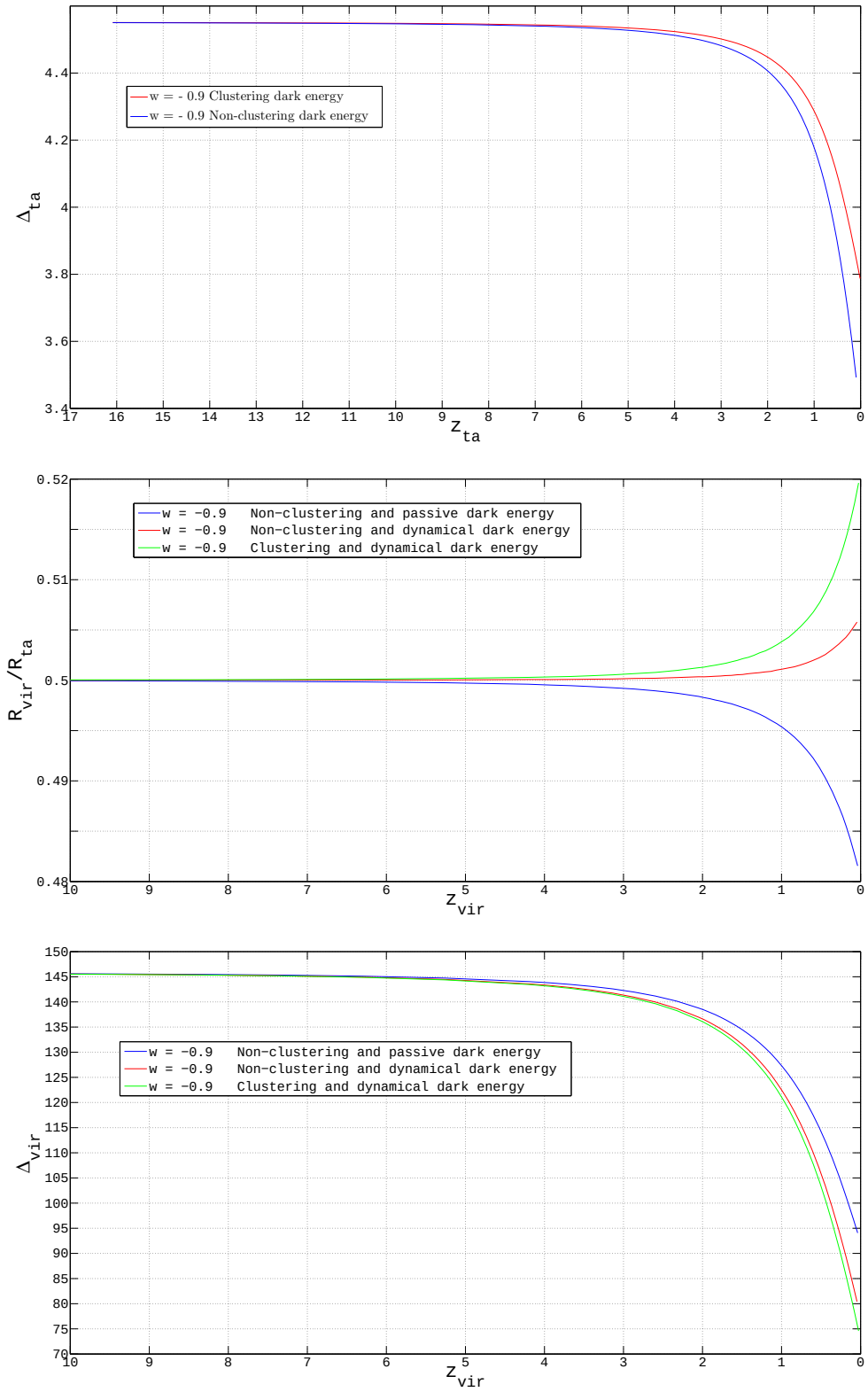

Figure 6.9: The collapsing sphere's dependence on three different properties imposed to the dark energy X in a dark energy model with an equation of state $w = -0.9$. These plots are a strong indication to expect that the shape of cosmological structures are able to reveal important information about the true nature of the dark energy and the equation of state of the Universe.

Chapter 7

Summary and Conclusions

Summary

Chapter two introduced the general theory of relativity and it was emphasized that it was the fundamental theory which physical cosmology is based on. In the same chapter the framework of basic cosmology needed for this text was presented and various derivations were made. In particular the Friedmann equations were emphasized because of its central roll in the code. In chapter three was the smooth Universe abandoned and the inhomogeneous Universe was introduced. First the linear perturbations was presented and a semi derivation of the equation which govern this evolution were made. Next in the same chapter nonlinear perturbations in the cosmic fluid was presented and a tool for describing its evolution was derived in general for universe models without a dark energy component. This tool was the spherical collapse model and in chapter 4 it got specified for the EdS universe. It was emphasized that it applied to a homogeneous overdensity. In the same chapter important analytical values related to this specified model were derived to be used in conjunction with simulations. Chapter 5 compared simulated spherical collapse in the EdS and ΛCDM universe and it was pointed out some fundamental differences of how spheres evolved and virialized. It also proved that the code were able to simulate the same values which was derived for the spherical collapse model in chapter 4. Chapter 6 was laid up in the same manner as chapter 5. It first studied and compared the dynamics of spheres evolving in different dark energy models. Then new virialization conditions were introduced which imposed different properties on the dark energy. Finally these new conditions were included in the simulations and the results were compared. They showed some fundamental differences.

Conclusions

In this text the evolution of structure formation in the Universe has been studied and the focus has been on the nonlinear regime. The tool used for this has been the spherical collapse model. It was first derived analytically and specified for the EdS universe.

Then, mainly based on the Friedmann equations, a program code was started to be developed with the aim of simulating this specified model in the EdS universe. When this was achieved the code was modified to simulate a new system which was spherical collapse inside the ΛCDM model. Finally it was modified to simulate spherical collapse in dark energy models with a constant equation of state. These last systems also took into account three different properties imposed to the dark energy. The simulations of spherical collapse in these systems have shown many important relations and a summary with conclusions will now follow.

• **Initial density contrast Δ_i:** In figure 4.1 the importance of the strength of the sphere's initial density contrast Δ_i related to when it reach turnaround and starts to collapse was shown for the EdS universe. This relation was also shown to apply for the other universe models considered and was (among others) shown in figure 5.1, 6.2 and 6.4. This trend was the same for all the considered models.

Conclusion: Stronger initial density contrasts leads to earlier turnaround and collapse.

• **Non-clustering or clustering dark energy X:** In the figures 6.2, 6.3, 6.4, and 6.5, the relation between non-clustering or clustering X and when the sphere reach turnaround and starts to collapse was shown. The simulations indicated that clustering X in models with $w = (-0.8, -0.6, -0.4)$ led to later turnaround and collapse than for non-clustering X in the same models. Based on the second Friedmann equation (6.6) of the sphere it was claimed that X inside the sphere for these models contributed with an outward force which slowed down the collapse. Therefore those spheres with clustering X contributes the most to this outward force.

Conclusion: Spheres with clustering X in the $w = (-0.8, -0.6, -0.4)$ models reach turnaround and starts to collapse later than corresponding spheres without clustering X.

• **The equation of state w:** Again in the figures 6.2, 6.3, 6.4, and 6.5, another important relation appeared. When the spheres reached turnaround and started to collapse depended of the value of the equation of state w. Regardless of X was clustering or non-clustering the same trend appeared for all the spheres with the same initial density contrast Δ_i.

Conclusion: Spheres inside the $w = -1$ model collapsed fastest, corresponding spheres inside the $w = -0.8$ model collapsed second fastest, corresponding spheres inside the $w = -0.6$ model collapsed third fastest, and finally corresponding spheres in the $w = -0.4$ model collapsed most slowly. This also indicates that a similar relation can be given for any $-1 \leq w \leq -1/3$ in ascending order, where $w = -1/3$ states the limit for if a universe model have or will achieve positive accelerated expansion in the future. This was discussed in connection with figure 6.1.

• **Effects at virialization from properties imposed to the dark energy X:** The dark energy models indicated some important effects to be aware of when virialized structures in the Universe are studied. The middle plot of figure 6.8 serves as an illustration of this. It shows that, based on the properties imposed to X, for the same universe model the radius R_{vir} of some virialized structure change significantly.

Conclusion:

(1) Non-clustering and passive X $\quad\Longrightarrow\quad \left.\frac{R_{vir}}{R_{ta}}\right|_1 < \frac{1}{2}$

(2) Non-clustering and dynamical X $\quad\Longrightarrow\quad \left.\frac{R_{vir}}{R_{ta}}\right|_2 > \frac{1}{2}$

(3) Clustering and dynamical X $\quad\Longrightarrow\quad \left.\frac{R_{vir}}{R_{ta}}\right|_3 > \left.\frac{R_{vir}}{R_{ta}}\right|_2 > \frac{1}{2}$

'Passive' meant that X did not participate in the virialization process but only sat up an extra potential U_X 'felt' by the CDM. 'Dynamical' meant that X did participate in the virialization process in addition to set up an extra potential U_X 'felt' by the CDM. Note that there have been no characteristic length scales associated to the collapsing system so the spherical collapse remains independent of the size of the object. These differences in the virialization radius also have an effect on the density contrast Δ_{vir} at the same epoch which can be seen in the bottom plot of the same figure.

• **Degeneration of universe models:** The figures 6.6, 6.7 and 6.8 represented the density contrast Δ_{ta} at turnaround, and radius R_{vir} and Δ_{vir} at virialization, respectively, in a total of 21 dark energy models with a constant equation of state $w \in [-1, 0]$. It is clear from these figures that several lines cross each other, meaning that different models may predict the same values for the physical quantities: R_{vir} and Δ_{vir}.

Conclusion: These lines' intersections mean the dark energy models are degenerate. Hence, observational measurements of R_{vir} and Δ_{vir} may give the same physical values. To avoid such degeneracy and be able to distinguish the different models one should look at several redshifts.

Outlook

Future work could include other dark energy models (e.g. quintessence), and it could include simulations of the linear density contrast δ_{vir} at virialization and then use the Press-Schechter formalism for predicting cluster abundances of a certain mass within a given volume of the Universe. Also one could introduce a new density profile of the sphere because so far its density has been considered to be homogeneous. That is, one could assume a density which depends on its scale factor a_s instead.

Appendix A

Additional plots for chapter 6

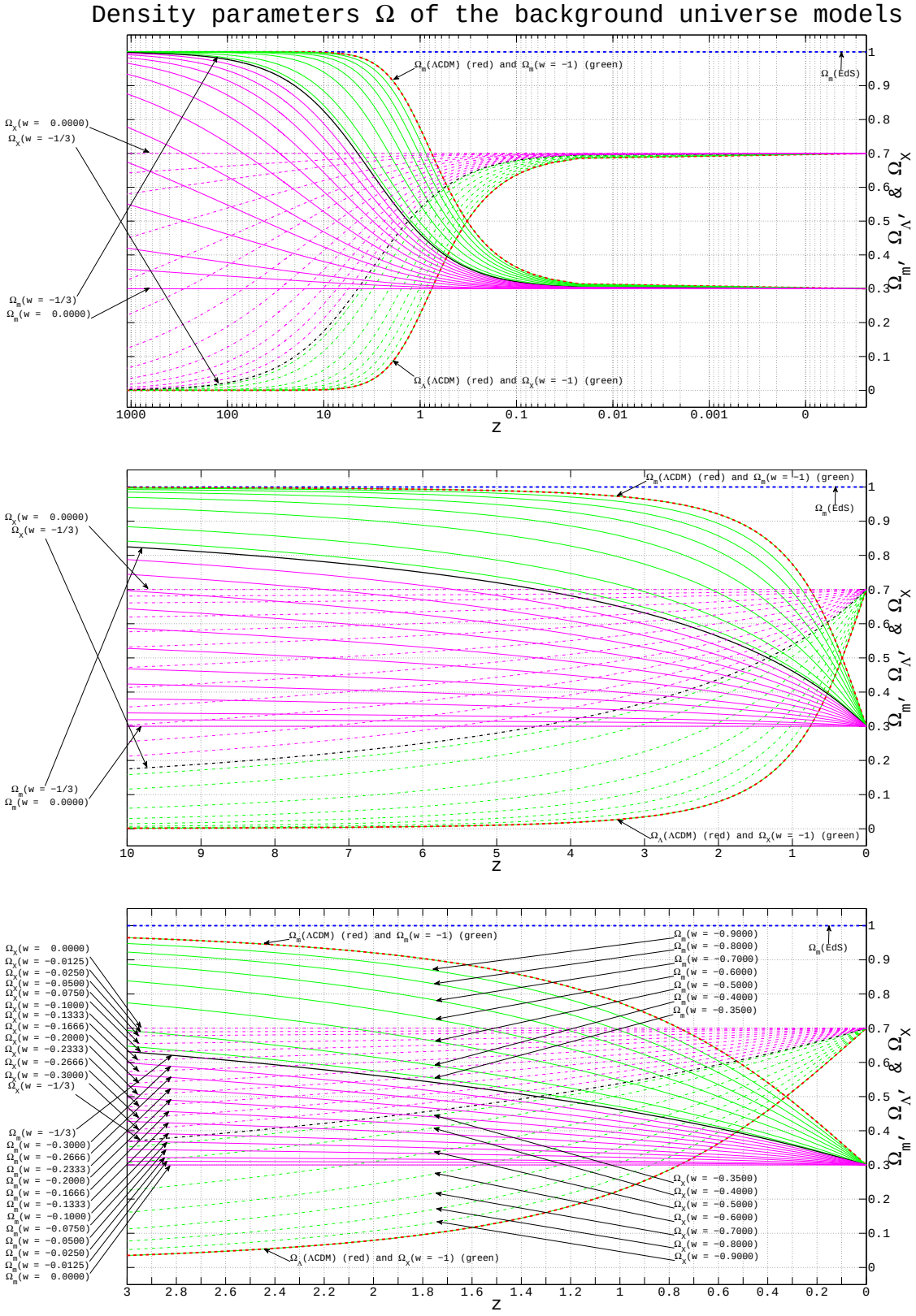

Figure A.1: Evolution of the energy density parameters in the EdS model, ΛCDM model, and dark energy models with a constant equation of state -1 ≤ w ≤ 0.

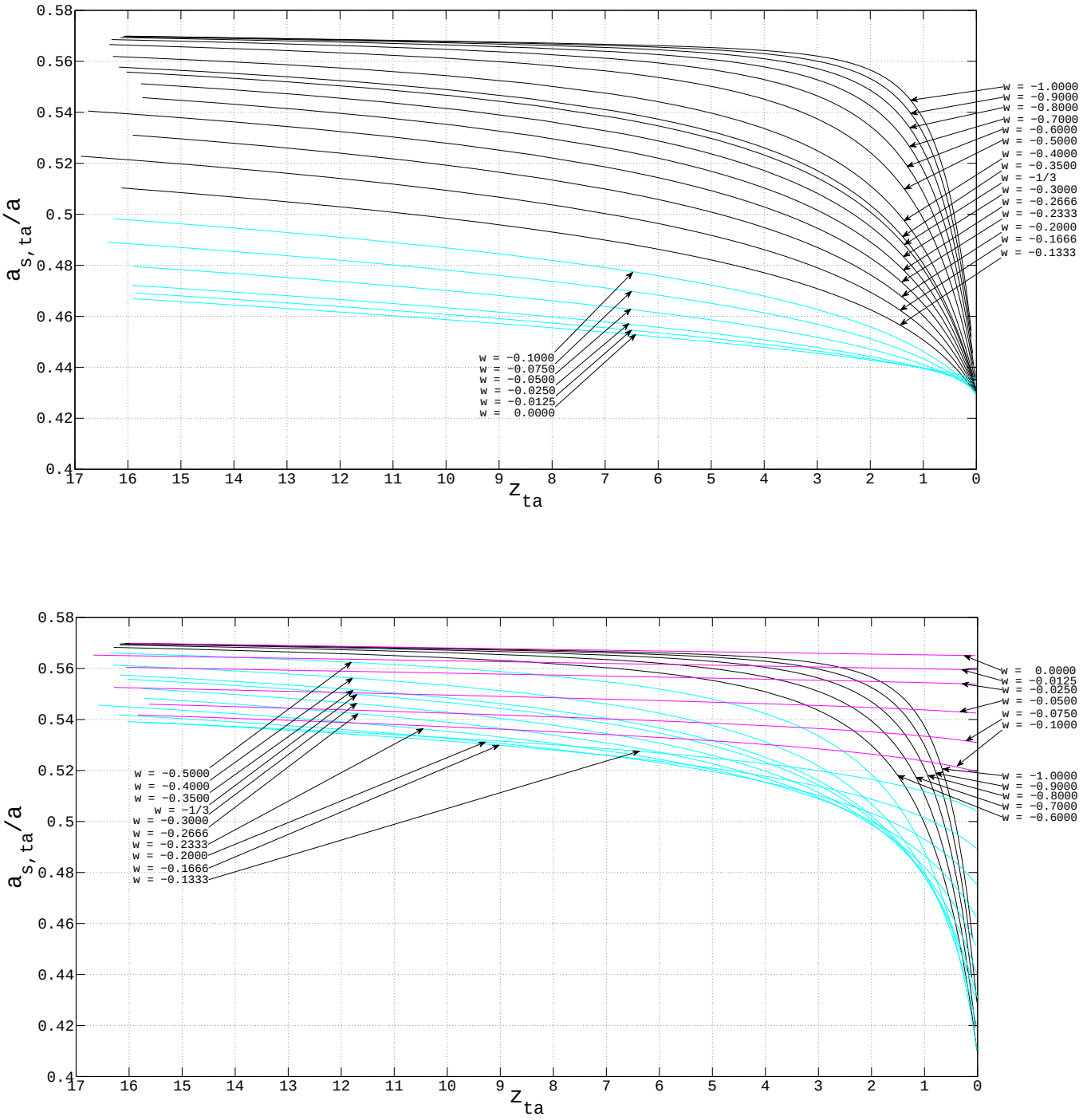

Figure A.2: $a_{s,ta}/a$ represents the turnaround radius R_{ta}. Top plot: Dark energy is not clustering, i.e. total energy of the sphere is not conserved. Bottom plot: Dark energy is clustering, i.e. total energy of the sphere is conserved.

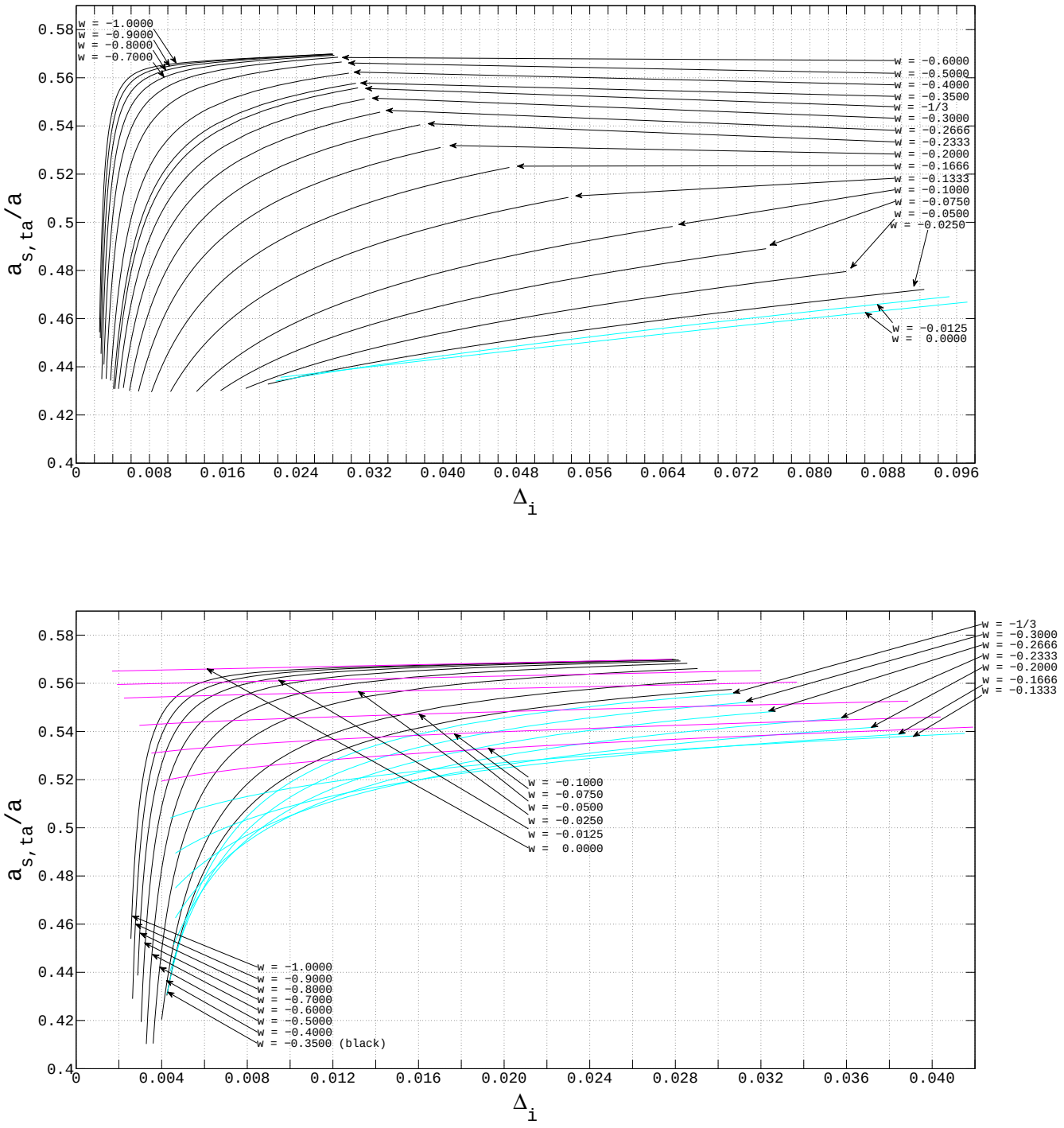

Figure A.3: $a_{s,ta}/a$ represents the turnaround radius R_{ta} where $a_{s,ta}$ and a is the scalefactor of the sphere and the background scalefactor at turnaround, respectively. Top plot: Dark energy is not clustering, i.e. total energy of the sphere is not conserved. Bottom plot: Dark energy is clustering, i.e. total energy of the sphere is conserved.

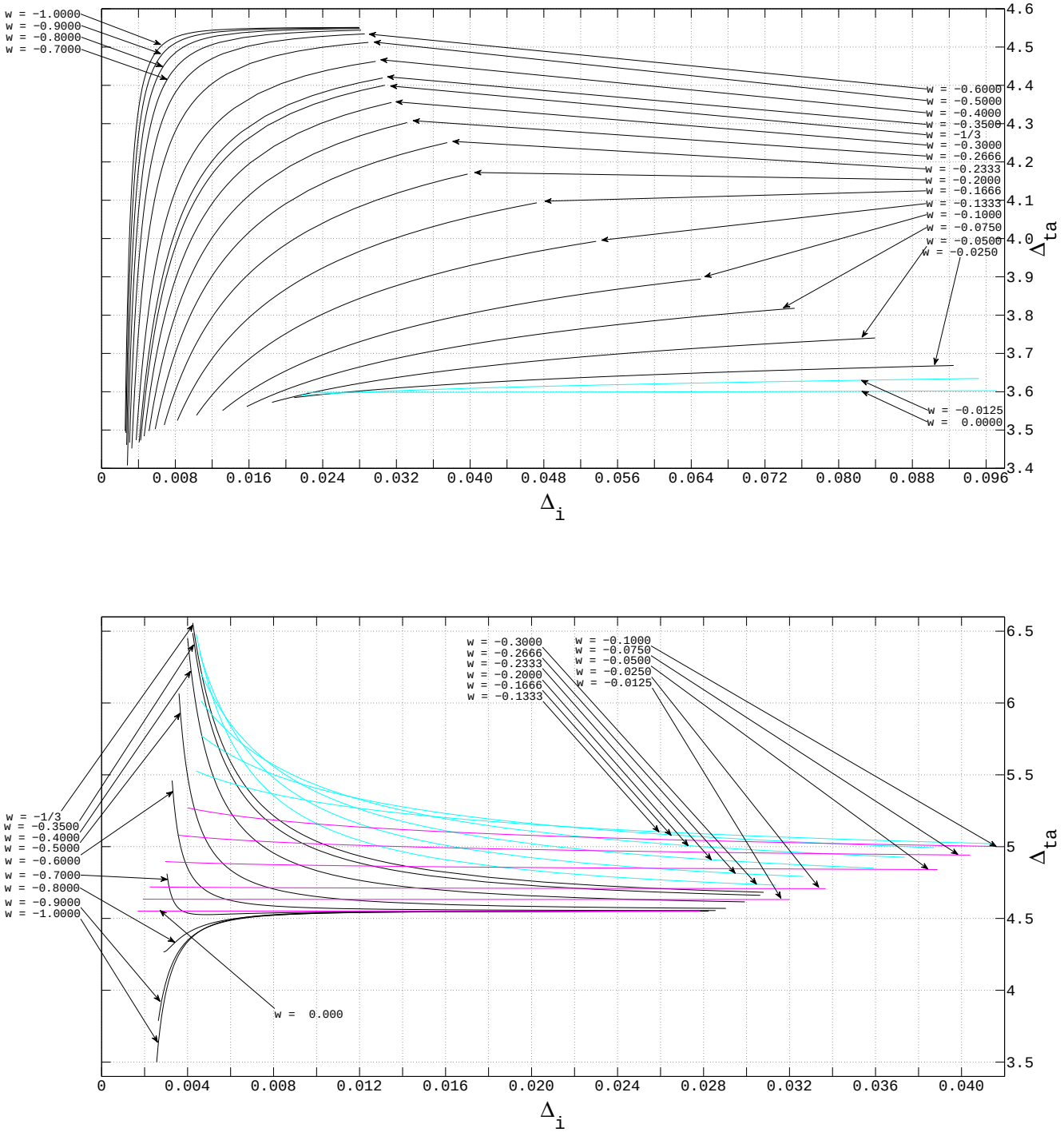

Figure A.4: Top plot: Dark energy component is not clustering, i.e. total energy of the sphere is not conserved. Bottom plot: Dark energy component is clustering, i.e. total energy of the sphere is conserved.

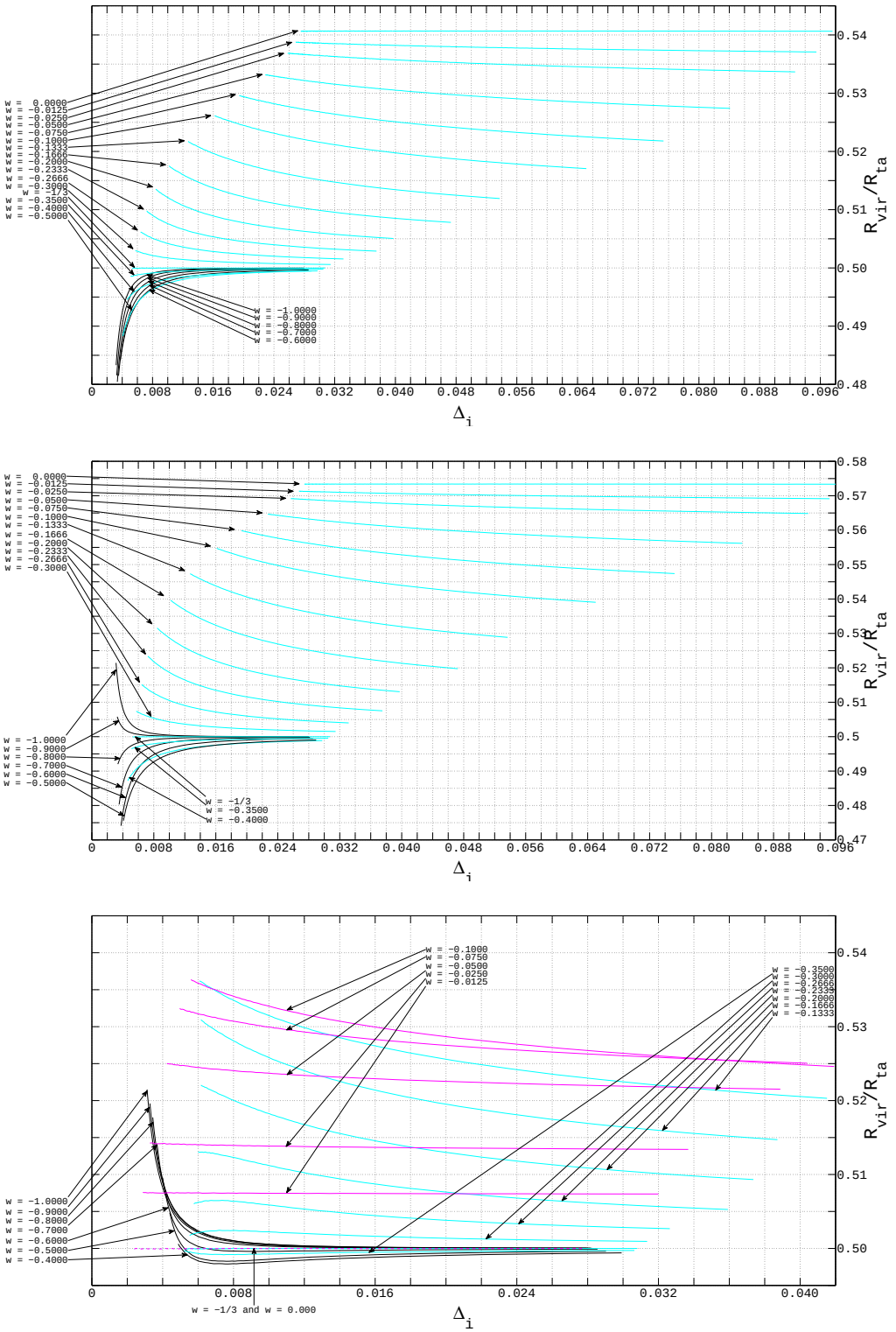

Figure A.5: All three plots shows the radius R_{vir} at virialization (presented as the ratio R_{vir}/R_{ta} where R_{ta} is the radius at turnaround) at virialization as a function of initial density contrast Δ_i. Top plot: The dark energy is not clustering and it is passive. Middle plot: The dark energy is not clustering but it is dynamical, i.e. total energy of the sphere is not conserved. Bottom plot: The dark energy is clustering and it is dynamical, i.e. total energy of the sphere is conserved.

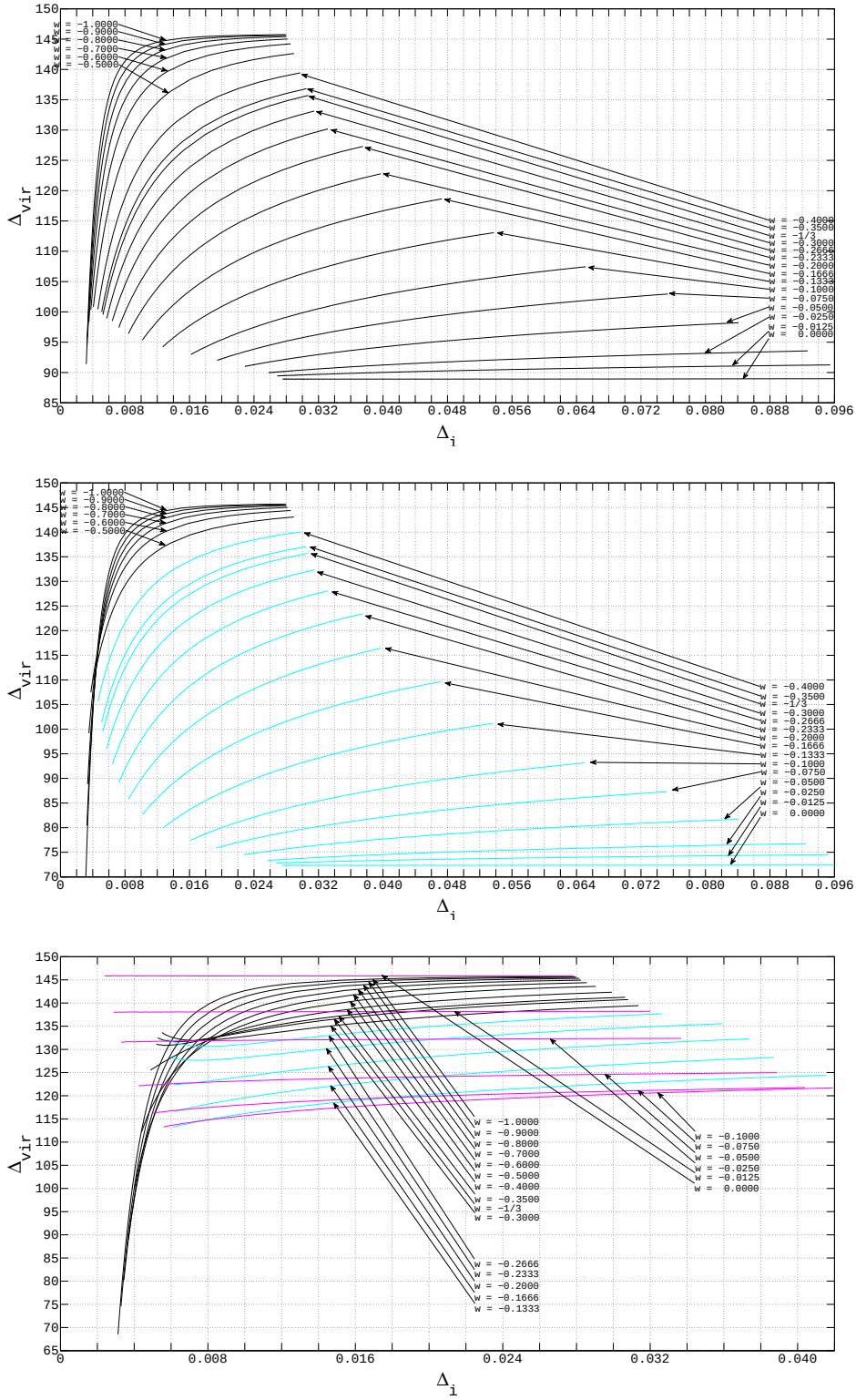

Figure A.6: All three plots shows the density contrast Δ_{vir} at virialization as a function of initial density contrast Δ_i. Top plot: The dark energy is not clustering and it is passive. Middle plot: The dark energy is not clustering but it is dynamical, i.e. total energy of the sphere is not conserved. Bottom plot: The dark energy is clustering and it is dynamical, i.e. total energy of the sphere is conserved.

Appendix B

Friedmann Equations

B.1 The Friedmann Equations Implemented in the Code

From (2.60) and (2.61), the general expressions for the first and second Friedmann equation within the realm of GR are

$$\frac{\dot{a}^2}{a^2} + \frac{kc^2}{a^2} = \frac{8\pi G}{3}\rho + \frac{\Lambda c^2}{3} \tag{B.1}$$

$$\frac{\ddot{a}}{a} = -\frac{4\pi G}{3}\Big(\rho + \frac{3p}{c^2}\Big) + \frac{\Lambda c^2}{3} \tag{B.2}$$

In addition that these two equations gets specified for a given universe model, they are also modified in this thesis so that they depend on the redshift z instead of the cosmic time t, i.e. $a = a(z)$. Thus

$$\dot{a} \equiv \frac{da}{dt} \quad \rightarrow \quad a' \equiv \frac{da}{dz} \qquad \text{and} \qquad \ddot{a} \equiv \frac{d^2a}{dt^2} \quad \rightarrow \quad a'' \equiv \frac{d^2a}{dz^2} \qquad \text{etc.} \tag{B.3}$$

This appendix derives the following for the given universe models

- Background universe: a', a'', $H = H(a)$, and $H' \equiv \frac{dH}{dz}$
- Perturbed sphere: a_s''

Note: The definition $H \equiv \frac{\dot{a}}{a}$ and the relation $1 + z = \frac{1}{a}$ are used frequently. The background scalefactor is a, and the scalefactor of the sphere is a_s.

B.1.1 Spherical Collapse in the EdS Universe Model

Because $k = 0$, $\Lambda = 0$ and $p = p_m = 0$, (B.1) and (B.2) specifies to

$$\frac{\dot{a}^2}{a^2} = \frac{8\pi G}{3}\rho \tag{B.4}$$

$$\frac{\ddot{a}}{a} = -\frac{4\pi G}{3}\rho \tag{B.5}$$

where

$$\rho = \rho_m = \rho_m(a) = \rho_{m0}a^{-3} \tag{B.6}$$

and ρ_{m0} is the background CDM density at present time t_0.

$\underline{a'}$**:**

$$(B.4) \quad \Longrightarrow \quad \dot{a} = \Big(\frac{8\pi G}{3}\rho_m\Big)^{\frac{1}{2}} a$$

$$\text{LHS:} \quad \dot{a} \equiv \frac{da}{dt} = \frac{dz}{dt}\frac{da}{dz} = a'\frac{d}{dt}\Big(\frac{1}{a} - 1\Big) = a'\Big(-\frac{1}{a^2}\frac{da}{dt}\Big) = \underline{-a'\frac{H}{a}}$$

$$\longrightarrow \quad -a'\frac{H}{a} = \Big(\frac{8\pi G}{3}\rho_m\Big)^{\frac{1}{2}} a \quad \Longleftrightarrow \quad \boxed{a' = -\Big(\frac{8\pi G}{3}\rho_m\Big)^{\frac{1}{2}}\frac{a^2}{H}} \tag{B.7}$$

$\underline{a''}$**:**

$$(B.5) \quad \Longrightarrow \quad \ddot{a} = -\frac{4\pi G}{3}\rho_m a$$

$$\text{LHS:} \quad \ddot{a} \equiv \frac{d^2a}{dt^2} = \frac{d}{dt}\Big(\frac{da}{dt}\Big) = \frac{dz}{dt}\frac{d}{dz}\Big(\frac{dz}{dt}\frac{da}{dz}\Big)$$

$$= \Big(\frac{d}{dt}\Big(\frac{1}{a} - 1\Big)\Big)\frac{d}{dz}\Big(a'\frac{d}{dt}\Big(\frac{1}{a} - 1\Big)\Big) = -\frac{H}{a}\frac{d}{dz}\Big(-a'\frac{H}{a}\Big)$$

$$= \frac{H}{a}\Big(\frac{H}{a}\frac{da'}{dz} + a'\frac{d}{dz}\Big(\frac{H}{a}\Big)\Big) = \frac{H}{a}\Big(\frac{Ha''}{a} + a'\Big(\frac{H'}{a} + H\frac{d}{dz}\Big(\frac{1}{a}\Big)\Big)\Big)$$

$$= \underline{\frac{H}{a}\Big(\frac{Ha''}{a} + \frac{H'a'}{a} + Ha'\Big)}$$

$$\longrightarrow \quad \frac{H}{a}\Big(\frac{Ha''}{a} + \frac{H'a'}{a} + Ha'\Big) = -\frac{4\pi G}{3}\rho_m a$$

$$\Longleftrightarrow \quad \boxed{a'' = -\frac{4\pi G}{3}\rho_m\frac{a^3}{H^2} - a'\Big(\frac{H'}{H} + a\Big)} \tag{B.8}$$

$\underline{H(a)}$**:**

$$(B.4) \quad \Longrightarrow \quad \frac{\dot{a}}{a} \equiv H = \Big(\frac{8\pi G}{3}\rho_m\Big)^{\frac{1}{2}}$$

$$H = \Big(\frac{8\pi G}{3}\rho_{m0}a^{-3}\Big)^{\frac{1}{2}} = \Big(\frac{8\pi G}{3}\rho_{m0}\Big)^{\frac{1}{2}}a^{-\frac{3}{2}} = H_0\Big(\frac{8\pi G}{3H_0^2}\rho_{m0}\Big)^{\frac{1}{2}}a^{-\frac{3}{2}}$$

$$= H_0\Big(\frac{\rho_{m0}}{\rho_{c0}}\Big)^{\frac{1}{2}}a^{-\frac{3}{2}} \quad \Longleftrightarrow \quad \boxed{H(a) = H_0 a^{-\frac{3}{2}}}$$

where ρ_{c0} is the critical density and $\rho_{c0} \equiv \frac{3H_0^2}{8\pi G} = \rho_{m0} \Rightarrow \frac{\rho_{m0}}{\rho_{c0}} = 1$ in the EdS universe.

(B.9)

$\underline{H'}$**:**

$$(B.9) \quad \longrightarrow \quad H = H_0 a^{-\frac{3}{2}}$$

LHS: $\quad \frac{dH}{dz} \equiv \underline{H'}$

RHS: $\quad \frac{d}{dz}\Big(H_0 a^{-\frac{3}{2}}\Big) = \underline{-\frac{3}{2}H_0 a^{-\frac{5}{2}}a'}$

$$\longrightarrow \quad \boxed{H' = -\frac{3}{2}H_0 a^{-\frac{5}{2}}a'}$$

(B.10)

$\underline{a_s''}$**:**

$$(B.5) \quad \Longrightarrow \quad \ddot{a}_s = -\frac{4\pi G}{3}\rho_s a_s$$

where $\rho_s = \rho_{m,s} = \rho_{m,s}(a_s) = \rho_{m,s,init}\Big(\frac{a_{s,init}}{a_s}\Big)^3$ is the density of the sphere, $\rho_{m,s,init}$ is the density of the sphere at the initial time for the calculation of its evolution and $a_{s,init}$ is the sphere's scalefactor at that same initial time.

$$\text{LHS:} \quad \ddot{a}_s \equiv \frac{d^2 a_s}{dt^2} = \frac{d}{dt}\Big(\frac{da_s}{dt}\Big) = \frac{dz}{dt}\frac{d}{dz}\Big(\frac{dz}{dt}\frac{da_s}{dz}\Big)$$

$$= \bigg(\frac{d}{dt}\Big(\frac{1}{a}-1\Big)\bigg)\frac{d}{dz}\bigg(a_s'\frac{d}{dt}\Big(\frac{1}{a}-1\Big)\bigg) = \Big(-\frac{H}{a}\Big)\frac{d}{dz}\Big(-a_s'\frac{H}{a}\Big)$$

$$= \frac{H}{a}\bigg(\frac{H}{a}a_s'' + a_s'\frac{d}{dz}\Big(\frac{H}{a}\Big)\bigg) = \frac{H}{a}\bigg(\frac{H}{a}a_s'' + a_s'\bigg(\frac{H'}{a} + H\frac{d}{dz}\Big(\frac{1}{a}\Big)\bigg)\bigg)$$

$$= \frac{H}{a}\bigg(\frac{H}{a}a_s'' + a_s'\bigg(\frac{H'}{a} + H\Big(-\frac{a'}{a^2}\Big)\bigg)\bigg) = \frac{H}{a}\bigg(\frac{H}{a}a_s'' + \frac{a_s'}{a}\Big(H' - H\frac{a'}{a}\Big)\bigg)$$

$$= \underline{\frac{H^2}{a^2}\bigg(a_s'' + a_s'\Big(\frac{H'}{H} - \frac{a'}{a}\Big)\bigg)}$$

$$\longrightarrow \quad \frac{H^2}{a^2}\bigg(a_s'' + a_s'\Big(\frac{H'}{H} - \frac{a'}{a}\Big)\bigg) = -\frac{4\pi G}{3}\rho_{m,s}a_s$$

$$\Longleftrightarrow \quad \boxed{a_s'' = a_s'\Big(\frac{a'}{a} - \frac{H'}{H}\Big) - \frac{4\pi G}{3}\frac{a_s a^2}{H^2}\rho_{m,s}} \tag{B.11}$$

B.1.2 Spherical Collapse in the ΛCDM Universe Model

Because $k = 0$, $\Lambda \neq 0$ and $p_\Lambda \neq 0$, only (B.1) of the Friedmann equations gets specified. Thus

$$\frac{\dot{a}^2}{a^2} = \frac{8\pi G}{3}\rho + \frac{\Lambda c^2}{3} \tag{B.12}$$

$$\frac{\ddot{a}}{a} = -\frac{4\pi G}{3}\Big(\rho + \frac{3p}{c^2}\Big) + \frac{\Lambda c^2}{3} \tag{B.13}$$

where

$$\rho = \rho_m = \rho_{m0} a^{-3} \quad \text{and} \quad p = p_m = 0 \tag{B.14}$$

and ρ_{m0} is the CDM background density at present time t_0.

Firstly, rewriting (B.12) and (B.13) on a simplified form is useful. The equations (2.15) and (2.84) gives

$$\rho_\Lambda = \rho_{\Lambda 0} = \frac{\Lambda c^2}{8\pi G} \qquad \text{and} \qquad p_\Lambda = -\rho_{\Lambda 0} c^2 \tag{B.15}$$

where the first gets substituted for Λ in both (B.12) and (B.13) which gives

$$\frac{\dot{a}^2}{a^2} = \frac{8\pi G}{3}\rho_m + \frac{c^2}{3}\Big(\frac{8\pi G}{c^2}\rho_\Lambda\Big) \quad \Longrightarrow \quad \frac{\dot{a}^2}{a^2} = \frac{8\pi G}{3}(\rho_m + \rho_\Lambda) \tag{B.16}$$

and

$$\begin{aligned} \frac{\ddot{a}}{a} &= -\frac{4\pi G}{3}\Big(\rho_m + \frac{3p_m}{c^2}\Big) + \frac{c^2}{3}\Big(\frac{8\pi G}{c^2}\rho_\Lambda\Big) = -\frac{4\pi G}{3}\Big(\rho_m + \frac{3p_m}{c^2} - 2\rho_\Lambda\Big) \\ &= -\frac{4\pi G}{3}\Big(\rho_m + \rho_\Lambda + \frac{3p_m}{c^2} - 3\rho_\Lambda\Big) \end{aligned} \tag{B.17}$$

Now, by substituting the second equation in (B.15) into the last term of (B.17), and also redefine the density $\rho = \rho_m \longrightarrow \rho = \rho_m + \rho_\Lambda$ and the pressure $p = p_m \longrightarrow p = p_m + p_\Lambda$ yields

$$\frac{\dot{a}^2}{a^2} = \frac{8\pi G}{3}\rho \tag{B.18}$$

$$\frac{\ddot{a}}{a} = -\frac{4\pi G}{3}\Big(\rho + \frac{3p}{c^2}\Big) \tag{B.19}$$

where, said ones again,

$$\rho = \rho_m + \rho_\Lambda \equiv \rho_{m0}a^{-3} + \rho_{\Lambda 0} \quad \text{and} \quad p = p_m + p_\Lambda \equiv 0 + (-\rho_{\Lambda 0}c^2) \tag{B.20}$$

$\underline{a' :}$

$$(B.18) \quad \Longrightarrow \quad \dot{a} = \left(\frac{8\pi G}{3}\Big(\rho_{m0}a^{-3} + \rho_{\Lambda 0}\Big)\right)^{\frac{1}{2}} a$$

LHS: During the derivation of $(B.7)$ it is shown that $\dot{a} = \underline{-a'\frac{H}{a}}$

RHS: $$\left(\frac{8\pi G}{3}\Big(\rho_{m0}a^{-3} + \rho_{\Lambda 0}\Big)\right)^{\frac{1}{2}} a = \left(\frac{H_0^2}{\frac{3H_0^2}{8\pi G}}\Big(\rho_{m0}a^{-3} + \rho_{\Lambda 0}\Big)\right)^{\frac{1}{2}} a$$

$$= H_0\Big(\frac{\rho_{m0}}{\rho_{c0}}a^{-3} + \frac{\rho_{\Lambda 0}}{\rho_{c0}}\Big)^{\frac{1}{2}} a = H_0\Big(\Omega_{m0}a^{-3} + \Omega_{\Lambda 0}\Big)^{\frac{1}{2}} a$$

$$= \underline{H_0\Big(\Omega_{m0}(a^{-3} - 1) + 1\Big)^{\frac{1}{2}} a} \qquad \text{where}$$

$$\Omega_{m0} \equiv \frac{\rho_{m0}}{\rho_{c0}}, \quad \Omega_{\Lambda 0} \equiv \frac{\rho_{\Lambda 0}}{\rho_{c0}}, \quad \text{and} \quad \Omega_{m0} + \Omega_{\Lambda 0} = 1 \quad \text{implied}$$

from (2.68) and (2.69), respectively.

Thus $$-a'\frac{H}{a} = H_0\Big(\Omega_{m0}(a^{-3} - 1) + 1\Big)^{\frac{1}{2}} a$$

$$\Longleftrightarrow \quad \boxed{a' = -H_0\Big(\Omega_{m0}(a^{-3} - 1) + 1\Big)^{\frac{1}{2}} \frac{a^2}{H}} \tag{B.21}$$

$\underline{a'' :}$

Substituting (B.20) in $(B.19)$ $\quad\Longrightarrow\quad$ $\ddot{a} = -\frac{4\pi G}{3}\Big(\rho_m + \rho_{\Lambda 0} + \frac{3}{c^2}(-\rho_{\Lambda 0}c^2)\Big)a$

LHS: During the derivation of $(B.8)$ it is shown that

$$\ddot{a} = \underline{\frac{H}{a}\Big(\frac{Ha''}{a} + \frac{H'a'}{a} + Ha'\Big)}$$

RHS: $$-\frac{4\pi G}{3}\Big(\rho_m + \rho_{\Lambda 0} + \frac{3}{c^2}(-\rho_{\Lambda 0}c^2)\Big)a = \underline{-\frac{4\pi G}{3}\Big(\rho_m - 2\rho_{\Lambda 0}\Big)a}$$

$$\longrightarrow \quad \frac{H}{a}\Big(\frac{Ha''}{a} + \frac{H'a'}{a} + Ha'\Big) = -\frac{4\pi G}{3}\Big(\rho_m - 2\rho_{\Lambda 0}\Big)a$$

$$\Longleftrightarrow \quad \boxed{a'' = -\frac{4\pi G}{3}\Big(\rho_m - 2\rho_{\Lambda 0}\Big)\frac{a^3}{H^2} - a'\Big(\frac{H'}{H} + a\Big)} \tag{B.22}$$

$\underline{H(a) :}$

LHS: During the derivation of $(B.21)$ it is shown that:

$$\dot{a} = H_0\Big(\Omega_{m0}(a^{-3} - 1) + 1\Big)^{\frac{1}{2}}a$$

$$\Longleftrightarrow \quad \frac{\dot{a}}{a} \equiv \boxed{H(a) = H_0\Big(\Omega_{m0}(a^{-3} - 1) + 1\Big)^{\frac{1}{2}}} \tag{B.23}$$

$\underline{H'}$:

$$(B.23) \quad \Longrightarrow \quad H = H_0\Big(\Omega_{m0}(a^{-3}-1)+1\Big)^{\frac{1}{2}}$$

LHS: $\dfrac{dH}{dz} \equiv \underline{H'}$

RHS: $\dfrac{d}{dz}\Big(H_0\Big(\Omega_{m0}(a^{-3}-1)+1\Big)^{\frac{1}{2}}\Big)$

$$= \frac{H_0}{2}\Big(\Omega_{m0}(a^{-3}-1)+1\Big)^{-\frac{1}{2}}(-3\Omega_{m0}a^{-4}a')$$

$$= \underline{-\frac{3}{2}H_0\Omega_{m0}\frac{a'}{a^4}\Big(\Omega_{m0}(a^{-3}-1)+1\Big)^{-\frac{1}{2}}}$$

$$\longrightarrow \quad \boxed{H' = -\frac{3}{2}H_0\Omega_{m0}\frac{a'}{a^4}\Big(\Omega_{m0}(a^{-3}-1)+1\Big)^{-\frac{1}{2}}} \tag{B.24}$$

$\underline{a_s'' :}$

$$(B.19) \quad \Longrightarrow \quad \ddot{a}_s = -\frac{4\pi G}{3}\Big(\rho_s + \frac{3p_s}{c^2}\Big)a_s$$

where $\rho_s = \rho_{m,s} + \rho_{\Lambda,s}$, and $\rho_{m,s} = \rho_{m,s,init}\Big(\frac{a_{s,init}}{a_s}\Big)^3$ is the CDM density of the sphere, $\rho_{m,s,init}$ is the density of the sphere at the initial time for the calculation of its evolution, $a_{s,init}$ is the sphere's scalefactor at that same initial time, $\rho_{\Lambda,s} \equiv \rho_{\Lambda 0}$, and $p_s = p_{m,s} + p_{\Lambda,s}$, where $p_{m,s} = 0$ for CDM and $p_{\Lambda,s} \equiv p_\Lambda$ is given by the equation of state $p_\Lambda = p_{\Lambda 0} = -\rho_{\Lambda 0}c^2$ implied by (2.84).

LHS: During the derivation of $(B.11)$ it is shown that $\ddot{a}_s = \underline{\frac{H^2}{a^2}\Big(a_s'' + a_s'\Big(\frac{H'}{H} - \frac{a'}{a}\Big)\Big)}$

RHS: $$-\frac{4\pi G}{3}\Big(\rho_s + \frac{3p_s}{c^2}\Big)a_s = -\frac{4\pi G}{3}\Big(\rho_{m,s} + \rho_{\Lambda 0} + \frac{3}{c^2}(-\rho_{\Lambda 0}c^2)\Big)a_s$$

$$= \underline{-\frac{4\pi G}{3}\Big(\rho_{m,s} - 2\rho_{\Lambda 0}\Big)a_s}$$

$$\longrightarrow \quad \frac{H^2}{a^2}\Big(a_s'' + a_s'\Big(\frac{H'}{H} - \frac{a'}{a}\Big)\Big) = -\frac{4\pi G}{3}\Big(\rho_{m,s} - 2\rho_{\Lambda 0}\Big)a_s$$

$$\Longleftrightarrow \quad \boxed{a_s'' = a_s'\Big(\frac{a'}{a} - \frac{H'}{H}\Big) - \frac{4\pi G}{3}\Big(\rho_{m,s} - 2\rho_{\Lambda 0}\Big)\frac{a^2 a_s}{H^2}} \quad \text{where} \quad \rho_{m,s} = \rho_{m,s,init}\Big(\frac{a_{s,init}}{a_s}\Big)^3.$$

(B.25)

B.1.3 Spherical Collapse in Dark Energy Universe Models

The Friedmann equations which describes universes that includes a dark energy component has the same form as (B.18) and (B.19), and also follows the same derivation that led to these. But there are some important differences such as the density ρ_X, which represents the density of the dark energy, which in general no longer is a constant, but a function of the scalefactor. Thus

$$\rho_\Lambda \equiv \rho_{\Lambda 0} \quad \longrightarrow \quad \rho_X = \rho_{X0} a^{-3(1+w)} \tag{B.26}$$

where ρ_{X0} is the density of the dark energy at present cosmic time, and w is related to the equation of state $p_X = w\rho_X$ of the universe model. Now, this opens for two different cases to be considered separately

$$\begin{aligned} &\underline{1:}\ \text{The dark energy is homogeneous all over the universe} \\ &\quad \Longrightarrow \quad \text{the dark energy within the sphere is} \propto a^{-3(1+w)}. \end{aligned} \tag{B.27}$$

$$\begin{aligned} &\underline{2:}\ \text{The dark energy is clustering and thus is } \textit{not} \text{ homogeneous} \\ &\quad \text{all over the universe} \\ &\quad \Longrightarrow \quad \text{the dark energy within the sphere is} \propto a_s^{-3(1+w)}. \end{aligned} \tag{B.28}$$

From now on the dark energy is characterized by $w \in [-1, 0]$. The renaming $\Lambda \longrightarrow X$ is to emphasize that there is now no *cosmological constant* in these universe models (except when $w = -1$). Thus, the Friedmann equations in this context are

$$\frac{\dot{a}^2}{a^2} = \frac{8\pi G}{3}\rho \tag{B.29}$$

$$\frac{\ddot{a}}{a} = -\frac{4\pi G}{3}\Big(\rho + \frac{3p}{c^2}\Big) \tag{B.30}$$

where

$$\rho = \rho_m + \rho_X \equiv \rho_{m0} a^{-3} + \rho_{X0} a^{-3(1+w)} \quad \text{and} \quad p = p_m + p_X \equiv 0 + w\rho_X c^2 \tag{B.31}$$

Note that, in all of the following equations, one gets the corresponding equations used in the ΛCDM universe model (B.1.2) when one sets $w = -1$. That is, $\rho_X = \rho_{X0} a^{-3(1+w)} = \rho_{X0} a^{-3(1+(-1))} = \rho_{X0} = \rho_{\Lambda 0}$ and $p = p_m + p_X \equiv 0 + w\rho_X c^2 = -\rho_\Lambda c^2$.

$\underline{a' :}$

$(B.29)$ and $(B.31)$ $\quad\Longrightarrow\quad$ $\dot{a} = \left(\frac{8\pi G}{3}\left(\rho_{m0}a^{-3} + \rho_{X0}a^{-3(1+w)}\right)\right)^{\frac{1}{2}} a$

LHS: During the derivation of $(B.7)$ it is shown that $\dot{a} = \underline{-a'\frac{H}{a}}$

RHS: $\left(\frac{8\pi G}{3}\left(\rho_{m0}a^{-3} + \rho_{X0}a^{-3(1+w)}\right)\right)^{\frac{1}{2}} a = \left(\frac{H_0^2}{\frac{3H_0^2}{8\pi G}}\left(\rho_{m0}a^{-3} + \rho_{X0}a^{-3(1+w)}\right)\right)^{\frac{1}{2}} a$

$= H_0\left(\frac{\rho_{m0}}{\rho_{c0}}a^{-3} + \frac{\rho_{X0}}{\rho_{c0}}a^{-3(1+w)}\right)^{\frac{1}{2}} a = \underline{H_0\left(\Omega_{m0}a^{-3} + \Omega_{X0}a^{-3(1+w)}\right)^{\frac{1}{2}} a}$

where $\quad \Omega_{m0} \equiv \frac{\rho_{m0}}{\rho_{c0}}, \quad \Omega_{X0} \equiv \frac{\rho_{X0}}{\rho_{c0}}, \quad$ and $\quad \Omega_{m0} + \Omega_{X0} = 1 \quad$ implied

from (2.68) and (2.69), respectively.

Thus $\quad -a'\frac{H}{a} = H_0\left(\Omega_{m0}a^{-3} + \Omega_{X0}a^{-3(1+w)}\right)^{\frac{1}{2}} a$

$\Longleftrightarrow \quad \boxed{a' = -H_0\left(\Omega_{m0}a^{-3} + \Omega_{X0}a^{-3(1+w)}\right)^{\frac{1}{2}} \frac{a^2}{H}}$ $\qquad$ (B.32)

$\underline{a'' :}$

$$(B.30) \text{ and } (B.31) \quad \Longrightarrow \quad \ddot{a} = -\frac{4\pi G}{3}\Big(\rho_m + \rho_X + \frac{3}{c^2}(w\rho_X c^2)\Big)a$$

where $\rho_m = \rho_{m0}a^{-3}$ and $\rho_X = \rho_{X0}a^{-3(1+w)}$.

LHS: During the derivation of $(B.8)$ it is shown that

$$\ddot{a} = \underline{\frac{H}{a}\Big(\frac{Ha''}{a} + \frac{H'a'}{a} + Ha'\Big)}$$

RHS: $$-\frac{4\pi G}{3}\Big(\rho_m + \rho_X + \frac{3}{c^2}(w\rho_X c^2)\Big)a = \underline{-\frac{4\pi G}{3}\Big(\rho_m + (1+3w)\rho_X\Big)a}$$

$$\longrightarrow \quad \frac{H}{a}\Big(\frac{Ha''}{a} + \frac{H'a'}{a} + Ha'\Big) = -\frac{4\pi G}{3}\Big(\rho_m + (1+3w)\rho_X\Big)a$$

$$\Longleftrightarrow \quad \boxed{a'' = -\frac{4\pi G}{3}\Big(\rho_m + (1+3w)\rho_X\Big)\frac{a^3}{H^2} - a'\Big(\frac{H'}{H} + a\Big)} \tag{B.33}$$

$\underline{H(a) :}$

LHS: During the derivation of $(B.32)$ it is shown that:

$$\dot{a} = H_0\Big(\Omega_{m0}a^{-3} + \Omega_{X0}a^{-3(1+w)}\Big)^{\frac{1}{2}}a$$

$$\Longleftrightarrow \quad \frac{\dot{a}}{a} \equiv \boxed{H(a) = H_0\Big(\Omega_{m0}a^{-3} + \Omega_{X0}a^{-3(1+w)}\Big)^{\frac{1}{2}}} \tag{B.34}$$

$\underline{H'}$:

$$(B.34) \quad \Longrightarrow \quad H = H_0\Big(\Omega_{m0}a^{-3} + \Omega_{X0}a^{-3(1+w)}\Big)^{\frac{1}{2}}$$

LHS: $\dfrac{dH}{dz} \equiv \underline{H'}$

RHS: $\dfrac{d}{dz}\left(H_0\Big(\Omega_{m0}a^{-3} + \Omega_{X0}a^{-3(1+w)}\Big)^{\frac{1}{2}}\right)$

$$= \frac{H_0}{2}\Big(\Omega_{m0}a^{-3} + \Omega_{X0}a^{-3(1+w)}\Big)^{-\frac{1}{2}}\Big(-3\Omega_{m0}a^{-4}a' - 3(1+w)\Omega_{X0}a^{-3(1+w)-1}a'\Big)$$

$$= \underline{-\frac{3}{2}H_0\Big(\Omega_{m0}a^{-3} + \Omega_{X0}a^{-3(1+w)}\Big)^{-\frac{1}{2}}\Big(\Omega_{m0}a^{-4} + (1+w)\Omega_{X0}a^{-3(1+w)-1}\Big)a'}$$

$$\longrightarrow \quad \boxed{H' = -\frac{3}{2}H_0\Big(\Omega_{m0}a^{-3} + \Omega_{X0}a^{-3(1+w)}\Big)^{-\frac{1}{2}}\Big(\Omega_{m0}a^{-4} + (1+w)\Omega_{X0}a^{-3(1+w)-1}\Big)a'}$$

(B.35)

$\underline{a_s'' :}$

$$(B.30) \text{ and } (B.31) \quad \Longrightarrow \quad \ddot{a}_s = -\frac{4\pi G}{3}\Big(\rho_s + \frac{3p_s}{c^2}\Big)a_s$$

where $\rho_s = \rho_{m,s} + \rho_{X,s}$, $\rho_{m,s} = \rho_{m,s,init}\Big(\frac{a_{s,init}}{a_s}\Big)^3$ is the CDM density of the sphere and $\rho_{X,s}$ is the dark energy density of the sphere and is explained at the end of this page. $\rho_{m,s,init}$ is the CDM density of the sphere at the initial time for the calculation of its evolution. $a_{s,init}$ is the sphere's scalefactor at that same initial time. $p_s = p_{m,s} + p_{X,s}$, where $p_{m,s} = 0$ for CDM, and $p_{X,s}$ is given by the equation of state, $p_{X,s} = w\rho_{X,s}c^2$, implied by (2.65).

LHS: During the derivation of $(B.11)$ it is shown that $\ddot{a}_s = \underline{\frac{H^2}{a^2}\Big(a_s'' + a_s'\Big(\frac{H'}{H} - \frac{a'}{a}\Big)\Big)}$

RHS: $$-\frac{4\pi G}{3}\Big(\rho_s + \frac{3p_s}{c^2}\Big)a_s = -\frac{4\pi G}{3}\Big(\rho_{m,s} + \rho_{X,s} + \frac{3}{c^2}(w\rho_{X,s}c^2)\Big)a_s$$

$$= \underline{-\frac{4\pi G}{3}\Big(\rho_{m,s} + (1+3w)\rho_{X,s}\Big)a_s}$$

$$\longrightarrow \quad \frac{H^2}{a^2}\Big(a_s'' + a_s'\Big(\frac{H'}{H} - \frac{a'}{a}\Big)\Big) = -\frac{4\pi G}{3}\Big(\rho_{m,s} + (1+3w)\rho_{X,s}\Big)a_s$$

$$\Longleftrightarrow \quad \boxed{a_s'' = a_s'\Big(\frac{a'}{a} - \frac{H'}{H}\Big) - \frac{4\pi G}{3}\Big(\rho_{m,s} + (1+3w)\rho_{X,s}\Big)\frac{a^2 a_s}{H^2}} \quad \text{where}$$

$\rho_{X,s}$ represent the two different cases (B.27) and (B.28), respectively:

Case 1: $\rho_{X,s} = \rho_{X0}a^{-3(1+w)}$

Case 2: $\rho_{X,s} = \rho_{X,s,init}\Big(\frac{a_{s,init}}{a_s}\Big)^{3(1+w)}$

where ρ_{X0} is the background dark energy density at present, and $\rho_{X,s,init}$ is the dark energy density at the initial time for the calculation of the sphere's evolution.

(B.36)

Appendix C

Verification of the Code

C.1 Verification of the Code

It is important that the data simulated by the code can be verified by comparison with analytical values. These analytical values where derived from the spherical collapse model in chapter 4.4 and presented in the boxes (4.35), (4.36), (4.37), (4.38), and (4.44). More credence can be given new data when the code is modified to simulate spherical collapse in other types of universe models, and for which it do not exists analytical data to compare with.

Below is three plots showing the simulated data of a spherical collapse in the EdS universe. In the same plots is the related analytical value for comparison. These simulations are satisfactory enough in the context of the spherical collapse model. The data which are being compared are

- ***The turnaround point*** (4.38): Δ_{ta}
- ***The virialization point*** (4.44): Δ_{vir} and R_{vir}

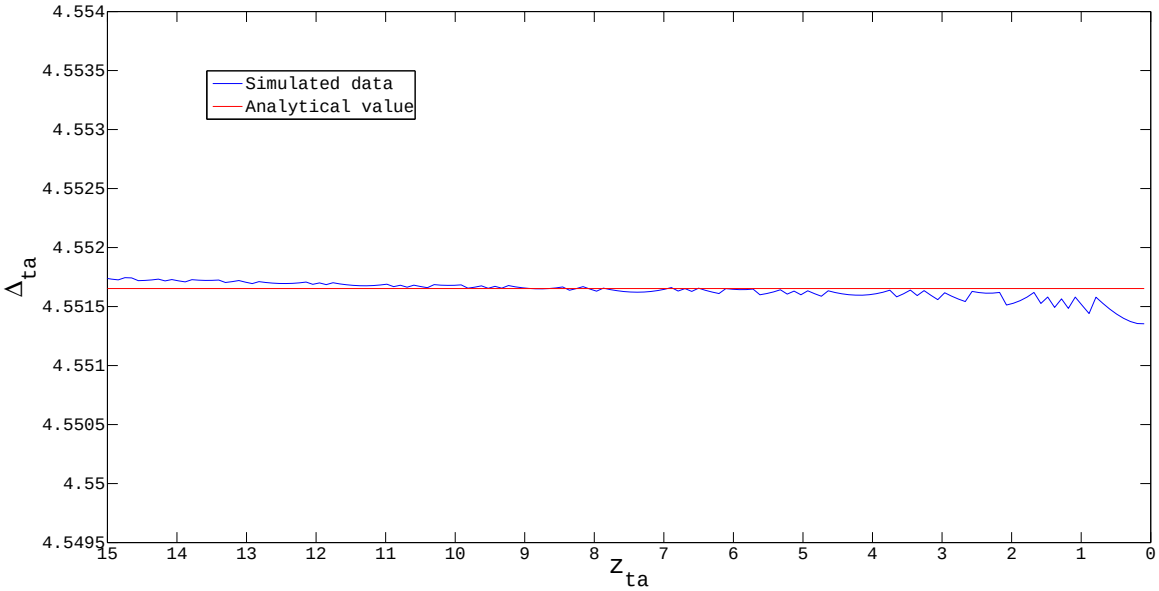

Figure C.1: The numerical data for the density contrast Δ_{ta} at turnaround. From the box (4.44), its analytical value is ≈ 4.551653.

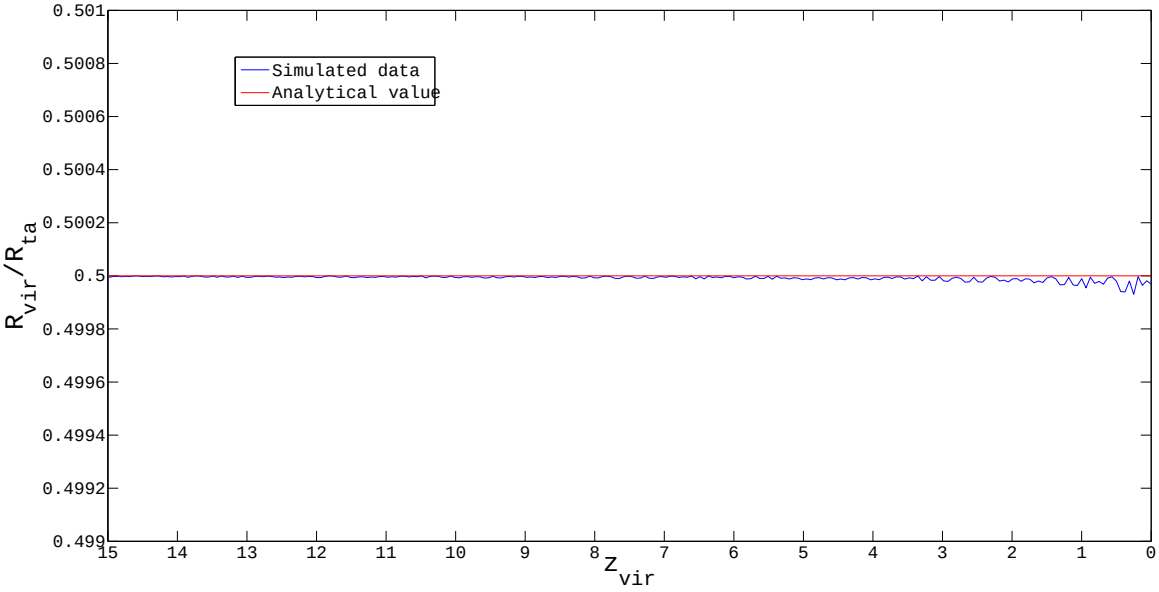

Figure C.2: The numerical data for the virialization radius given as R_{vir}/R_{ta}. From the box (4.44), its analytical value is 0.5.

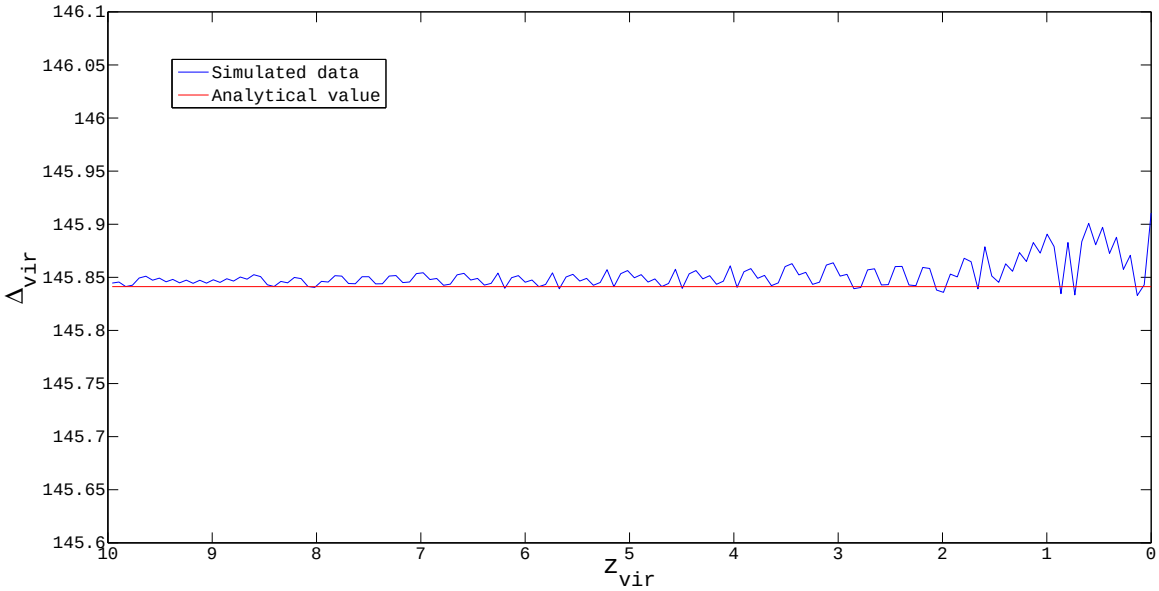

Figure C.3: The numerical data for the density contrast Δ_{vir} at virialization. For the bottom plot in figure 5.6 in section 5.3 it was emphasized that instead of using the constant analytical value derived and then given in (4.44), this thesis relate to another constant analytical value $\approx$ 145.8412454. This also represents the density contrast Δ_{vir} at virialization for the EdS universe but it is derived from another definition of virialization. For more info see John A. Peacock [14] p. 489.

Bibliography

[1] J. E. Gunn and J. R. Gott, III. On the Infall of Matter Into Clusters of Galaxies and Some Effects on Their Evolution. , 176:1–+, August 1972.

[2] O. Lahav, P. B. Lilje, J. R. Primack, and M. J. Rees. Dynamical effects of the cosmological constant. , 251:128–136, July 1991.

[3] I. Maor and O. Lahav. On virialization with dark energy. , 7:3–+, July 2005.

[4] C. Horellou and J. Berge. Dark energy and the evolution of spherical overdensities. , 360:1393–1400, July 2005.

[5] David McMahon. *Relativity Demystified*. McGraw-Hill Companies Inc., 2006.

[6] James B. Hartle. *Gravity - An Introduction to Einstein's General Relativity*. Pearson Education, Inc. Addison Wesley, 2003.

[7] Øyvind Grøn and Sigbjørn Hervik. *Einstein's general theory of relativity*. Springer Science+Business Media, 2007.

[8] Øyvind Grøn. *Lecture Notes on the General Theory of Relativity*. Springer Science+Business Media, 2009.

[9] Peter Coles. *Cosmology - A Very Short Introduction*. Oxford University Press Inc., 2001.

[10] Andrew Liddle. *An Introduction To Modern Cosmology*. John Wiley & Sons Ltd, 2003.

[11] Øystein Elgarøy. *Lecture notes for the course AST4220: Cosmology I.* http://folk.uio.no/mota/LECTURES/COSMOLOGY_I/Lecture_Notes.pdf, 2008.

[12] V. Mukhanov. *Physical foundations of cosmology*. Cambridge University Press, 2005.

[13] Daniel V. Schroeder. *An Introduction To Thermal Physics*. Addison, Wesley & Longman, 2000.

[14] John A. Peacock. *Cosmological Physics*. Cambridge University Press, 1999.

[15] T. Padmanabhan. *Structure formation in the universe*. Cambridge University Press, 1993.

[16] Steven Weinberg. *Cosmology*. Oxford University Press, 2008.

[17] Marc L. Kutner. *Astronomy A physical perspective*. Cambridge University Press, 2003.

[18] Bernard Schutz. *Gravity from the ground up*. Cambrigde University Press, 2003.

[19] N. Wintergerst and V. Pettorino. Clarifying spherical collapse in coupled dark energy cosmologies. , 82(10):103516–+, November 2010.

[20] P. Creminelli, G. D'Amico, J. Noreña, L. Senatore, and F. Vernizzi. Spherical collapse in quintessence models with zero speed of sound. , 3:27–+, March 2010.

[21] S. Basilakos, J. C. B. Sanchez, and L. Perivolaropoulos. Spherical collapse model and cluster formation beyond the Λ cosmology: Indications for a clustered dark energy? , 80(4):043530–+, August 2009.

[22] Ole Eggers Bjaelde and Yvonne Y.Y. Wong. Spherical collapse of dark energy with an arbitrary sound speed. 2010. * Temporary entry *.

[23] Seokcheon Lee and Kin-Wang Ng. Spherical collapse model with non-clustering dark energy. *JCAP*, 1010:028, 2010. * Brief entry *.

[24] Irit Maor. Spherical collapse with dark energy. *Int.J.Theor.Phys.*, 46:2274–2282, 2007.

[25] Ujjal Debnath and Subenoy Chakraborty. Role of modified Chaplygin gas as a dark energy model in collapsing spherically symmetric cloud. *Int.J.Theor.Phys.*, 47:2663–2671, 2008.

[26] Ding-Fang Zeng and Yi-Hong Gao. Spherical collapse model and dark energy(II). 2005.

[27] D.F. Mota and C. van de Bruck. On the Spherical collapse model in dark energy cosmologies. *Astron.Astrophys.*, 421:71–81, 2004.